

## 2.6.2 PHARMACOLOGY WRITTEN SUMMARY

This document contains confidential information belonging to BioNTech/Pfizer. Except as may be otherwise agreed to in writing, by accepting or reviewing these materials, you agree to hold such information in confidence and not to disclose it to others (except where required by applicable law), nor to use it for unauthorized purposes. In the event of actual or suspected breach of this obligation, BioNTech/Pfizer should be promptly notified.

## TABLE OF CONTENTS

LIST OF TABLES .....	4
LIST OF FIGURES .....	4
LIST OF ABBREVIATIONS .....	9
2.6.2. PHARMACOLOGY WRITTEN SUMMARY .....	11
2.6.2.1. Introduction .....	11
2.6.2.2. SARS-CoV-2 S as a Vaccine Target .....	11
2.6.2.3. In Vitro Expression of Antigens From BNT162b2 RNA .....	13
2.6.2.4. Structural and Biophysical Characterization of P2 S as a Vaccine Antigen .....	15
2.6.2.5. Immunogenicity of BNT162b2 in Mice .....	18
2.6.2.6. Immunogenicity of BNT162b2 Monovalent Omicron BA.4/BA.5 and BNT162b2 Bivalent Original and Omicron BA.4/BA.5 in Mice .....	25
2.6.2.7. Immunogenicity of BNT162b2 Monovalent Omicron XBB.1.5 and Bivalent Omicron XBB.1.5 and Omicron BA.4/BA.5 in Mice .....	35
2.6.2.7.1. Vaccine-Experienced Study .....	35
2.6.2.7.1.1. T Cell Response .....	39
2.6.2.7.2. Primary Series Study .....	39
2.6.2.7.2.1. Functional Antibody Response .....	40
2.6.2.7.2.2. T Cell Response .....	42
2.6.2.8. Immunogenicity of BNT162b2 Monovalent Omicron KP.2 Vaccine Compared to BNT162b2 Monovalent Omicron JN.1 and BNT162b2 Monovalent Omicron XBB.1.5 Vaccines in Mice .....	42
2.6.2.8.1. Vaccine-Experienced Study .....	42
2.6.2.8.2. Primary Series Study .....	46
2.6.2.8.2.1. Functional Antibody Response .....	47
2.6.2.8.2.2. T Cell Response .....	48
2.6.2.9. Immunogenicity of BNT162b2 Monovalent Omicron JN.1 and Monovalent Omicron XBB.1.5 in Mice .....	51
2.6.2.9.1. Vaccine-Experienced Study .....	51
2.6.2.9.1.1. Functional Antibody Response .....	53
2.6.2.9.1.2. T Cell Response .....	55
2.6.2.9.2. Primary Series Study .....	58
2.6.2.9.2.1. Functional Antibody Response .....	58

2.6.2.9.2.2. T Cell Response .....	60
2.6.2.10. Immunogenicity of BNT162b2 Monovalent Omicron LP.8.1 and Monovalent Omicron KP.2 in Mice .....	63
2.6.2.10.1. Vaccine-Experienced Study.....	63
2.6.2.10.1.1. Functional Antibody Response .....	63
2.6.2.10.1.2. T Cell Response .....	66
2.6.2.10.2. Primary Series Study .....	69
2.6.2.10.2.1. Functional Antibody Response .....	69
2.6.2.10.2.2. T Cell Response .....	70
2.6.2.11. BNT162b2 Vaccine Immunogenicity and Evaluation of Protection Against SARS-CoV-2 Challenge in Rhesus Macaques .....	74
2.6.2.11.1. Immunogenicity in Rhesus Macaques .....	74
2.6.2.11.2. SARS-CoV-2 Challenge of BNT162b2-Immunized Nonhuman Primates.....	78
2.6.2.12. Immunogenicity Testing of Rats in the GLP Compliant Repeat Dose Toxicity Studies and Developmental and Reproductive Toxicity Study .....	82
2.6.2.12.1. Repeat-Dose Toxicity Study of Three LNP-Formulated RNA Platforms Encoding for Viral Proteins by Repeated Intramuscular Administration to Wistar Han Rats.....	82
2.6.2.12.2. 17-Day Intramuscular Toxicity Study of BNT162b2 in Wistar Han Rats With a 3-Week Recovery .....	84
2.6.2.12.3. A Combined Fertility and Developmental Study (Including Teratogenicity and Postnatal Investigations) of BNT162b1, BNT162b2 and BNT162b3 by Intramuscular Administration in the Wistar Han Rat .....	84
2.6.2.13. Secondary Pharmacodynamics.....	85
2.6.2.14. Safety Pharmacology.....	85
2.6.2.15. Pharmacodynamic Drug Interactions .....	85
2.6.2.16. Discussion and Conclusions.....	85
2.6.2.17. Immunogenicity and Efficacy Methods .....	86
2.6.2.17.1. SARS-CoV-2 S1 and RBD Direct ELISA.....	86
2.6.2.17.2. VSV/SARS-CoV-2 S Pseudovirus Neutralization Assay.....	86
2.6.2.17.3. SARS-CoV-2 S1-Binding and RBD-Binding Kinetics Using Surface Plasmon Resonance Spectroscopy.....	87
2.6.2.17.4. SARS-CoV-2 S1-Binding IgG Luminex Assay .....	87
2.6.2.17.5. SARS-CoV-2 Neutralization Assay .....	87
2.6.2.17.6. Cytokine Profiling Immunoassays in Mice .....	88

2.6.2.17.7. ELISpot and Intracellular Cytokine Staining Assays in NHPs .....	89
2.6.2.17.8. Quantitative RT-PCR for Detection of SARS-CoV-2 Viral RNA .....	90
2.6.2.17.9. Lung Radiographs and Computed Tomography Scans .....	90
2.6.2.17.10. Macroscopic and Microscopic Pathology.....	90
2.6.2.18. References .....	91

## LIST OF TABLES

Table 2.6.2-1. Summary of IgG Concentrations at Day 28 Post Immunization .....	21
Table 2.6.2-2. Study Design.....	26
Table 2.6.2-3. Omicron XBB.1.5 Sublineage Booster Vaccine Mouse Immunogenicity Study Design .....	36
Table 2.6.2-4. Omicron XBB.1.5 Sublineage Primary Series Vaccine Mouse Immunogenicity Study Design .....	40
Table 2.6.2-5. Study Design.....	52
Table 2.6.2-6. JN.1 Primary Series Vaccine Mouse Immunogenicity Study Design .....	58
Table 2.6.2-7. IgG Antibody Concentration [mg/mL] Against the Viral Antigen in Wistar Han Rats After BNT162b2 Immunization .....	83
Table 2.6.2-8. Group Mean Titers of SARS-CoV-2 Neutralizing Antibodies.....	84
Table 2.6.2-9. Group Mean Titers of SARS-CoV-2 Neutralizing Antibodies.....	85

## LIST OF FIGURES

Figure 2.6.2-1. Replication Cycle of a Coronavirus.....	12
Figure 2.6.2-2. Schematic of the Organization of the SARS-CoV-2 S Glycoprotein.....	13
Figure 2.6.2-3. Flow Cytometry Analysis of BNT162b2 Transfection Frequency.....	14
Figure 2.6.2-4. Immunofluorescence Detection of P2 S in BNT162b2 Transfected Cells .....	15
Figure 2.6.2-5. Binding to Cell Surface-Expressed Recombinant P2 S.....	16
Figure 2.6.2-6. Biolayer Interferometry Sensorgrams for Binding of P2 S to ACE-2-PD and B38 mAb .....	17
Figure 2.6.2-7. CryoEM P2 S Structure at 3.29 Å Resolution .....	18
Figure 2.6.2-8. Anti-S IgG Response 7, 14, 21, and 28 Days After Immunization With BNT162b2 .....	19
Figure 2.6.2-9. Binding Kinetics of Murine SARS-CoV-2 S1- and RBD-Specific IgGs.....	20

Figure 2.6.2-10.	BNT162b2 Pseudovirus Neutralizing Titers 14, 21, and 28 Days After Immunization .....	21
Figure 2.6.2-11.	ELISpot Analysis Using Splenocytes Obtained on Day 28 After One Immunization .....	22
Figure 2.6.2-12.	Cytokine Release Analysis Using Splenocytes Obtained on Day 28 After One Immunization.....	23
Figure 2.6.2-13.	B and T Cell Phenotyping in Lymph Nodes of BNT162b2 Immunized Mice.....	24
Figure 2.6.2-14.	Functional Neutralizing Antibodies Elicited by Immunization of Naïve Mice With 2-Doses of Variant-Modified Vaccines .....	27
Figure 2.6.2-15.	Functional Neutralizing Antibody Responses Elicited by Immunization of Naïve Mice With 2 Doses of BNT162b2 (Groups 4 and 5) .....	28
Figure 2.6.2-16.	Neutralizing Antibodies Elicited by Immunization of BNT162b2 Experienced Mice With Omicron BA.4/BA.5 Variant Modified Monovalent and Bivalent modRNA Vaccines as a Third Dose Booster .....	29
Figure 2.6.2-17.	Neutralizing Antibodies Elicited by Immunization of BNT162b2 Experienced Mice With Omicron BA.1 and BA.4/BA.5 Variant Modified Monovalent and Bivalent modRNA Vaccines as a Third Dose Booster.....	30
Figure 2.6.2-18.	Spike-Specific B Cell Response in Lymph Nodes Following Immunization of BNT162b2-Experienced Mice With Omicron BA.4/BA.5 Variant Modified Monovalent and Bivalent modRNA Vaccines as a Third Dose Booster .....	32
Figure 2.6.2-19.	Spike-Specific T Cell Response in Spleens Following Immunization of BNT162b2-Experienced Mice With Omicron BA.4/BA.5 Variant Modified Monovalent and Bivalent modRNA Vaccines as a Third Dose Booster .....	34
Figure 2.6.2-20.	Functional Neutralizing Antibodies Elicited by Immunization of Naïve Mice With 2 Doses of BNT162b2 and 1 Dose of Bivalent BNT162b2 (WT + BA.4/5) at 1 Month Post Dose 3 .....	37
Figure 2.6.2-21.	Neutralizing Antibody Geometric Mean Titers (GMT) at 1 Month Post Dose 4 Elicited by XBB.1.5 Monovalent and Bivalent Vaccines as a Fourth Dose Booster .....	38
Figure 2.6.2-22.	Neutralizing Antibody Geometric Mean Ratios (GMR) at 1 Month Post Dose 4 Elicited by XBB.1.5 Monovalent and Bivalent Vaccines as a Fourth Dose Booster .....	38
Figure 2.6.2-23.	Neutralizing Antibody Geometric Mean Titers (GMT) at 1 Month Post Dose 2 Elicited by XBB.1.5 Monovalent and Bivalent Vaccines as a Primary Series .....	41

Figure 2.6.2-24.	Neutralizing Antibody Geometric Mean Ratios (GMR) at 1 Month Post Dose 2 Elicited by XBB.1.5 Monovalent and Bivalent Vaccines as a Primary Series .....	41
Figure 2.6.2-25.	Study Design for Immunogenicity of a Fourth Dose With BNT162b2 KP.2 Vaccine Compared to BNT162b2 XBB.1.5 and JN.1 Vaccines .....	43
Figure 2.6.2-26.	Weeks Post Dose 3 Neutralizing Geometric Mean Titers (GMT) Following Immunization With 2 Doses of BNT162b2 Original, and 1 Dose of Bivalent BNT162b2 (Original +BA.4/5) .....	43
Figure 2.6.2-27.	2 Weeks Post Dose 4 Vaccination Neutralizing Geometric Mean Titers (GMT) Elicited by XBB.1.5, JN.1, and KP.2 Vaccines .....	45
Figure 2.6.2-28.	Neutralizing Antibody Titer Geometric Mean Fold Rise (GMFR) 2 Weeks Post Dose 4 Compared to Prior Vaccination .....	46
Figure 2.6.2-29.	Study Design for Immunogenicity of a Primary Series With BNT162b2 KP.2 Vaccine Compared to BNT162b2 XBB.1.5 and JN.1 Vaccines .....	47
Figure 2.6.2-30.	1 Month Post Dose 2 Neutralizing Geometric Mean Titers (GMT) With BNT162b2 XBB.1.5, BNT162b2 JN.1, or BNT162b2 KP.2 Monovalent Vaccines as a Primary Series .....	47
Figure 2.6.2-31.	Geometric Mean Ratios (GMR) of the 1 Month Post Dose 2 Neutralizing Geometric Mean Titers (GMT) Elicited by KP.2 and JN.1 Vaccines, Relative to XBB.1.5 Vaccine, as a Primary Series .....	48
Figure 2.6.2-32.	Spike-Specific CD4+ T Cell Response in Spleens Following Immunization With XBB.1.5, JN.1, or KP.2 Vaccine as a Primary Series .....	49
Figure 2.6.2-33.	Spike-Specific CD8+ T Cell Response in Spleens Following Immunization With XBB.1.5, JN.1 or KP.2 Vaccine as a Primary Series .....	50
Figure 2.6.2-34.	5 Weeks Post Dose 4 Neutralizing Geometric Mean Titers (GMT) Following Immunization With 2 Doses of BNT162b2 Original, 1 Dose of Bivalent BNT162b2 (WT + BA.4/5) and 1 Dose of Monovalent BNT162b2 XBB.1.5 .....	53
Figure 2.6.2-35.	1 Month Post Fifth Dose Vaccination Neutralizing Geometric Mean Titers (GMT) with BNT162b2 JN.1 and BNT162b2 XBB.1.5 Monovalent Vaccines .....	54
Figure 2.6.2-36.	Neutralizing Antibody Geometric Mean Fold Rise (GMFR) 1 Month Post Dose 5 Compared to Prior Vaccination .....	54
Figure 2.6.2-37.	Spike-Specific CD4+ T Cell Response in Spleens Following Immunization of BNT162b2 Experienced Mice With JN.1 or XBB.1.5 as a Fifth Vaccination .....	56

Figure 2.6.2-38.	Spike-Specific CD8 <sup>+</sup> T Cell Response in Spleens Following Immunization of BNT162b2 Experienced Mice With JN.1 or XBB.1.5 as a Fifth Vaccination.....	57
Figure 2.6.2-39.	2 Weeks Post Dose 2 Neutralizing Geometric Mean Titers (GMT) With BNT162b2 JN.1 and BNT162b2 XBB.1.5 Monovalent Vaccines as a Primary Series.....	59
Figure 2.6.2-40.	1 Month Post Dose 2 Neutralizing Geometric Mean Titers (GMT) With BNT162b2 JN.1 and BNT162b2 XBB.1.5 Monovalent Vaccines as a Primary Series.....	60
Figure 2.6.2-41.	Spike-Specific CD4 <sup>+</sup> T Cell Response in Spleens Following Immunization With BNT162b2 JN.1 or BNT162b2 XBB.1.5 as a Primary Series.....	61
Figure 2.6.2-42.	Spike-Specific CD8 <sup>+</sup> T Cell Response in Spleens Following Immunization With BNT162b2 JN.1 or BNT162b2 XBB.1.5 as a Primary Series.....	62
Figure 2.6.2-43.	Study Design for the Immunogenicity Evaluation of a Fourth Dose of the BNT162b2 LP.8.1 Vaccine Compared to KP.2 .....	63
Figure 2.6.2-44.	Neutralizing Antibody Geometric Mean Titers (GMT) Following Immunization with 2 Doses of BNT162b2 (Original) and 1 Dose of Bivalent BNT162b2 (Original + BA.4/5) (Pre-Boost) .....	64
Figure 2.6.2-45.	Neutralizing Antibody Geometric Mean Titers (GMT) Following Immunization of BNT162b2 Experienced Mice with BNT162b2 KP.2 or LP.8.1 as a Fourth Vaccination .....	65
Figure 2.6.2-46.	Geometric Mean Ratio (GMR) of Neutralizing Antibody GMTs Elicited by the LP.8.1 Vaccine Groups Relative to KP.2 Vaccine.....	65
Figure 2.6.2-47.	Neutralizing Antibody Geometric Mean Fold Rise (GMFR) 1 Month Post Dose 4 Compared to Pre-Boost.....	66
Figure 2.6.2-48.	SARS-CoV-2 Spike-Specific CD4 <sup>+</sup> T Cell Response in Spleens Following Immunization of BNT162b2 Experienced Mice with BNT162b2 KP.2 or LP.8.1 as a Fourth Vaccination .....	67
Figure 2.6.2-49.	SARS-CoV-2 Spike-Specific CD8 <sup>+</sup> T Cell Response in Spleens Following Immunization of BNT162b2 Experienced Mice with BNT162b2 KP.2 or LP.8.1 as a Fourth Vaccination .....	68
Figure 2.6.2-50.	Study Design for the Immunogenicity Evaluation of a Primary Series of the BNT162b2 LP.8.1 Vaccine Compared to KP.2.....	69
Figure 2.6.2-51.	Neutralizing Antibody Geometric Mean Titers (GMT) Following Immunization of Naïve Mice with BNT162b2 KP.2 or LP.8.1 as a Primary Series.....	70
Figure 2.6.2-52.	Geometric Mean Ratio (GMR) of Neutralizing Antibody GMTs Elicited by the LP.8.1 Vaccine Groups Relative to KP.2 Vaccine.....	70



Figure 2.6.2-53.	SARS-CoV-2 Spike-Specific CD4 <sup>+</sup> T Cell Responses in Spleens Following Immunization of Naïve Mice with BNT162b2 KP.2 or LP.8.1 as a Primary Series .....	72
Figure 2.6.2-54.	SARS-CoV-2 Spike-Specific CD8 <sup>+</sup> T Cell Responses in Spleens Following Immunization of Naïve Mice with BNT162b2 KP.2 or LP.8.1 as a Primary Series .....	73
Figure 2.6.2-55.	S1-Binding IgG Levels Elicited by Immunization of Rhesus Macaques With BNT162b2 .....	74
Figure 2.6.2-56.	50% Serum Neutralizing Titers Elicited by Immunization of Rhesus Macaques With BNT162b2 .....	75
Figure 2.6.2-57.	IFN $\gamma$ and IL-4 ELISpot Results in BNT162b2 Immunized Animals .....	76
Figure 2.6.2-58.	S-Specific CD4 <sup>+</sup> and CD8 <sup>+</sup> T Cell Response in BNT162b2 Immunized Animals as Measured by ICS Assay .....	77
Figure 2.6.2-59.	Viral RNA in BAL Fluid and Nasal and Oropharyngeal Swabs of Rhesus Macaques After Infectious SARS-CoV-2 Challenge.....	79
Figure 2.6.2-60.	Clinical Signs in Rhesus Macaques After Immunization With BNT162b2 and Challenge With Infectious SARS-CoV-2 .....	80
Figure 2.6.2-61.	Radiograph and CT Scores of Rhesus Macaque Lungs After Infectious SARS-CoV-2 Challenge .....	81
Figure 2.6.2-62.	Lung Inflammation Area Score After IN/IT SARS-CoV-2 Challenge .....	82
Figure 2.6.2-63.	Pseudovirus Neutralization Activity in Rats After BNT162b2 Immunization .....	83



## LIST OF ABBREVIATIONS

Abbreviation	Term
ACE-2	Angiotensin Converting Enzyme 2
BAL	Bronchoalveolar lavage
BSL3	Biosafety level 3
CD	Cluster of differentiation
CH	Central helix
COVID-19	Coronavirus disease 2019
CT	Cytoplasmic tail
DART	Developmental And Reproductive Toxicology
dLIA	Direct Luminex Immunoassay
DSPC	1,2-distearoyl- <i>sn</i> -glycero-3-phosphocholine
ELISA	Enzyme-Linked Immunosorbent Assay
ELISpot	Enzyme-Linked Immunospot
ER	Endoplasmic Reticulum
FITC	Fluorescein Isothiocyanate
FP	Fusion Peptide
GD	Gestation Day
GFP	Green Fluorescent Protein
GMC	Geometric Mean Concentration
GMFR	Geometric Mean Fold Rise
GMR	Geometric Mean Ratio
GMT	Geometric Mean Titer
HCS	Human Convalescent Sera
HR	Heptad Repeat
HR1	Heptad Repeat 1
HRP	Horseradish Peroxidase
ICOS	Inducible Costimulatory Molecule
ICS	Intracellular cytokine staining
IFN	Interferon
IgG	Immunoglobulin G
IL	Interleukin
IM	Intramuscular
IN	Intranasal
IT	Intratracheal
LD	Lactation day
LN	Lymph nodes
LNP	Lipid nanoparticle
LLOQ	Lower limit of quantification
mAb	Monoclonal antibody
MERS	Middle East respiratory syndrome
MFI	Mean fluorescence intensity
mL	Milliliter

Abbreviation	Term
mNG	mNeongreen
modRNA	Modified mRNA
NHP	Nonhuman primate
OP	Oropharyngeal
ORF	Open reading frame
P2 S	stable prefusion S including two proline substitutions
PBMC	Peripheral blood mononuclear cells
PBS	Phosphate-buffered saline
PD	Protease domain
PFU	Plaque forming unit
PND	Postnatal day
PVDF	Polyvinylidene fluoride
pVNT	Pseudotype neutralization titer
pVNT <sub>50</sub>	50% pseudovirus neutralizing titer
pVNT <sub>90</sub>	90% pseudovirus neutralizing titer
RBD	Receptor binding domain
RNA	Ribonucleic acid
RT-PCR	Reverse transcription-polymerase chain reaction
RT-qPCR	Reverse transcription-quantitative polymerase chain reaction
S	SARS-CoV-2 spike glycoprotein
S1 / S2	SARS-CoV-2 spike glycoprotein subdomains 1 / 2
S2'	S2 protease cleavage site
SARS-CoV-2	Severe Acute Respiratory Syndrome Coronavirus 2
SS	Signal Sequence
Tfh	T follicular helper cell
Th1 / Th2	Type 1 T-helper cell / Type 2 T-helper cell
TLR	Toll-Like Receptor
TM	Transmembrane
TMB	3, 3', 5, 5'-tetramethylbenzidine
TNF	Tumor Necrosis Factor
µg	Microgram
ULOQ	Upper Limit Of Quantification
US	United States
USA	United States of America
VSV	Vesicular Stomatitis Virus
VNT <sub>50</sub>	50% Virus Neutralizing Titer
WHO	World Health Organization
WT	Wild Type
1MPD4	1 Month post dose 4

## 2.6.2. PHARMACOLOGY WRITTEN SUMMARY

### 2.6.2.1. Introduction

BNT162b2 (BioNTech code number BNT162, Pfizer code number PF-07302048) is a nucleoside-modified mRNA (modRNA) vaccine that encodes the SARS-CoV-2 full-length spike glycoprotein (S). The S glycoprotein encoded by BNT162b2 includes two amino acid substitutions to proline (P2 S) locking the transmembrane protein in an antigenically optimal prefusion conformation (Pallesen et al, 2017; Wrapp et al, 2020).

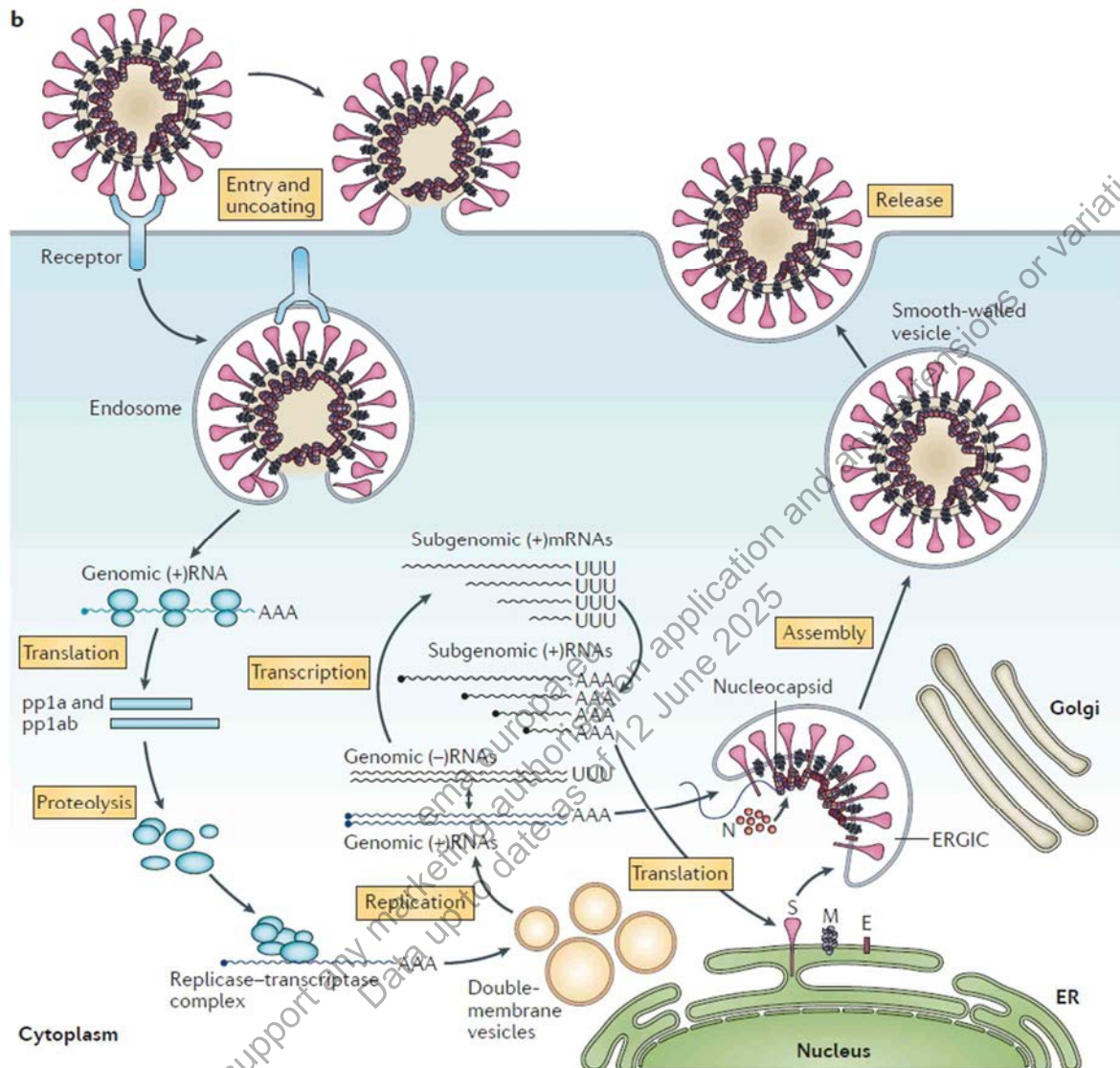
The RNA is formulated with functional and structural lipids, which protect the RNA from degradation and enable transfection of the RNA into host cells after IM injection. The formulation contains two functional lipids, ALC-0315 and ALC-0159, and two structural lipids, DSPC (1,2-distearoyl-*sn*-glycero-3-phosphocholine) and cholesterol.

The modRNA comprises a single-stranded, 5'-capped mRNA that is translated upon entering the cell. In addition to the open reading frame (ORF) encoding the SARS-CoV-2 P2 S antigen, each modRNA contains common structural elements optimized for high translational efficacy of the RNA. ModRNA also contains a substitution of 1-methyl-pseudouridine for uridine. This substitution decreases recognition of the vaccine RNA by innate immune sensors, such as toll-like receptors (TLRs) 7 and 8, resulting in decreased innate immune activation and increased protein translation (Kariko et al, 2005). Vaccination with modRNA is characterized by the strong expansion of Th1-skewed antigen-specific T follicular helper (Tfh) cells, which stimulate and expand germinal center B cells, thereby resulting in particularly strong, long-lived, high-affinity antibody responses (Sahin et al, 2014; Pardi et al, 2018). The structural elements of BNT162b2 contain non-coding sequences optimized for prolonged and strong translation of the P2 S antigen-encoding RNA component.

### 2.6.2.2. SARS-CoV-2 S as a Vaccine Target

SARS-CoV-2 is an enveloped, positive sense, single-stranded RNA virus that is coated with S, which gives the virion its characteristic corona or “crown” appearance (Figure 2.6.2-1). Coronavirus S is a major target of virus neutralizing antibodies and is a key antigen for vaccine development. S is a transmembrane glycoprotein responsible for receptor recognition, attachment to the cell, and viral envelope fusion with a host cell membrane resulting in genome release, which is driven by the S conformation change leading to the fusion of viral and host cell membranes. For infection, S requires proteolytic cleavage by two host proteases, a furin-like protease between the S1 and S2 subunits, and by the serine protease TMPRSS2 at a conserved site directly preceding the fusion peptide (S2') (Figure 2.6.2-2; Hoffmann et al, 2020). While the membrane-proximal S2 furin cleavage fragment is responsible for membrane fusion, the membrane-distal S1 fragment, with its receptor-binding domain (RBD), recognizes the host receptor and binds to the target host cell. SARS-CoV S and SARS-CoV-2 S have similar structural properties and bind to the same host cell receptor, angiotensin converting enzyme 2 (ACE-2) (Zhou et al, 2020).

**Figure 2.6.2-1. Replication Cycle of a Coronavirus**

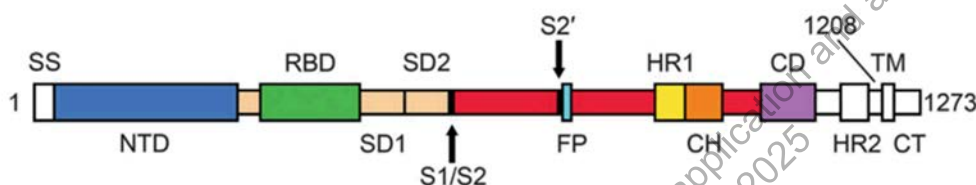


Source: [de Wit et al, 2016](#)

S is a large, trimeric glycoprotein that exists predominantly in a prefusion conformation on the virion ([Ke et al, 2020](#)). Spontaneously and during cell entry, the S1 fragment dissociates, and the S2 fragment undergoes a fold-back rearrangement to the post-fusion conformation in a process that facilitates fusion of viral and host cell membranes. S is critical for the induction of virus neutralizing antibodies by the host immune system ([Zakhartchouk et al, 2007](#); [Yong et al, 2019](#)). Some monoclonal antibodies against S, particularly those directed against the RBD, neutralize SARS-CoV and Middle East respiratory syndrome (MERS)-CoV infection in vitro and in vivo ([Hulswit et al, 2016](#)). Vaccines targeting the S protein are sufficient to induce strong neutralizing immune responses ([Al-Amri et al, 2017](#)).

The RBD forms membrane distal “heads” on the S trimer that are connected to the body by a hinge. In the native S, the RBD alternates between an open (up) and closed (down) position. Although potent neutralizing epitopes have been described when the RBD is in the “heads down” closed conformation, the “heads up” receptor accessible conformation exposes a potentially greater breadth of neutralizing antibody targets (Brouwer et al, 2020; Liu et al, 2020; Robbani et al, 2020). A P2 mutant (P2 S) variant of S contains two consecutive prolines introduced at amino acid positions 986 and 987, between the central helix (CH) and heptad repeat 1 (HR1) (Figure 2.6.2-2). These mutations lock S in the prefusion conformation (Pallesen et al, 2017; Wrapp et al, 2020). A proportion of P2 S has one RBD in the “heads up” and two RBDs in the “heads down” position, and there is probably a dynamic equilibrium as the heads hinge up and down (Cai et al, 2020; Henderson et al, 2020).

**Figure 2.6.2-2. Schematic of the Organization of the SARS-CoV-2 S Glycoprotein**



The S1 furin cleavage fragment includes the signal sequence (SS), the N terminal domain (NTD), the receptor binding domain (RBD, which binds the human cellular receptor, ACE-2), subdomain 1 (SD1), and subdomain 2 (SD2). The furin cleavage site (S1/S2) separates S1 from the S2 fragment, which contains the S2 protease cleavage site (S2') followed by a fusion peptide (FP), heptad repeats (HR1 and HR2), a central helix (CH) domain, the connector domain (CD), the transmembrane domain (TM) and a cytoplasmic tail (CT).  
Source: modified from Wrapp et al, 2020.

BNT162b2 encodes for a full-length P2 S. The RNA-expressed P2 S is membrane anchored. It elicits of a potent humoral neutralizing antibody response and Th1-type CD4<sup>+</sup> and CD8<sup>+</sup> T cell response to block virus infection and kill virus infected cells, respectively.

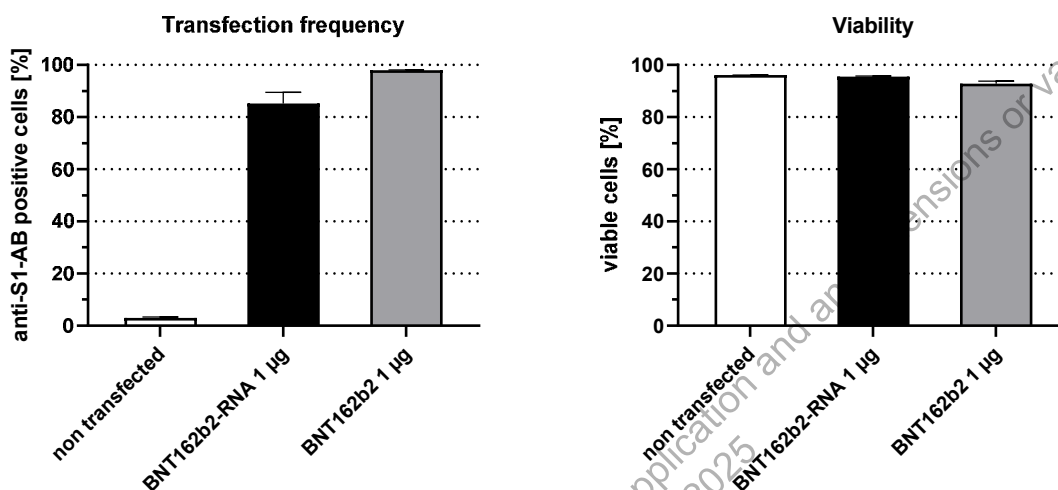
### 2.6.2.3. In Vitro Expression of Antigens From BNT162b2 RNA

Different in vitro methods were performed to analyze SARS-CoV-2 P2 S expression. To assess transfection frequencies in cells exposed to BNT162b2 RNA mixed with a commercial transfection reagent or exposed to BNT162b2 (which is LNP-formulated), flow cytometry analysis was performed. Immunofluorescence staining of transfected cells was used to assess cellular localization.

Flow cytometry analysis of HEK293T cells transfected with either BNT162b2 RNA or LNP-formulated BNT162b2 led to high frequencies of cells being transfected, with BNT162b2-transfected cells being transfected at a slightly higher frequency than cells exposed to BNT162b2 RNA mixed with a commercial transfection reagent (Figure 2.6.2-3). There were no differences in cell viability after transfection with BNT162b2 RNA or BNT162b2 compared to non-transfected cells. Furthermore, co-localization of the S protein

antigen with an ER marker was detected by immunofluorescence experiments in HEK293T cells expressing BNT162b2-RNA suggesting the S protein is processed within the ER (Figure 2.6.2-4).

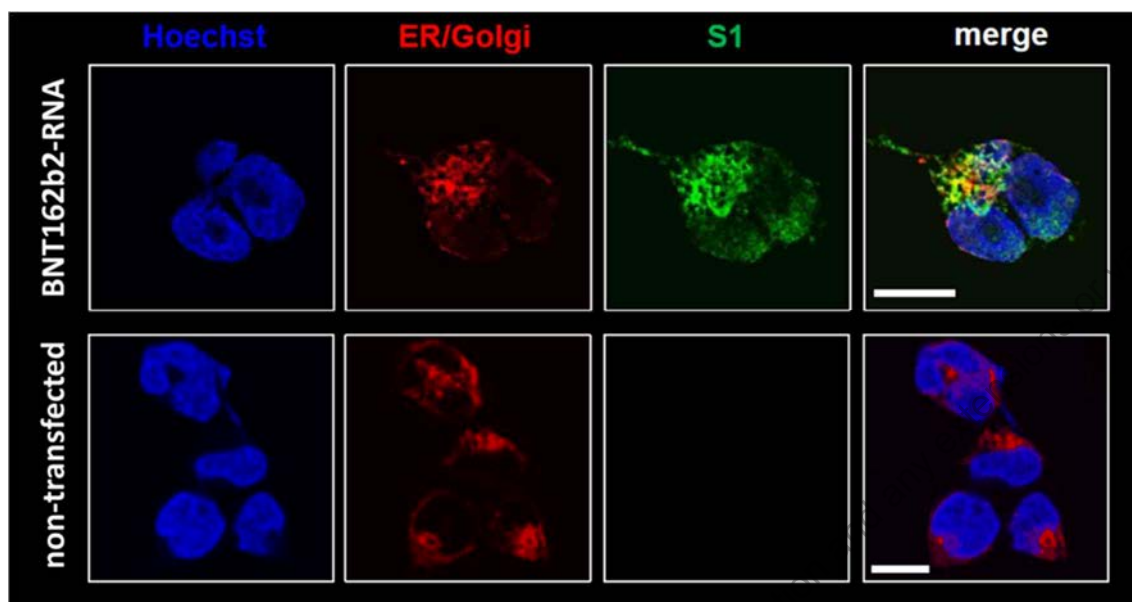
**Figure 2.6.2-3. Flow Cytometry Analysis of BNT162b2 Transfection Frequency**



HEK 293T cells were transfected using RiboJuice™ mRNA transfection reagent (Merck Millipore) with 1 µg of the RNA encoding BNT162b2 P2 S (BNT162b2 RNA) or the BNT162b2 (LNP-formulated RNA). After 18 hours in culture, cells were stained with a viability dye, fixed, permeabilized and stained with a monoclonal rabbit antibody recognizing S1 and labelled with AlexaFluor647. Non-transfected cells were used as a control.



**Figure 2.6.2-4. Immunofluorescence Detection of P2 S in BNT162b2 Transfected Cells**



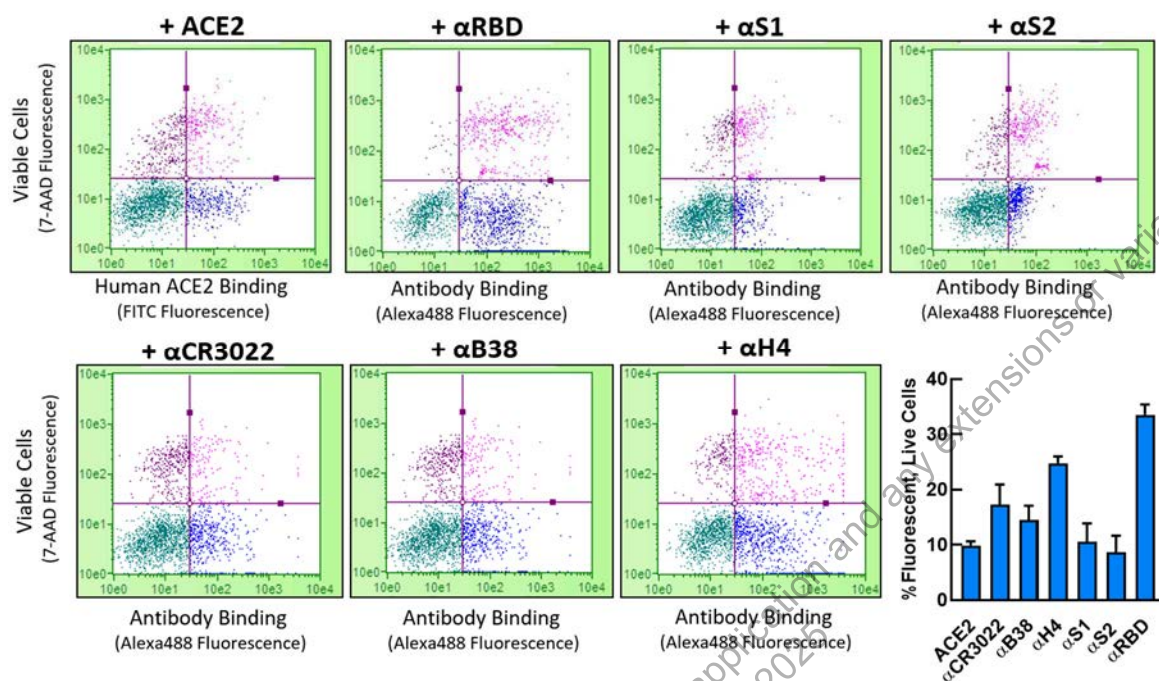
HEK293T cells were transfected with BNT162b2 RNA using RiboJuice™ RNA transfection reagent (Merck Millipore). After 18 hours in culture, cells were fixed, permeabilized and stained for DNA to visualize the nucleus with Hoechst (blue), for the endoplasmic reticulum and Golgi (ER/ Golgi) with concanavalin A and Golgi tracker, both Alexa Fluor™ 594 conjugated (red). Cells were stained for P2 S with a monoclonal anti-S1 antibody and Alexa Fluor® 488 (green). The merged color panels show that the P2 S expressed by BNT162 colocalizes with the ER/ Golgi marker (scale: 10 µm). A control of non-transfected cells is shown in the lower row.

#### 2.6.2.4. Structural and Biophysical Characterization of P2 S as a Vaccine Antigen

For structural characterization, P2 S was expressed in Expi293F cells from DNA that encodes the same amino acid sequence as BNT162b2 RNA, with the addition of a C-terminal TwinStrep tag for affinity purification ([VR-VTR-10741](#)). To confirm surface expression of untagged P2 S as well as the ability of P2 S to bind to human ACE-2, flow cytometry experiments were performed on nonpermeabilized cells ([Figure 2.6.2-5](#)). Antibodies to the RBD, S1, and S2 were pre-incubated with Alexa-488 anti-IgG Fab for staining, and a nucleic acid dye was used to separate live and dead cells. To confirm binding of human ACE-2, P2 S-expressing cells were labeled with the extracellular domain of human ACE-2 pre-incubated with a FITC -labeled antibody against an affinity tag on the ACE-2. Finally, anti-RBD human neutralizing antibodies B38 and H4 isolated from a COVID-19 convalescent patient ([Wu et al, 2020](#)) as well as the anti-RBD therapeutic antibody CR3022 ([Yuan et al, 2020](#)) were similarly confirmed to bind the surface-expressed P2 S.



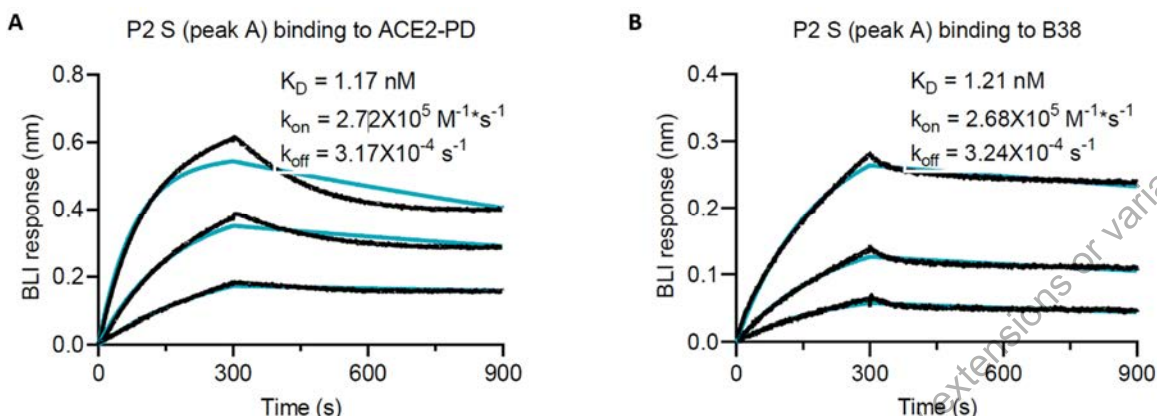
**Figure 2.6.2-5. Binding to Cell Surface-Expressed Recombinant P2 S**



P2 S antigen was over-expressed in Expi293F cells, and surface expression confirmed by staining with antibodies against the RBD, S1, and S2 regions of the full-length S protein. Human ACE2 extracellular domain (ACE-2) as well as the therapeutic antibody CR3022 and two neutralizing antibodies isolated from a COVID-19 convalescent patient, B38 and H4, were further confirmed to bind to surface express P2 S. The nucleic acid dye 7-AAD was used to identify viable cells (lower quadrants in flow plots). Binding to surface expressed P2 S over background in live cells is quantified across replicates in the bar graph.

Purification of the recombinant P2 S was based on a procedure described previously (Cai et al, 2020), with minor modifications. Upon cell lysis, P2 S was solubilized in 1% NP-40 detergent. The TwinStrep-tagged protein was then captured with StrepTactin Sepharose HP resin in 0.5% NP-40. P2 S was further purified by size-exclusion chromatography and eluted as three distinct peaks in 0.02% NP-40 as previously reported (Cai et al, 2020). Protein from the first peak of a size exclusion column, containing intact P2 S and dissociated S1 and S2, was assayed by bilayer interferometry (Figure 2.6.2-6). The trimeric P2 S bound to the human ACE-2 peptidase domain (ACE-2-PD), and an anti-RBD human neutralizing antibody B38 with high affinity (apparent  $K_D = 1$  nM).

**Figure 2.6.2-6. Biolayer Interferometry Sensorgrams for Binding of P2 S to ACE-2-PD and B38 mAb**

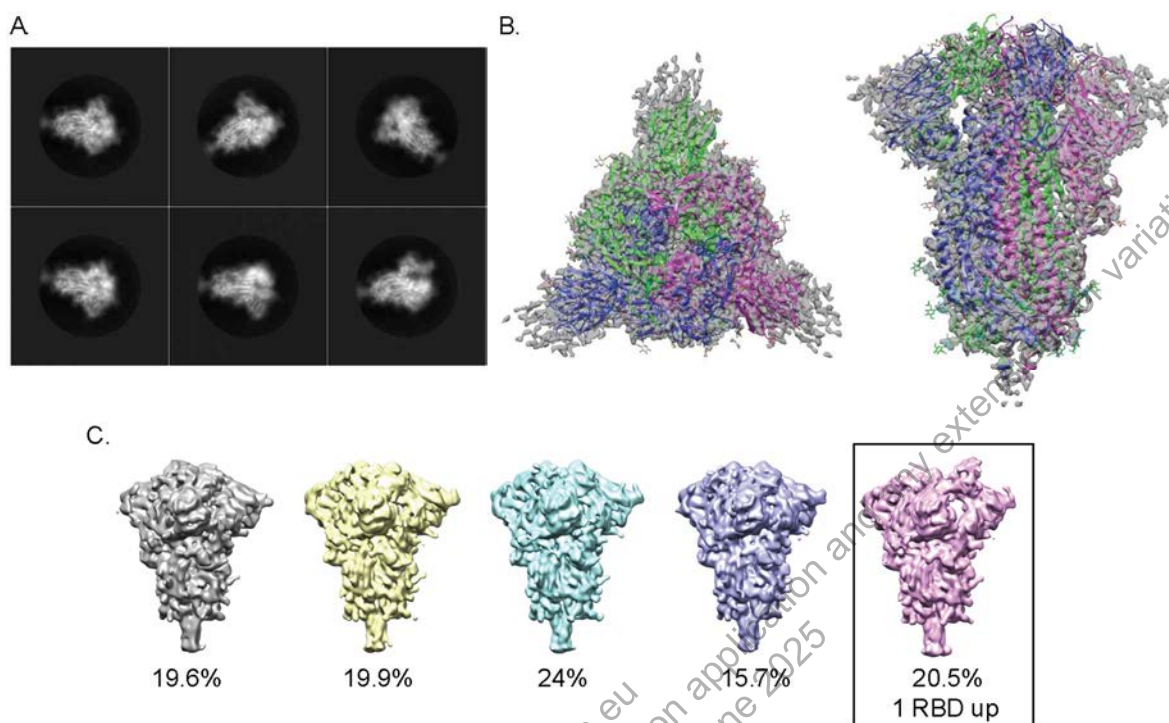


P2 S with a C-terminal TwinStrep tag expressed in Expi293F cells, was detergent solubilized and purified by affinity and size exclusion chromatography. Protein from the first peak of a size exclusion column, containing intact P2 S and dissociated S1 and S2, was assayed by biolayer interferometry on an Octet RED384 (FortéBio) at 25°C in running buffer consisting of 25 mM Tris pH 7.5, 150 mM NaCl, 1mM EDTA and 0.02% NP-40. Sensorgrams showing the binding kinetics of TwinStrep-tagged P2 S to immobilized (A), human ACE-2-PD and (B), B38 monoclonal antibody. The highest concentration tested for P2 S was 71 nM with 2 more 3-fold dilutions. The binding curves were globally fit to a 1:1 Langmuir binding model with  $R^2$  values greater than 0.95. Actual binding data (black) and the best fit of the data to a 1:1 binding model (green). Apparent kinetic parameters are provided in the graphs.

Purified TwinStrep-tagged P2 S was characterized structurally using cryo-electron microscopy (cryoEM). 2D classification of particles from cryoEM data revealed a particle population that closely resembles the prefusion conformation of SARS-CoV-2 spike protein (Figure 2.6.2-7A). Processing and refinement of this dataset yielded a high-quality 3D map with a nominal resolution of 3.29 Å (Figure 2.6.2-7B), into which a previously published atomic model (PDB ID: 6VSB) was fitted and rebuilt. The rebuilt model shows good agreement with reported structures of prefusion full-length wild type S (Cai et al, 2020) and its ectodomain with P2 mutations (Wrapp et al, 2020). Three-dimensional classification of the dataset (Figure 2.6.2-7C) showed a class of particles that was in the one RBD ‘up’ (accessible for receptor binding), two RBD ‘down’ (closed) conformation and represented 20.4% of the trimeric molecules. The remainder were in the all RBD ‘down’ conformation. The RBD in the ‘up’ conformation was less well resolved than other parts of the structure, suggesting conformational flexibility and a dynamic equilibrium between RBD ‘up’ and RBD ‘down’ states as also suggested by others (Cai et al, 2020; Henderson et al, 2020).

The well-resolved trimeric prefusion structure and the high affinity binding to ACE-2 and human neutralizing antibodies demonstrate that the recombinant P2 S authentically presents the ACE-2 binding site and other epitopes targeted by many SARS-CoV-2 neutralizing antibodies.

**Figure 2.6.2-7. CryoEM P2 S Structure at 3.29 Å Resolution**



(A) 2D class averages of TwinStrep-tagged P2 S particles extracted from cryoEM micrographs. Box size is 39.2 nm in each dimension. (B) 3.29 Å cryoEM map of TwinStrep-tagged P2 S, with fitted atomic model, showing top (perpendicular to the three-fold axis) and side (parallel to the three-fold axis) views. CryoEM model is based on PDB 6VSB and was fitted into the structure using manual rebuilding in Coot and real-space refinement in Phenix. ~28,000 micrographs were collected using a Titan Krios electron microscope operating at 300 kV accelerating voltage, and image processing and 3D reconstructions were performed using Warp and RELION. (C) Maps of P2 S produced by 3D classification indicate some heterogeneity in positioning of the RBD domains. Percentages of the particle population represented in each class are indicated below the models.

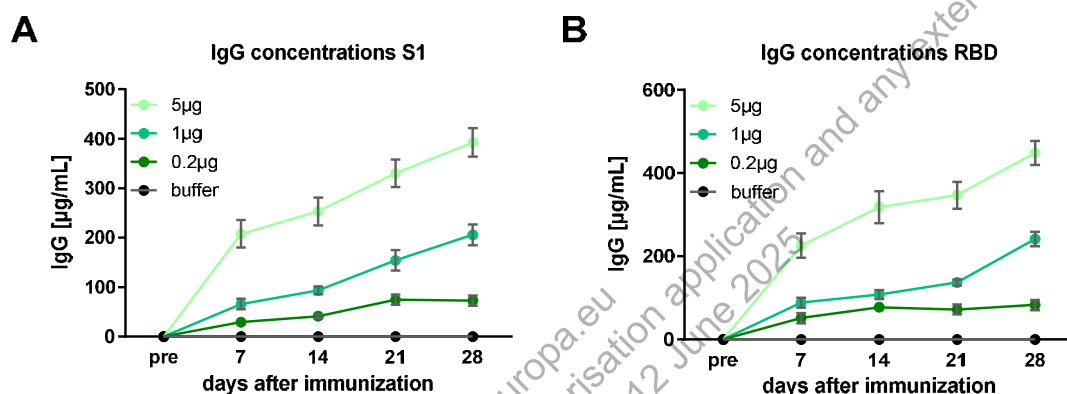
#### 2.6.2.5. Immunogenicity of BNT162b2 in Mice

The immunogenicity of BNT162b2 in mice was investigated ([Report R-20-0085](#)).

Four groups of eight female BALB/c mice were immunized on Day 0 with 0.2 µg, 1 µg or 5 µg RNA/animal of BNT162b2, or with buffer alone (control group). Blood was collected on Days 7, 14, 21 and 28 after immunization to analyze the antibody response by SARS-CoV-2-RBD or S1 IgG ELISA and pseudovirus neutralization test (pVNT) (detailed methods described in [Section 2.6.2.17.1](#) for ELISA and [Section 2.6.2.17.2](#) for pVNT). Binding kinetics of SARS-CoV-2 S1- and RBD-specific IgGs were determined with sera generated at Day 28.

Immunization with BNT162b2 induced IgGs that bind S1 and RBD, while these antibodies were not detected in samples from buffer control animals. A dose-dependent increase in S1-binding IgGs was observed. Antibody concentrations in the serum samples were calculated using a mouse IgG monoclonal standard; the kinetics of IgGs against S1 and RBD are shown in Figure 2.6.2-8. At Day 28, the differences in concentrations of IgGs against S1 and RBD in the test groups compared to the buffer control group were statistically significant (S1:  $p = 0.0259$  for 0.2  $\mu\text{g}$ ,  $p < 0.0001$  for 1  $\mu\text{g}$  and 5  $\mu\text{g}$ ; RBD:  $p = 0.0072$  for 0.2  $\mu\text{g}$ ,  $p < 0.0001$  for 1  $\mu\text{g}$  and 5  $\mu\text{g}$ ).

**Figure 2.6.2-8. Anti-S IgG Response 7, 14, 21, and 28 Days After Immunization With BNT162b2**

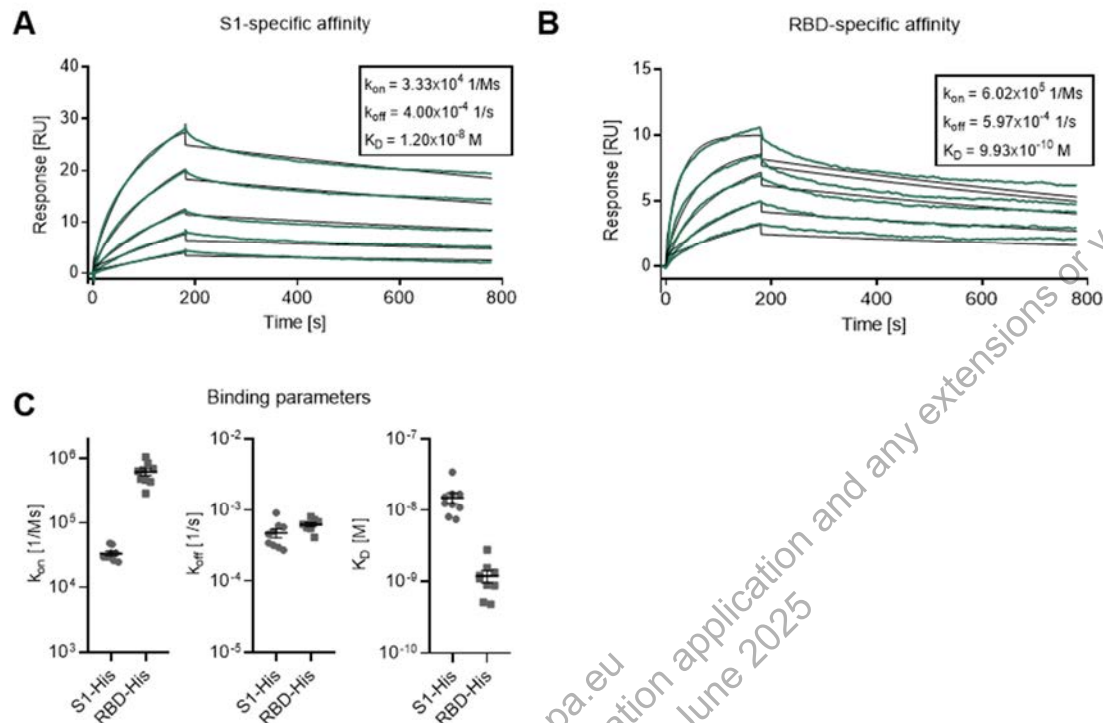


BALB/c mice were immunized IM once with 0.2, 1 and 5  $\mu\text{g}$  BNT162b2 or buffer. On 7, 14, 21, and 28 days after immunization, animals were bled. For individual  $\Delta\text{OD}$  values, the antibody concentrations in the serum samples were calculated. The serum samples were tested by ELISA against (A) recombinant S1 and (B) recombinant RBD. Group mean antibody concentrations are shown ( $\pm\text{SEM}$ ). Group size  $n=8$ . Statistical significance of the differences in IgG concentrations between the test groups and the control group was assessed by one-way ANOVA test with Dunnett's multiple comparison post-test on Day 28.

At Day 28 after immunization, vaccine-elicited IgG against the S1 domain showed a very strong binding affinity (geometric mean KD 12 nM) including IgG binding the RBD with high affinity (geometric mean KD 0.99 nM), both with high on-rate (geometric mean  $k_{\text{on}}$ :  $3.33 \times 10^4/\text{Ms}$  for S1-specific affinity;  $6.02 \times 10^5/\text{Ms}$  for RBD-specific affinity) and low off-rate (geometric mean  $k_{\text{off}}$ :  $4.00 \times 10^{-4}/\text{s}$  for S1-specific affinity;  $5.97 \times 10^{-4}/\text{s}$  for RBD-specific affinity) (Figure 2.6.2-9).



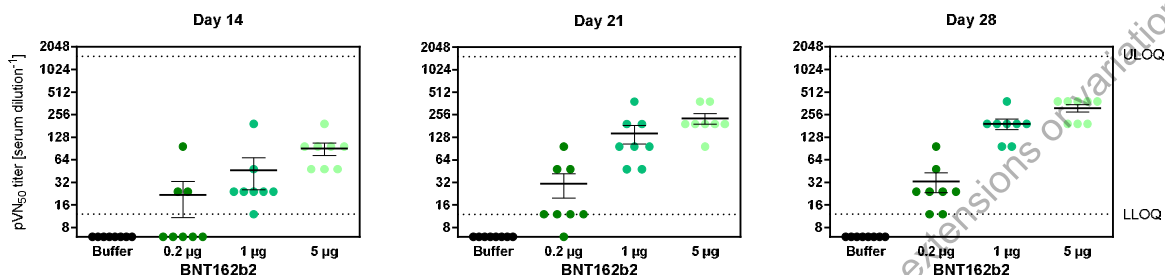
**Figure 2.6.2-9. Binding Kinetics of Murine SARS-CoV-2 S1- and RBD-Specific IgGs**



BALB/c mice were immunized IM once with 5 µg BNT162b2. On Day 28 after immunization, animals were bled. IgG in the sera were tested for binding to recombinant histidine-tagged S1 (A) or recombinant histidine tagged RBD (B) (Sino Biological) using surface plasmon resonance spectroscopy in multi-cycle mode with concentrations ranging from 25-400 nM (S1-His) or 1.562-50 nM (RBD-His). Binding kinetics were calculated using a global kinetic fit to a 1:1 Langmuir model. Binding parameters are given in (C). Actual binding data (black) and the best fit of the data to a 1:1 binding model (green). One point in the graphs stands for one mouse. Group size n=8. Mean ± SEM is shown by horizontal bars with whiskers for each group.

In pVNT analysis, dose-dependent increases in neutralizing antibodies were observed (Figure 2.6.2-10).

**Figure 2.6.2-10. BNT162b2 Pseudovirus Neutralizing Titers 14, 21, and 28 Days After Immunization**



BALB/c mice were immunized IM once with 0.2, 1 and 5 µg BNT162b2 or buffer. On 14, 21, and 28 days after immunization, animals were bled. The sera were tested for SARS-CoV-2 pseudovirus neutralization. Graphs depict pVNT<sub>50</sub> serum dilutions (50% reduction of infectious events, compared to positive controls without serum). One point in the graphs stands for one mouse. Every mouse sample was measured in duplicate. Group size n=8. Mean ± SEM is shown by horizontal bars with whiskers for each group. LLOQ, lower limit of quantification. ULOQ, upper limit of quantification.

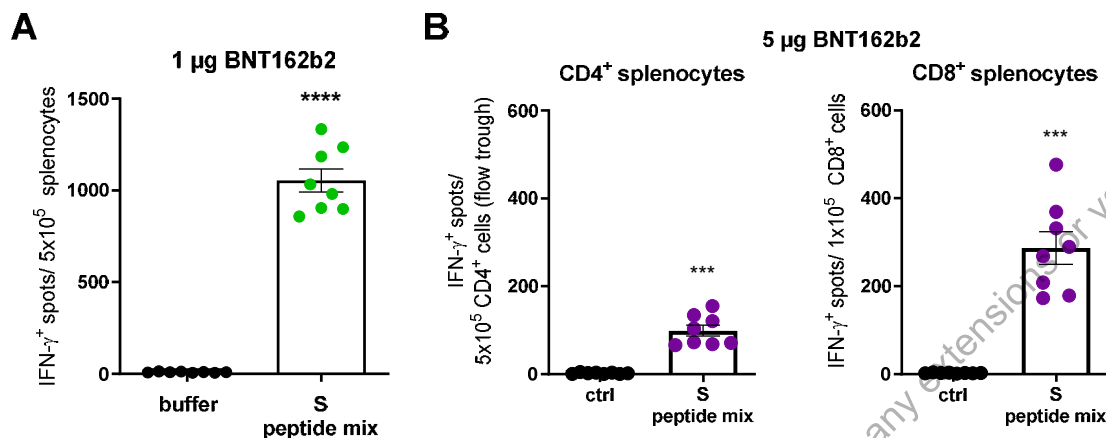
The summary of antibody titers on Day 28 is as follows:

**Table 2.6.2-1. Summary of IgG Concentrations at Day 28 Post Immunization**

	BNT162b2 0.2 µg	BNT162b2 1 µg	BNT162b2 5 µg
Anti S1 total IgG [µg/mL]	73.0 ± 10.4	205.9 ± 21.0	392.7 ± 28.9
Anti RBD total IgG [µg/mL]	83.1 ± 12.3	241.7 ± 17.2	448.6 ± 28.6
pVN <sub>50</sub> titer [reciprocal dilution]	33.0 ± 9.8	192.0 ± 31.4	312.0 ± 35.1

In addition, the cellular immune response was analyzed. At Day 28 after one immunization, spleens were collected and splenocytes tested for IFN $\gamma$  release after antigen stimulation by ELISpot. Stimulation of fresh splenocytes with an S-specific overlapping peptide pool induced IFN $\gamma$  responses in T cells of immunized animals. Splenocytes of the groups immunized with BNT162b2 had significantly higher spot numbers than splenocytes from the groups that received buffer control (Figure 2.6.2-11). To identify the T cell subtype, an additional ELISpot analysis was performed after separation of fresh CD4+ and CD8+ T cells by MACS isolation from splenocytes obtained from the group immunized with 5 µg BNT162b2. Both CD4+ and CD8+ T cells displayed IFN $\gamma$  responses.

**Figure 2.6.2-11. ELISpot Analysis Using Splenocytes Obtained on Day 28 After One Immunization**

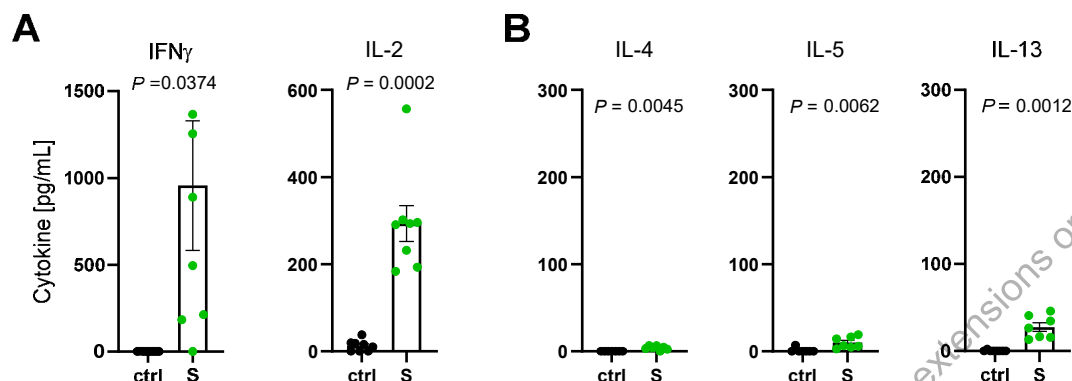


ELISpot assay was performed using (A) bulk splenocytes isolated on Day 28 after IM immunization of mice with 1  $\mu$ g BNT162b2 or (B) CD4<sup>+</sup> and CD8<sup>+</sup> T cells after magnetic cell separation from the 5  $\mu$ g BNT162b2 immunized group. Splenocytes were stimulated with S-specific overlapping peptide pools, buffer or an irrelevant control peptide (ctrl), and IFN- $\gamma$  secretion was measured to assess S-specific T cell number. Individual spot counts are shown by dots; group mean values are indicated by bars ( $\pm$ SEM). P-values were determined by one-way ANOVA analysis followed by Dunnett's multiple comparisons test. \*\*\* p < 0.001, \*\*\*\* p < 0.0001.

Furthermore, cytokine release data from the S-peptide mix stimulated splenocytes was acquired 28 days after immunization with 5  $\mu$ g BNT162b2. High levels of the Th1 cytokines IFN $\gamma$  and IL-2 but minute amounts of the Th2 cytokines IL-4, IL-5 and IL-13 in multiplex immunoassays were detected (Figure 2.6.2-12).



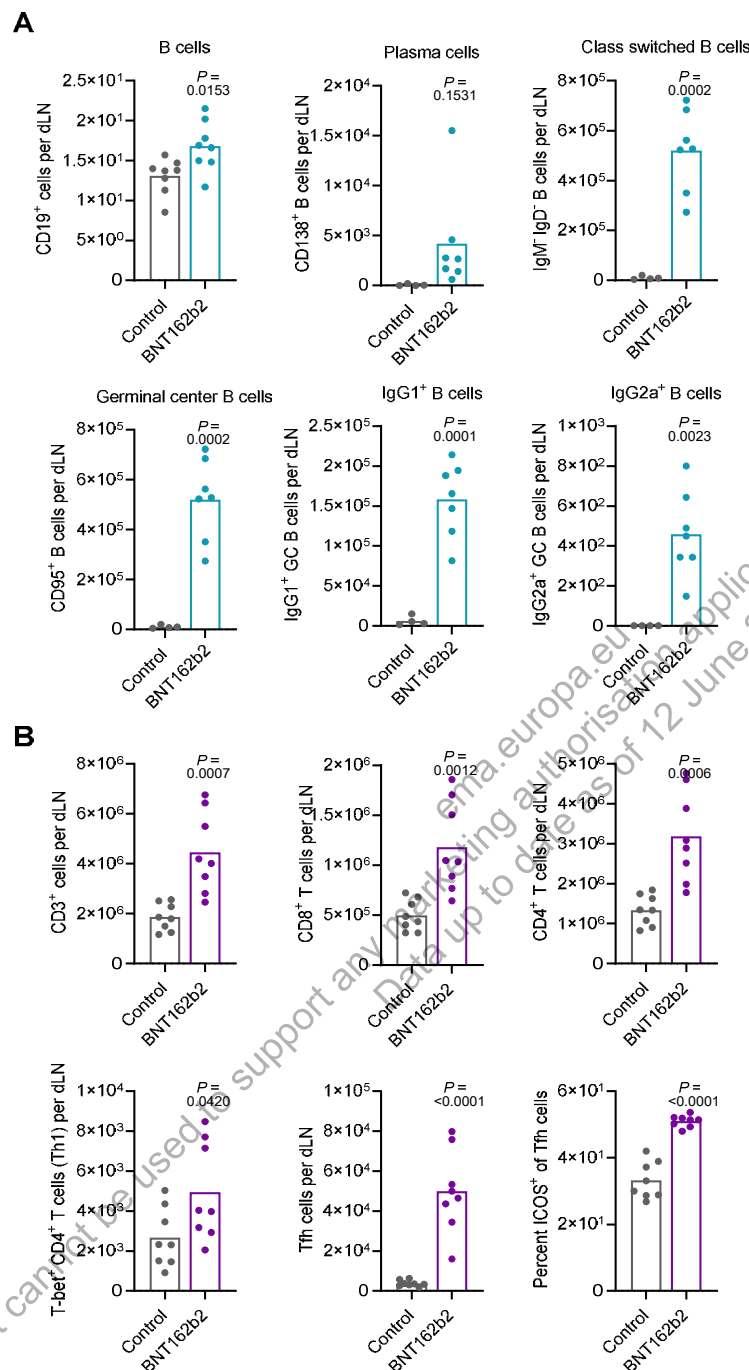
**Figure 2.6.2-12. Cytokine Release Analysis Using Splenocytes Obtained on Day 28 After One Immunization**



Splenocytes of BALB/c mice immunized IM with 1  $\mu$ g BNT162b2 were stimulated ex vivo with full-length S peptide mix and cytokine multiplex analysis of supernatants was performed (n=8 per group). Splenocytes of buffer treated mice served as control. Cytokine production was determined by bead-based multiplex analysis (n=8 per group, n=7 for IL-4, IL-5 and IL-13 as one outlier was removed via routs test [Q=1%] for the S peptide stimulated samples). Individual dots indicate results from one animal; group mean values are indicated by bars. P-values were determined by a two-tailed paired t-test.

To dissect the cellular response after BNT162b2 immunization in more detail, mice were immunized with 5  $\mu$ g BNT162b2 and 12 days after immunization draining lymph nodes (dLNs) were collected to perform B cell and T cell phenotyping analysis by flow cytometry (Figure 2.6.2-13). Much higher numbers of B cells (including plasma cells, class switched IgG1- and IgG2a-positive B cells, and germinal center B cells) were observed in the samples from mice that received BNT162b2 compared to controls. In addition, dLNs from BNT162b2-immunized mice also displayed an elevation in T cell counts, particularly numbers of T follicular helper (Tfh) cells, including subsets with ICOS upregulation, which is known to play an essential role in the formation of germinal centers (Hutloff, 2015).

**Figure 2.6.2-13. B and T Cell Phenotyping in Lymph Nodes of BNT162b2 Immunized Mice**



Mice (n=8 per group) were immunized with 5 µg BNT162b2 or buffer (Control). (A) B cell and (B) T cell numbers 12 days after immunization in the subsets indicated by the y-axis labels were analysed in draining lymph nodes by flow cytometry. P-values were determined by an unpaired two-tailed t-test. The percentage of ICOS<sup>+</sup> cells among T follicular helper cells (Tfh) in draining lymph nodes (dLNs) is depicted on the lower right.

In summary, BNT162b2 induced a strong antibody response, with high total IgG, high binding affinity to S1 and the RBD, and high pVNT titers. Both CD4+ and CD8+ T cell responses were detectable 12 and 28 days after one immunization with an overall significant increase in T cell reactivity compared to control animals. Taking the phenotyping of B and T cells in aggregate, the data indicates a strong and concurrent induction of SARS-CoV-2-specific neutralizing antibody titers and a Th1-driven T cell response by BNT162b2.

#### **2.6.2.6. Immunogenicity of BNT162b2 Monovalent Omicron BA.4/BA.5 and BNT162b2 Bivalent Original and Omicron BA.4/BA.5 in Mice**

The immunogenicity of BNT162b2 monovalent Omicron BA.4/BA.5 and bivalent BNT162b2 Original and Omicron BA.4/BA.5 in mice was investigated ([VR-VTR-10976](#)).

This study was designed to evaluate immunogenicity of monovalent or bivalent Omicron BA.4/BA.5 vaccine as either a two-dose primary series or as a third dose booster in BNT162b2-experienced mice. Five groups of 10 female BALB/c mice each were immunized and serum collected according to the schedule outlined in [Figure 2.6.2-2](#).

Table 2.6.2-2. Study Design

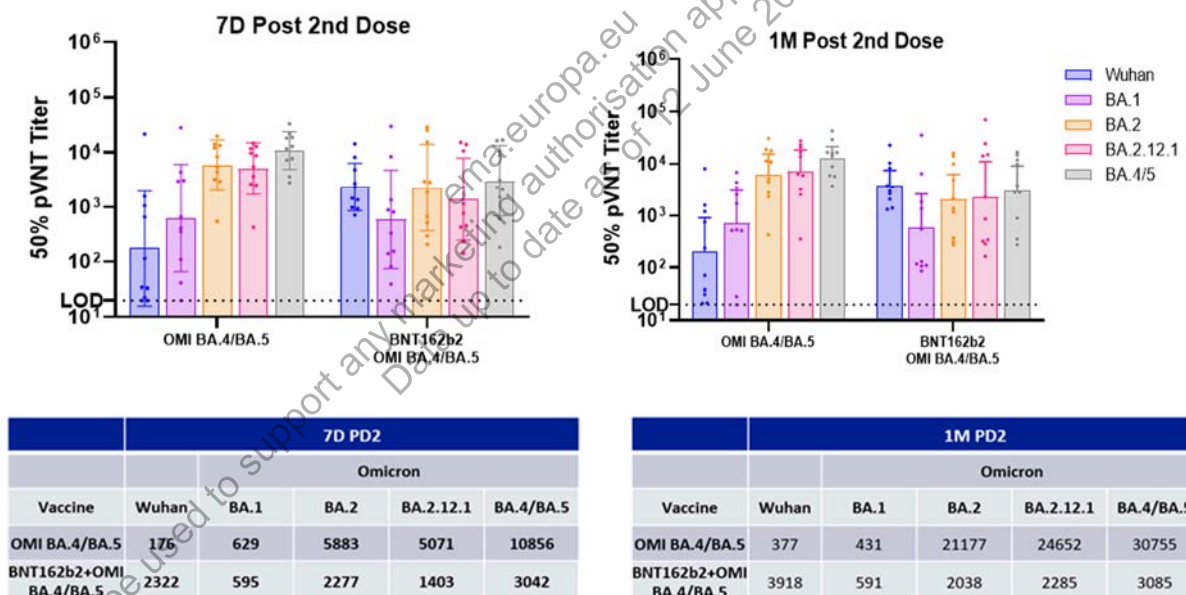
	Group #	N	Vaccination (Day 0) (µg)	Vaccination (Day 21) (µg)	Vaccination (Day 49) (µg)	Vaccination (Day 70) (µg)	Vaccination (Day of Study)	Bleed (Day of Study)	Tissue Harvest on Day 77 (n=5)
Neg Control	1	5 / 5	X	X	Saline	Saline	49, 70	77 (7DPD2) <sup>a</sup> 98 (1MPD2)	Spleen and LN
Two dose primary series cohort	2	10	X	X	Omicron BA.4/BA.5 P2 (0.5 µg)	Omicron BA.4/BA.5 P2 (0.5 µg)	49, 70	77 (7DPD2) 98 (1MPD2)	N/A
	3	10	X	X	BNT162b2 + Omicron BA.4/BA.5 P2 (0.25 µg + 0.25 µg)	BNT162b2 + Omicron BA.4/BA.5 P2 (0.25 µg + 0.25 µg)	49, 70	77 (7DPD2) 98 (1MPD2)	N/A
(BNT162b2 experienced) third dose booster cohort	4	10	BNT162b2 (0.5)	BNT162b2 (0.5)	Omicron BA.4/BA.5 P2 (0.5 µg)	X	0, 21, 49	49 (1MPD2) 56 (7DPD3) 77 (1MPD3) <sup>a</sup>	Spleen and LN
	5	10	BNT162b2 (0.5)	BNT162b2 (0.5)	BNT162b2 + Omicron BA.4/BA.5 P2 (0.25 µg + 0.25 µg)	X	0, 21, 49	49 (1MPD2) 56 (7DPD3) 77 (1MPD3) <sup>a</sup>	Spleen and LN

a. Tissue harvest performed, spleens and lymph nodes collected.

Blood was collected on Days 49, 56, 77, 98 and spleen and lymph nodes were harvested on Day 77 after immunization to analyze the antibody response by pVNT and the B cell and T cell response by flow cytometry, using methods described in [Section 2.6.2.5](#).

Intramuscular immunization of naïve BALB/c mice with BNT162b2 LNP-formulated modRNA vaccines encoding the SARS-COV-2 spike antigens induced robust neutralizing antibody responses as measured by pVNT. In naïve mice that were immunized with a two-dose primary series (Figure 2.6.2-14), monovalent Omicron BA.4/BA.5 elicited high neutralizing titers against Omicron pseudovirus strains BA.2, BA.2.12.1, and BA.4/BA.5 after two doses, but with reduced neutralizing activities against Wuhan, and BA.1 strains. Bivalent vaccines (combinations of BNT162b2 and BNT162b2 Omicron BA.4/BA.5) elicited a greater breadth of neutralizing antibody responses against all strains, but neutralizing activity against Omicron BA.1 was still 2- to 5-fold lower than that against other strains tested. This finding may be explained by the fact that Omicron BA.4/BA.5 is a sublineage that is derived from Omicron BA.2 sublineage, which has significant genetic divergence from BA.1.

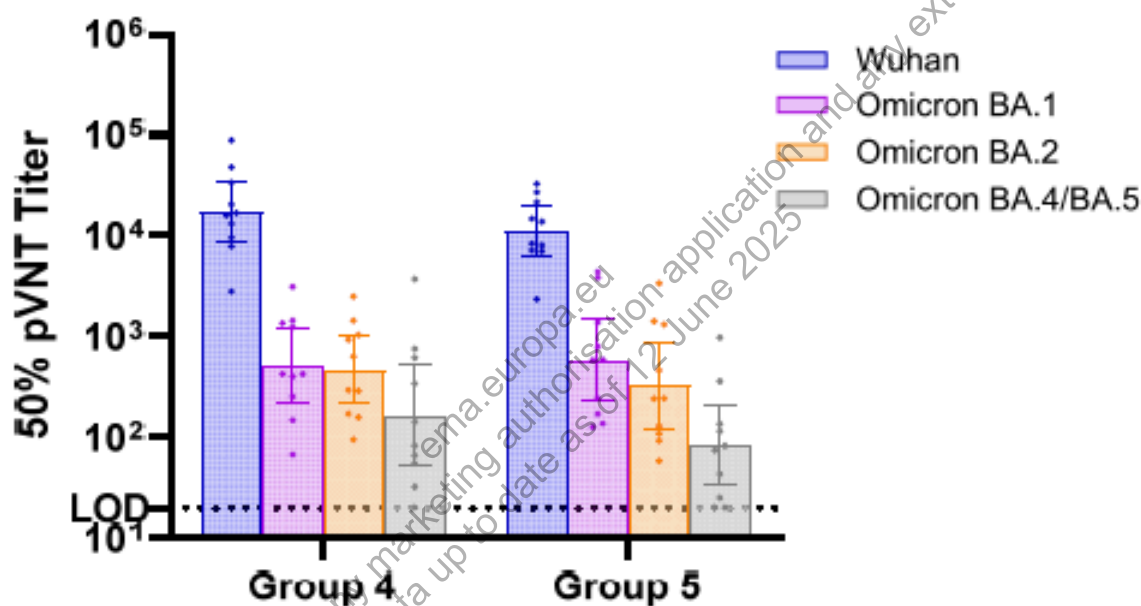
**Figure 2.6.2-14. Functional Neutralizing Antibodies Elicited by Immunization of Naïve Mice With 2-Doses of Variant-Modified Vaccines**



Ten BALB/c mice per group were immunized IM on Days 0 and 21 with 0.5 µg of either monovalent BNT162B2 Omicron BA.4/BA.5 or bivalent (1:1 mixture of BNT162b2 and BNT162b2 Omicron BA.4/BA.5). Neutralizing antibody responses against the Wuhan reference strain (blue) and Omicron BA.1 (purple), BA.2 (orange), BA.2.12.1 (pink), and BA.4/BA.5 (grey) variants of concern were measured by pseudovirus neutralization assay at 1 week and 1 month post second dose.

Initial immunization in a 2-dose primary series of BNT162b2 at a 0.5 µg dose level to establish the cohort of BNT162b2-experienced mice (Groups 4 and 5 from Table 2.6.2-2) showed a high neutralizing antibody response against the Wuhan strain and substantially lower neutralizing titers against Omicron BA.1, BA.2, and BA.4/BA.5 (Figure 2.6.2-15). Consistent with prior studies, BA.4/BA.5 titers were the lowest of the Omicron sublineages tested. Overall, the responses were similar across Group 4 (monovalent booster group) and Group 5 (bivalent booster group), with slightly lower Omicron BA.2 and BA.4/BA.5 titers observed in Group 5.

**Figure 2.6.2-15. Functional Neutralizing Antibody Responses Elicited by Immunization of Naïve Mice With 2 Doses of BNT162b2 (Groups 4 and 5)**



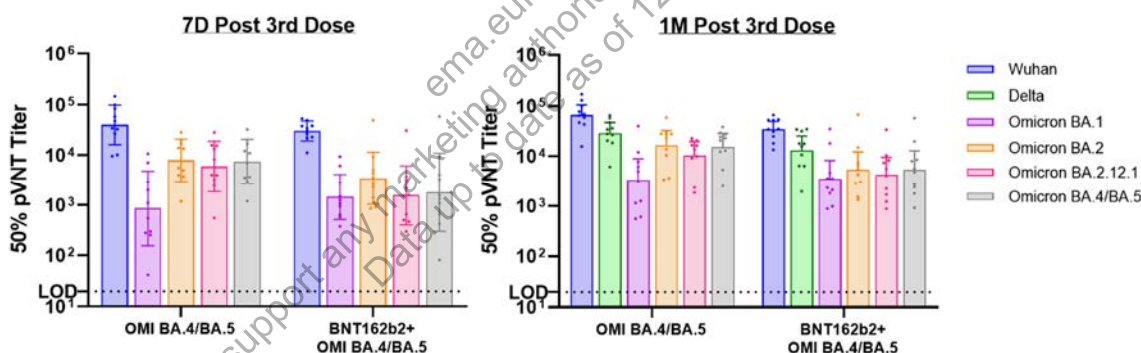
Vaccine	Wuhan	Omicron		
		BA.1	BA.2	BA.4/BA.5
BNT162b2 (Grp 4)	17110	516	465	166
BNT162b2 (Grp 5)	11187	582	324	82

Two groups of 10 female BALB/c mice were immunized IM on Days 0 and 21 with 0.5 µg of BNT162b2. Neutralizing antibody responses against pseudovirus of Wuhan reference strain (blue) and Omicron BA.1 (purple), BA.2 (orange), and BA.4/BA.5 (grey) variants of concern were measured by pseudovirus neutralization assay at 1 month post second dose.

IM immunization of BNT162b2-experienced BALB/c mice with a 0.5 µg dose level of LNP-formulated BA.4/BA.5 variant-modified vaccines as a third dose booster increased neutralizing antibody responses against the Wuhan reference strain, Delta, and Omicron BA.1, BA.2, BA.2.12.1, and BA.4/BA.5 (Figure 2.6.2-16). In the monovalent group, Wuhan, Omicron BA.1, BA.2 and BA.4/BA.5 neutralizing titers increased by 2, 2, 17, and 45-fold, respectively, at 7 days post booster compared to 1 month post BNT162b2 Dose 2. At 1 month post-third dose boost, the difference, as compared to 1 month post BNT162b2 Dose 2, was 4, 7, 36, and 94-fold for Wuhan, Omicron BA.1, BA.2 and BA.4/BA.5, respectively.

In the bivalent group, Wuhan, Omicron BA.1, BA.2, and BA.4/BA.5 neutralizing titers increased by 3, 3, 11, and 22-fold, respectively, 7 days post booster compared to 1 month post BNT162b2 Dose 2 and 3, 6, 17, and 66-fold, respectively, 1 month post booster compared to 1 month post BNT162b2 Dose 2. A broad response against Omicron sublineages was achieved with both monovalent (BNT162b2 BA.4/BA.5) and bivalent (BNT162b2 + BNT162b2 BA.4/BA.5) formulations. The monovalent BA.4/BA.5 formulation elicited slightly higher Omicron neutralizing titers compared to the bivalent BA.4/BA.5 formulation.

**Figure 2.6.2-16. Neutralizing Antibodies Elicited by Immunization of BNT162b2 Experienced Mice With Omicron BA.4/BA.5 Variant Modified Monovalent and Bivalent modRNA Vaccines as a Third Dose Booster**



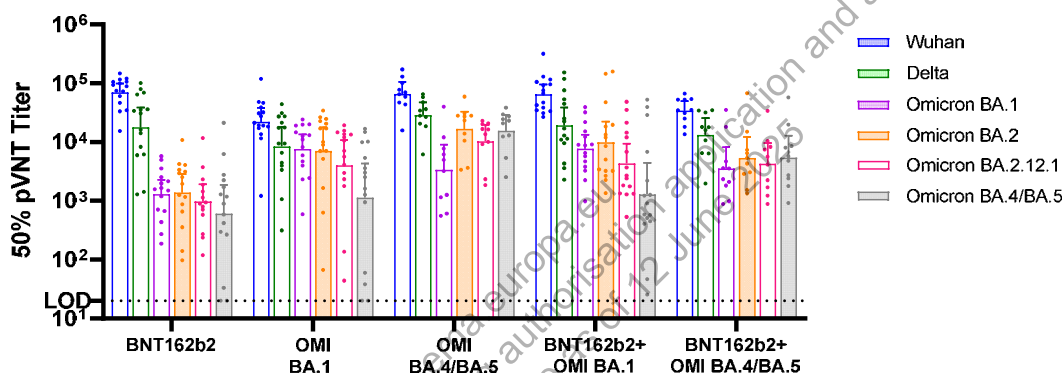
	7DPD3					1MPD3					
Vaccine	Wuhan	Omicron				Wuhan	Delta	Omicron			
		BA.1	BA.2	BA.2.12.1	BA.4/BA.5			BA.1	BA.2	BA.2.12.1	BA.4/BA.5
OMI BA.4/BA.5	40174	865	7884	5944	7454	65839	28865	3366	16677	10385	15522
BNT162b2+ OMI BA.4/BA.5	30316	1459	3478	1573	1813	34457	13291	3537	5391	4294	5446

Ten BALB/c mice per group were immunized IM on Days 0 and 21 with 0.5 µg of BNT162b2; one month following dose 2, mice were boosted with an additional dose of either monovalent vaccine BNT162b2 BA.4/BA.5 (0.5 µg) or bivalent vaccine BNT162b2 + BNT162b2 BA.4/BA.5 (0.25 µg of each). Neutralizing antibody responses against the Wuhan reference strain (blue) and Omicron BA.1 (purple), BA.2 (orange), BA.2.12.1 (pink), and BA.4/BA.5 (grey) variants of concern were measured by pseudovirus neutralization assay at 1 week post third dose and at 1 month post third dose with the addition of the Delta variant (green).



To compare immune responses elicited by Omicron BA.1 and Omicron BA.4/BA.5 variant-modified vaccine candidates, 1 month post third dose mouse sera from prior mouse immunogenicity study (VR-VTR-10944) were tested concurrently with 1 month post third dose sera from the present study in the same pseudovirus neutralization assay runs (Figure 2.6.2-17). BALB/c mice from both studies were of a similar age range, were vaccinated and boosted following the same dosing interval, and at the same dose level. The BA.4/BA.5 variant modified formulations elicited higher neutralizing titers against Omicron BA.4/BA.5 and a broader immune response across Omicron sublineages compared to the Omicron BA.1 variant-modified vaccine candidates and the prototype vaccine.

**Figure 2.6.2-17. Neutralizing Antibodies Elicited by Immunization of BNT162b2 Experienced Mice With Omicron BA.1 and BA.4/BA.5 Variant Modified Monovalent and Bivalent modRNA Vaccines as a Third Dose Booster**

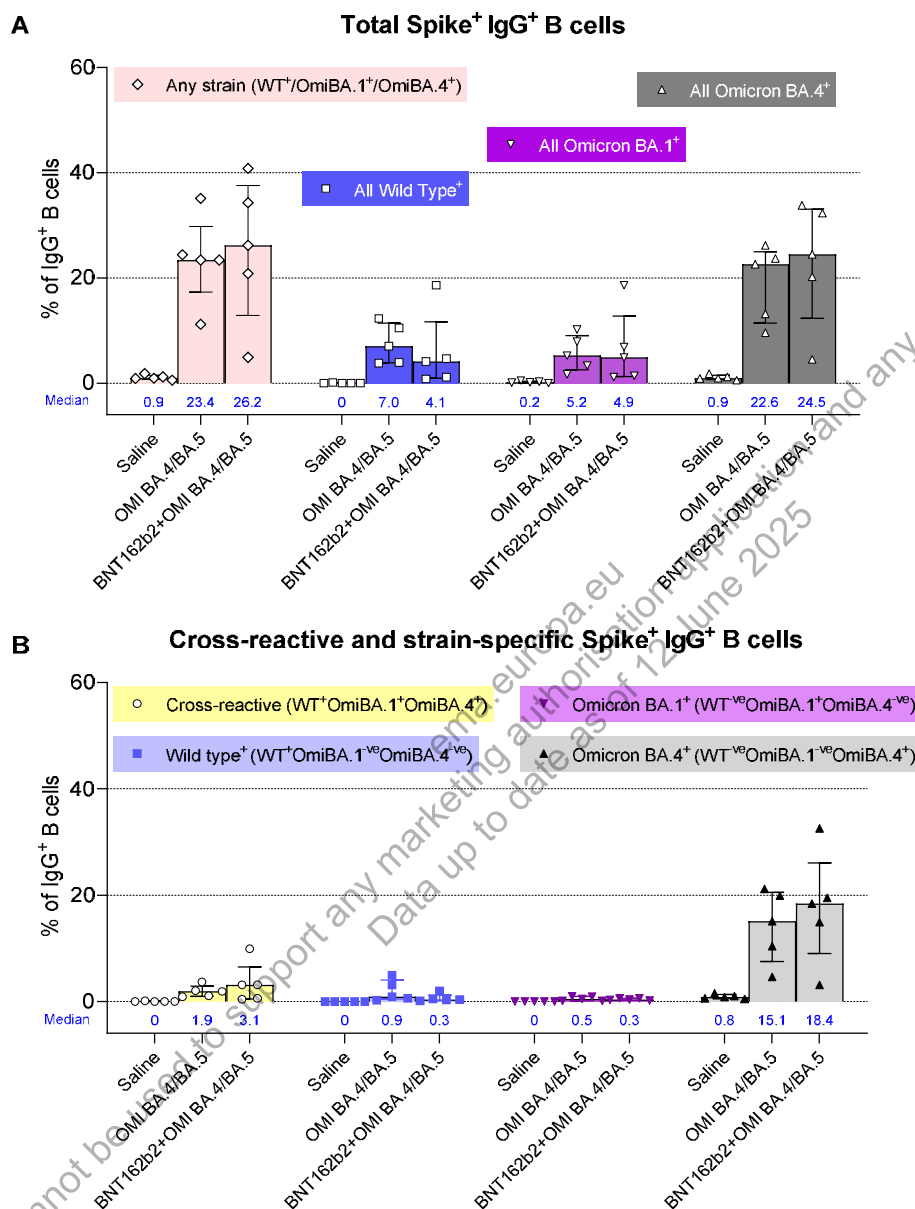


Vaccine	Wuhan	Delta	Omicron			
			BA.1	BA.2	BA.2.12.1	BA.4/BA.5
BNT162b2	70546	17911	1308	1378	973	603
OMI BA.1	21998	8454	7575	7030	4049	1136
OMI BA.4/5	65839	28865	3366	16677	10385	15522
BNT162b2 + OMI BA.1	65389	19206	7652	9855	4380	1294
BNT162b2 + OMI BA.4/BA.5	34457	13291	3537	5391	4294	5446

BALB/c mice were immunized IM on Days 0 and 21 with 0.5 µg of BNT162b2; one month following dose 2, mice were boosted with an additional dose of either monovalent Omicron modified vaccine (0.5 µg) or bivalent vaccine (0.25 µg of each; 0.5 µg total) or BNT162b2 prototype vaccine. Omicron BA.1 variant-modified vaccines and BNT162b2 prototype were administered in PRL-COVID-Ms-2022-01 (15 mice per group) and BA.4/BA.5 variant-modified vaccines were administered in PRL-COVID-Ms-2022-06 (10 mice per group). All sera were tested concurrently in the same pseudovirus neutralization assay runs. Neutralizing antibody responses against the Wuhan reference strain (blue), Delta (green), Omicron BA.1 (purple), BA.2 (orange), BA.2.12.1 (pink), and BA.4/BA.5 (grey) variants were measured by pseudovirus neutralization assay at 1 month post third dose.

Spike-specific IgG<sup>+</sup> B cells in lymph nodes of BNT162b2-experienced mice at 1 month following administration of a third dose booster of either monovalent (BNT162b2 BA.4/BA.5) or bivalent BA.4/BA.5 (BNT162b2 + BNT162b2 BA.4/BA.5) vaccines were measured by flow cytometry using fluorochrome-coupled spike trimer proteins for Wuhan/wild type (WT) reference, Omicron BA.1 (purple) and Omicron BA.4/BA.5 (grey) (Figure 2.6.2-18). In BNT162b2-experienced mice, both monovalent and bivalent vaccines administered as a third dose booster elicited a high frequency of total spike-specific B cells (any strain) (A), with the greatest proportion of the response accounted by Omicron BA.4/BA.5-antigen specific B cells (A). The third dose booster induced low levels of cross reactive Spike<sup>+</sup> B cells that could bind all three strains, WT, Omicron BA.1 and Omicron BA.4/BA.5, with slightly more cross-reactive B cells observed with the bivalent BNT162b2 + Omicron BA.4/BA.5 vaccine compared to the monovalent Omicron BA.4/BA.5 vaccine (B). Both monovalent Omicron BA.4/BA.5 and bivalent BNT162b2 + Omicron BA.4/BA.5 vaccines induced predominantly Omicron BA.4-specific Spike<sup>+</sup> B cells compared to a low frequency of WT or Omicron BA.1-specific Spike<sup>+</sup> B cells (B).

**Figure 2.6.2-18. Spike-Specific B Cell Response in Lymph Nodes Following Immunization of BNT162b2-Experienced Mice With Omicron BA.4/BA.5 Variant Modified Monovalent and Bivalent modRNA Vaccines as a Third Dose Booster**

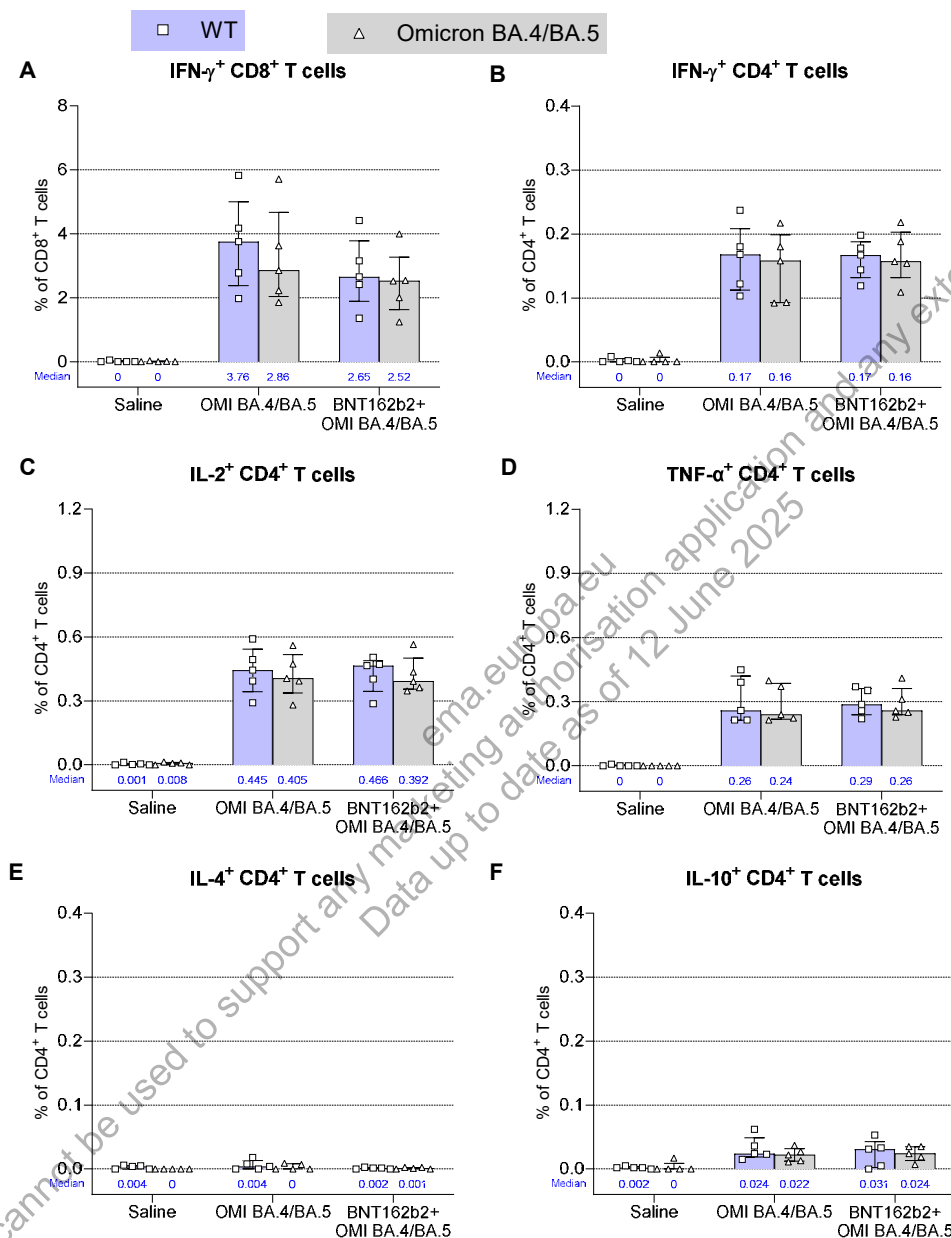


Ten BALB/c mice per group were immunized IM on Days 0 and 21 with 0.5 µg of BNT162b2; one month following dose 2, mice were boosted with an additional dose of either monovalent vaccine BNT162b2 BA.4/BA.5 (0.5 µg) or bivalent vaccine BNT162b2 + BNT162b2 BA.4/BA.5 (0.25 µg of each). Spike<sup>+</sup> IgG<sup>+</sup> B cells in lymph nodes (n=5) at 1 month post dose 3 following immunization were measured by flow cytometry using fluorochrome-coupled spike trimer proteins. Results are expressed as frequency of IgG<sup>+</sup> B cells. Spike<sup>+</sup> IgG<sup>+</sup> B cells to Wuhan/wild type (WT) reference in blue, Omicron BA.1 in Purple and Omicron BA.4 in grey, any of 3 strains in pink and all 3 strains cross-reactive cells in yellow. (A) Total spike<sup>+</sup> B cell response to all three strains and individual strains and (B) Cross-reactive and strain-specific spike<sup>+</sup> B cell response. Each symbol represents an individual animal; bars depict median frequency with interquartile range.

SARS-CoV-2 spike-specific T cell responses were measured in splenocytes at different timepoints following immunization by ICS assay using flow cytometry (Figure 2.6.2-19). To measure if variant specific mutations have an impact on the overall T cell response, peptide pools representing the spike protein from either the wild type (WT) virus or the Omicron BA.4/BA.5 variant were used.

In BNT162b2-experienced mice, both monovalent (BNT162b2 BA.4/BA.5) or bivalent (BNT162b2 + BNT162b2 BA.4/BA.5) vaccines administered as a third dose booster elicited a high frequency of spike-specific T cells, both CD8+ and CD4+ T cells. The frequency of IFN- $\gamma$  producing CD8+ T cells was higher than CD4+ T cells (Figure 2.6.2-19). The frequency of IL-2- and TNF- $\alpha$ -producing CD4+ T cells was slightly higher than the frequency of CD4+ T cells producing IFN- $\gamma$  (Panel B, C, D). There was a high frequency of IFN- $\gamma$ -expressing CD4+ T cells and very low levels of IL-4 or IL-10 expressing CD4+ T cells (Panel B, E and F), suggesting a Th1-biased T cell response, consistent with prior preclinical data for BNT162b2 (VR-VTR-10944 and Vogel et al, 2021). The magnitude of spike-specific T cell responses induced by both monovalent and bivalent vaccines was similar. Notably, the magnitude of the T cell response did not change based on the peptide pool (WT versus Omicron BA.4/BA.5), confirming that the variant-specific mutations have minimal impact on the polyclonal T cell response.

**Figure 2.6.2-19. Spike-Specific T Cell Response in Spleens Following Immunization of BNT162b2-Experienced Mice With Omicron BA.4/BA.5 Variant Modified Monovalent and Bivalent modRNA Vaccines as a Third Dose Booster**



Ten BALB/c mice per group were immunized IM on Days 0 and 21 with 0.5  $\mu$ g of BNT162b2; one month following dose 2, mice were boosted with an additional dose of either monovalent vaccine BNT162b2 BA.4/BA.5 (0.5  $\mu$ g) or bivalent vaccine BNT162b2 + BNT162b2 BA.4/BA.5 (0.25  $\mu$ g of each). Spike-specific T cells in spleens (n=5) at 1 month post dose 3 following immunization were measured by intracellular cytokine staining assay. All samples were stimulated separately with peptide pools for spike from Wuhan/WT (WT) reference in blue, and Omicron BA.4/BA.5 in Grey. Graphs show CD4<sup>+</sup> and CD8<sup>+</sup> T cells expressing different cytokines. Each symbol represents an individual animal; bars depict median frequency with interquartile range.

In summary, in naïve mice, two doses of the monovalent BA.4/BA.5 variant-modified vaccine elicited strong neutralizing antibody responses against Omicron BA.2, BA.2.12.1, and BA.4/BA.5 strains but reduced neutralizing activity against Wuhan and BA.1. The bivalent formulation induced a broader immune response against all strains tested. In BNT162b2 experienced mice, BA.4/BA.5 variant-modified vaccines induced robust and broad neutralizing antibody responses against the Wuhan reference strain and Omicron BA.1, BA.2, BA.2.12, and BA.4/BA.5 sublineages as well as a strong spike-specific B cell and T cell response when administered as a third dose booster. In comparison, reduced Omicron neutralizing antibody responses, in particular BA.4/BA.5, were generated following a third dose booster in mice ([VR-VTR-10944](#)). Both monovalent (BNT162b2 BA.4/BA.5) and bivalent (BNT162b2 + BNT162b2 BA.4/BA.5) vaccines administered as a third dose booster elicited an Omicron BA.4/BA.5-specific B cell response, with low levels of cross-reactive spike+ B cells. T cell responses were of a similar magnitude for WT and Omicron BA.4/BA.5 supporting that the polyclonal T cell response was not affected by Omicron BA.4/BA.5 variant-specific mutations.

#### **2.6.2.7. Immunogenicity of BNT162b2 Monovalent XBB.1.5 and Bivalent Omicron XBB.1.5 and Omicron BA.4/BA.5 in Mice**

The immunogenicity of BNT162b2 monovalent XBB.1.5 and bivalent XBB.1.5 + BA.4/BA.5, was evaluated as either a fourth dose booster in BNT162b2-experienced mice ([VR-VTR-11123](#)) or as a two-dose primary series in naïve mice ([VR-VTR-11122](#)). The bivalent BNT162b2 (WT + BA.4/BA.5) vaccine was used as a benchmark.

##### **2.6.2.7.1. Vaccine-Experienced Study**

BALB/c mice (10/group) were immunized with Original WT BNT162b2 vaccine (0.5 µg) at Day 0 and Day 21 and administered a third dose boost with bivalent BNT162b2 vaccine (WT (0.25 µg) + BA.4/BA.5(0.25 µg)) at Day 105 to establish the cohort of BNT162b2-experienced mice. A fourth dose booster was administered at Day 134 (1 month post dose 3) and sera were collected at Day 134 (pre boost) and Day 160 (1 month post boost) to measure neutralizing antibody responses. Spleens were collected on Day 160 to evaluate cell-mediated immune responses ([Table 2.6.2-3](#)).

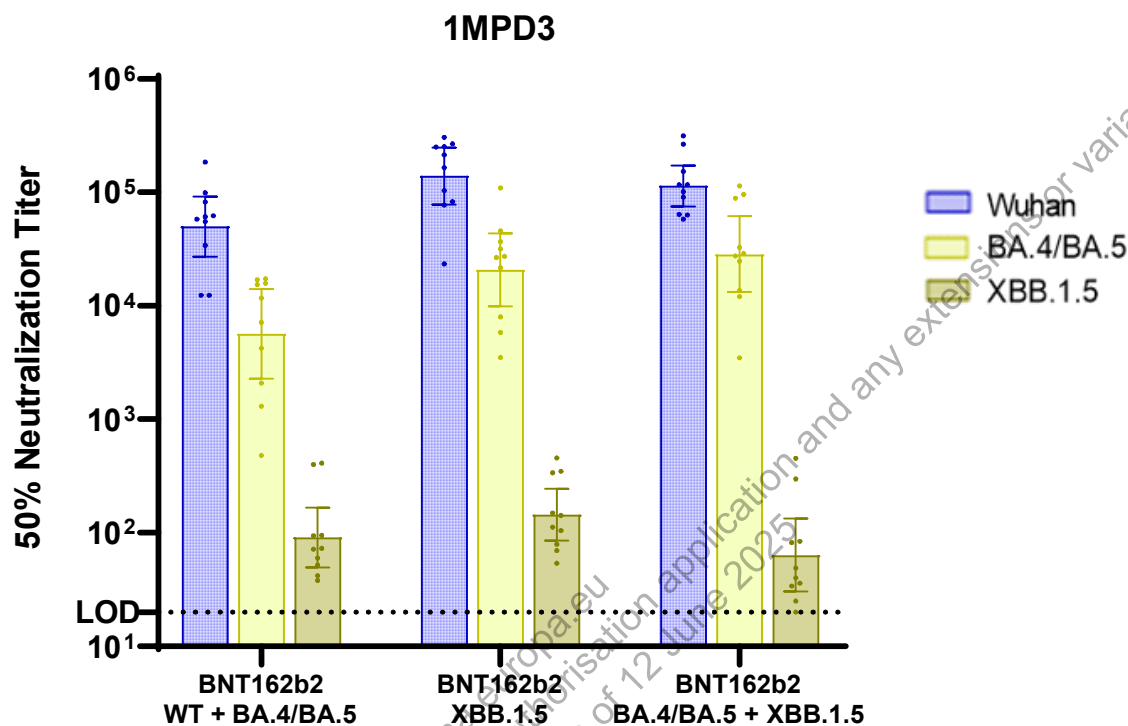
**Table 2.6.2-3. Omicron XBB.1.5 Sublineage Booster Vaccine Mouse Immunogenicity Study Design**

Group	Mice N/group	Vaccination #1 (Day 0)	Vaccination #2 (Day 21)	Vaccination #3 (Day 105)	Vaccination #4 (Day 134)	Tissue Harvest at D160 (n=5)
1	10	N/A	N/A	Saline	Saline	Spleen
2		BNT162b2 WT (0.5 µg)	BNT162b2 WT (0.5 µg)	BNT162b2 WT (0.25 µg)  +  BNT162b2 BA.4/5 (0.25 µg)  (0.5 µg total)	BNT162b2 BA.4/5 (0.5 µg)	
3					BNT162b2 WT (0.25 µg) + BNT162b2 BA.4/5 (0.25 µg)  (0.5 µg total)	
4					BNT162b2 XBB.1.5 (0.5 µg)	
5					BNT162b2 BA.4/5 (0.25 µg) + BNT162b2 XBB.1.5 (0.25 µg)  (0.5 µg total)	

Prior to the fourth dose boost, all mice showed a robust neutralizing antibody response against the Wuhan reference strain, substantially lower neutralizing titers against Omicron BA.4/BA.5, and minimal response to other more antigenically distant Omicron sublineages (eg, XBB.1.5) (Figure 2.6.2-20). Overall, the responses were similar across groups, with slightly higher titers against Wuhan and Omicron BA.4/BA.5 in groups with vaccines containing XBB.1.5.



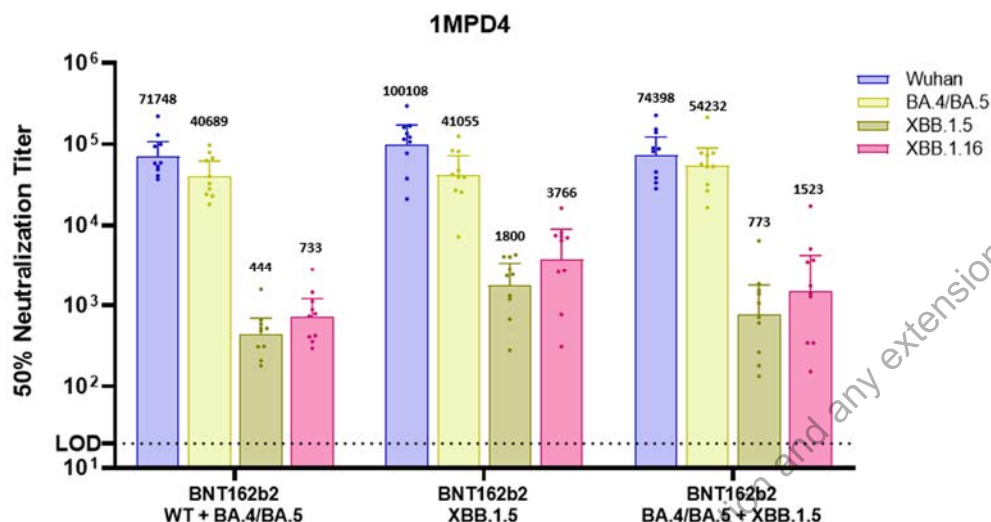
**Figure 2.6.2-20. Functional Neutralizing Antibodies Elicited by Immunization of Naïve Mice With 2 Doses of BNT162b2 and 1 Dose of Bivalent BNT162b2 (WT + BA.4/5) at 1 Month Post Dose 3**



Groups of 10 female BALB/c mice were immunized IM on Days 0 and 21 with 0.5 µg of BNT162b2 and on Day 105 with 0.5 µg of bivalent BNT162b2 (WT 0.25 µg + BA.4/BA.5 0.25 µg). Neutralizing antibody responses against pseudovirus of Wuhan reference strain (blue) and Omicron BA.4/BA.5 (yellow), and XBB.1.5 (tan) variants of concern were measured by pseudovirus neutralization assay at one month post third dose.

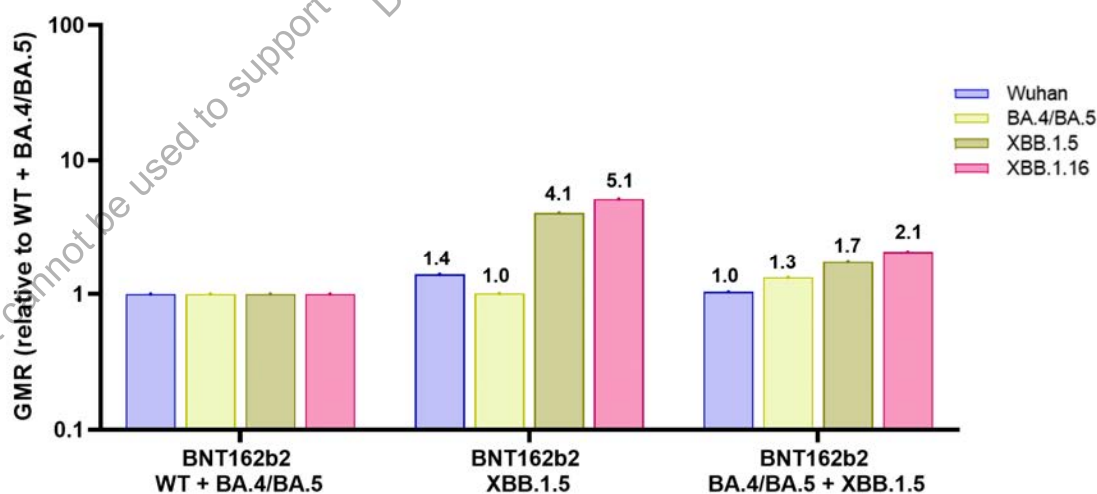
Intramuscular immunization of BNT162b2-experienced BALB/c mice with a 0.5 µg dose of monovalent or bivalent modRNA sublineage-adapted vaccines as a fourth dose booster increased neutralizing antibody responses against Omicron BA.4/BA.5, XBB.1.5 and XBB.1.16 (Figure 2.6.2-21). Higher geometric mean titers against XBB.1.5 and XBB.1.16 were elicited by the monovalent XBB.1.5 booster vaccine, approximately four-to-five-fold higher than those elicited by the bivalent WT + BA.4/BA.5 vaccine (Figure 2.6.2-22).

**Figure 2.6.2-21. Neutralizing Antibody Geometric Mean Titers (GMT) at 1 Month Post Dose 4 Elicited by XBB.1.5 Monovalent and Bivalent Vaccines as a Fourth Dose Booster**



Ten BALB/c mice per group were immunized IM on Days 0 and 21 with 0.5 µg of Original WT BNT162b2 vaccine and on Day 105 with 0.5 µg of bivalent BNT162b2 (WT 0.25 µg + BA.4/5 0.25 µg); one month following dose 3, mice were boosted with an additional dose of monovalent BNT162b2 BA.4/BA.5 (0.5 µg), bivalent BNT162b2 + BNT162b2 BA.4/BA.5 (0.25 µg of each), monovalent BNT162b2 XBB.1.5 (0.5 µg), bivalent BNT162b2 (BA.4/5 + XBB.1.5, 0.25 µg of each). Neutralizing antibody responses against the Wuhan reference strain and Omicron BA.4/BA.5 XBB.1.5 and XBB.1.16 sublineages were measures.

**Figure 2.6.2-22. Neutralizing Antibody Geometric Mean Ratios (GMR) at 1 Month Post Dose 4 Elicited by XBB.1.5 Monovalent and Bivalent Vaccines as a Fourth Dose Booster**



Note: The geometric mean ratio is defined as the geometric mean titer (GMT) of neutralization against a pseudovirus elicited the sublineage-adapted vaccine group divided by that elicited by the WT + BA.4/BA.5 vaccine.

#### 2.6.2.7.1.1. T Cell Response

SARS-CoV-2 spike-specific T cell responses were measured by ICS assay using flow cytometry in fresh splenocytes at 1 month following administration of a fourth dose (1 month post dose 4) of monovalent or bivalent modRNA vaccines encoding spike antigens of SARS-CoV-2 Omicron sublineages in mice that had received 2-dose primary series of BNT162b2 at a 0.5 µg dose level followed by a third dose booster with 0.5 µg of Bivalent BNT162b2 (original Wuhan 0.25 µg + BA.4/BA.5 0.25 µg). To assess if sublineage-specific mutations have an impact on the overall T cell response, peptide pools representing the spike protein from either the wild type (WT) virus or BA.4/BA.5 or XBB.1.5 sublineages were used.

High spike-specific CD4<sup>+</sup> and CD8<sup>+</sup> T cell responses were observed at 1 month post dose 4 after the fourth dose booster, with the frequency of IFN-γ producing CD8<sup>+</sup> T cells higher than IFN-γ producing CD4<sup>+</sup> T cells. The frequency of IL-2 producing CD4<sup>+</sup> T cells was slightly higher than the frequency of CD4<sup>+</sup> T cells producing IFN-γ. Very low levels of IL-4 expressing CD4<sup>+</sup> T cells were observed relative to the IFN-γ+CD4<sup>+</sup> T cell response, suggesting a Th1-biased T cell response, consistent with prior preclinical data for BNT162b2. The magnitude of the T cell response to each of the sublineages was similar across all the vaccine groups suggesting that polyclonal T cell responses in mice are not affected by mutations in the tested Omicron sublineages.

#### 2.6.2.7.2. Primary Series Study

This mouse study was performed to assess the immunogenicity and breadth of neutralization activity of LNP-formulated modRNA vaccine candidates encoding SARS-CoV-2 spike proteins of Omicron sublineage XBB.1.5 in naïve BALB/c mice as a 2-dose primary series. The vaccine candidates were evaluated as monovalent and bivalent formulations using bivalent BNT162b2 BA.4/5 (1:1 mixture of original Wuhan and Omicron BA.4/5 drug products) as a benchmark. SARS-CoV-2 pseudovirus neutralization tests (pVNT) were performed on serum collected at Day 49 (1 month post dose 2). XBB.1.5 sublineage-modified monovalent and bivalent (with Omicron BA.4/BA.5) vaccines induced higher immune response against the corresponding and genetically close related sublineages (XBB.1.5 and XBB.1.16). Compared to the bivalent BNT162b2 BA.4/5, the highest neutralizing antibody titers against XBB sublineages were observed in the monovalent BNT162b2 XBB.1.5 group. Additionally, monovalent and bivalent vaccine formulations containing WT, BA.4/5 and XBB.1.5 induced a robust CD4<sup>+</sup> and CD8<sup>+</sup> T cell response. Together these data suggest that XBB.1.5 and containing vaccine formulations enhance the breadth and quality of immune response and thus may provide improved protection against more distant current and future virus lineages and sublineages.

Groups containing 10 mice each were immunized with monovalent BNT162b2 (BA.4/5 or XBB.1.5) or bivalent BNT162b2 (1:1 mixture of two modRNA drug products) at Day 0 and 21. Sera were collected on Day 49 for assessment of neutralizing antibody responses on pseudovirus neutralization assay (pVNT). Spleens were collected to evaluate cell-mediated immune responses. (Table 2.6.2-4).

**Table 2.6.2-4. Omicron XBB.1.5 Sublineage Primary Series Vaccine Mouse Immunogenicity Study Design**

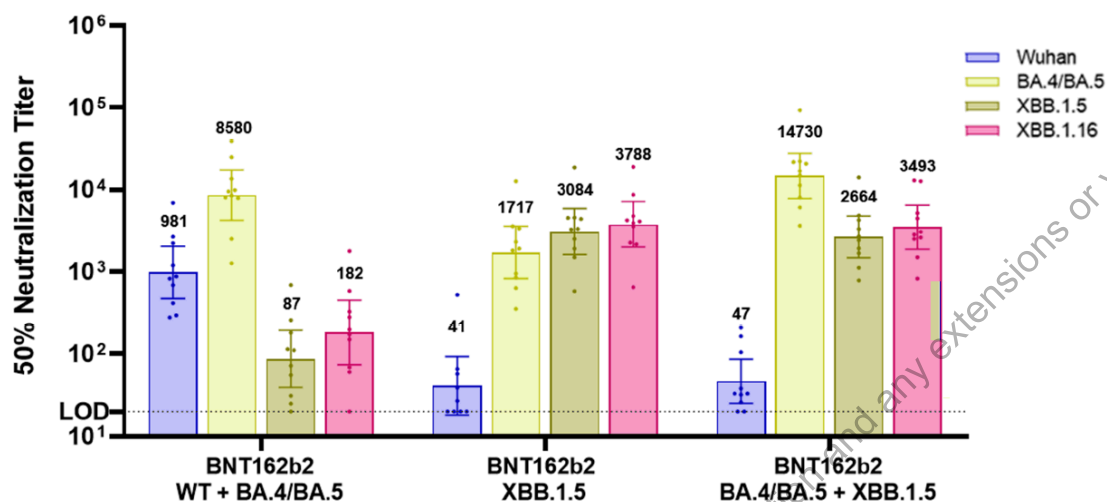
Group	Mice	Test Articles (Monovalent = 0.5 µg / Bivalent = 0.25 µg + 0.25 µg)	Vaccination (Day of Study)	Bleed (Day of Study)	Tissue Harvest (Day 49) (n=5)
1	10	Saline	0, 21	49	Spleen
2		BNT162b2 BA.4/5			
3		BNT162b2 WT + BNT162b2 BA.4/5			
4		BNT162b2 XBB.1.5			
5		BNT162b2 BA.4/5 + BNT162b2 XBB.1.5			

#### 2.6.2.7.2.1. Functional Antibody Response

Intramuscular immunization of naive BALB/c mice with two doses of 0.5 µg of LNP-formulated monovalent or bivalent modRNA vaccines encoding Omicron XBB.1.5 modified SARS-COV-2 spike antigen induced strong neutralizing antibody responses against matched or closely matched sublineages (Figure 2.6.2-23). Monovalent BNT162b2 XBB.1.5 stimulated high and comparable neutralizing antibody titers against XBB.1.5 and XBB.1.16 with slightly lower titers against BA.4/5, while neutralizing antibody response were much lower against the Wuhan strain. Bivalent formulation of 1:1 mixture of BNT162b2 XBB.1.5 and BNT162b2 BA.4/5 elicited a higher neutralizing response against BA.4/5 than the monovalent XBB.1.5 vaccine but lower against XBB.1.5 and XBB.1.16.

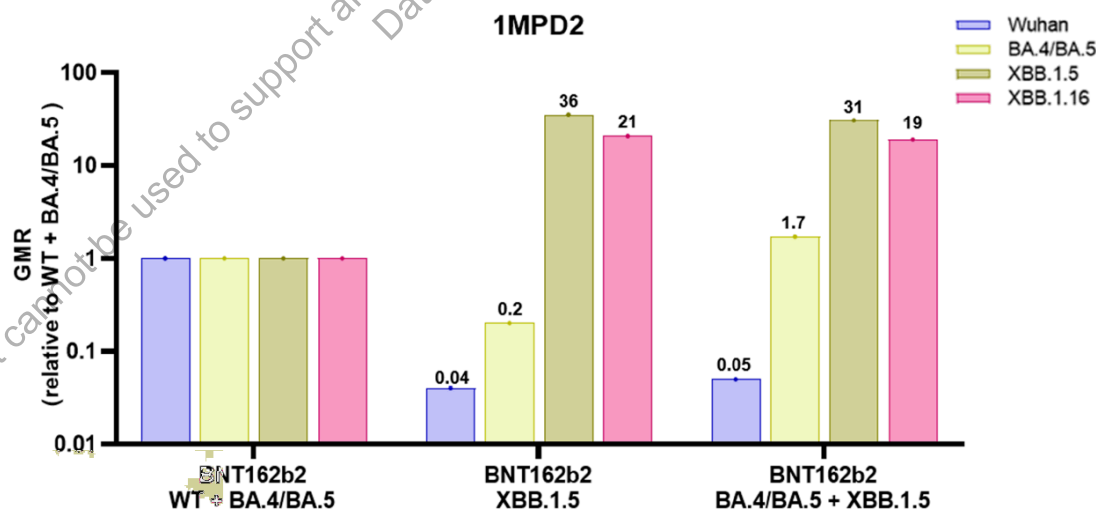
Compared to the bivalent BNT162b2 (WT + BA.4/5), a 36-fold higher neutralizing antibody response against the XBB.1.5 and XBB.1.16 pseudoviruses was elicited by the monovalent XBB.1.5 vaccine (Figure 2.6.2-24).

**Figure 2.6.2-23. Neutralizing Antibody Geometric Mean Titers (GMT) at 1 Month Post Dose 2 Elicited by XBB.1.5 Monovalent and Bivalent Vaccines as a Primary Series**



Note: Ten BALB/c mice per group were immunized IM on Days 0 and 21 with either 0.5 µg of bivalent BNT162b2 (WT 0.25 µg + BA.4/5 0.25 µg) or monovalent BNT162b2 XBB.1.5 (0.5 µg) or bivalent vaccine BNT162b2 (BA.4/BA.5 + XBB.1.5, 0.25 µg of each). Neutralizing antibody responses against the Wuhan reference strain (WT) and BA.4/BA.5, XBB.1.5 and XBB.1.16 sublineages were measured by pseudovirus neutralization assay at 1 month post-second dose.

**Figure 2.6.2-24. Neutralizing Antibody Geometric Mean Ratios (GMR) at 1 Month Post Dose 2 Elicited by XBB.1.5 Monovalent and Bivalent Vaccines as a Primary Series**



Note: The geometric mean ratio is defined as the geometric mean titer (GMT) of neutralization against a pseudovirus elicited the sublineage-adapted vaccine group divided by that elicited by the WT + BA.4/BA.5 vaccine.

#### 2.6.2.7.2.2. T Cell Response

SARS-CoV-2 spike-specific T cell responses were measured by ICS assay using flow cytometry in fresh splenocytes at 1 month following administration of 2 doses of monovalent or bivalent modRNA vaccines encoding spike antigens of SARS-COV-2 Omicron sublineage in naïve mice. To measure if sublineage-specific mutations have an impact on the overall T cell response, peptide pools representing the spike protein from either the wild type (WT) virus or BA.4/5 or XBB.1.5 were used.

Spike-specific T cell responses at 1 month post dose 2 showed that the monovalent or bivalent modRNA vaccines encoding spike antigens of wild type or Omicron sublineages induced moderate and variable frequencies of spike-specific T cells, both CD8+ and CD4+ T cells. The frequency of IFN- $\gamma$  producing CD8+ T cells was higher than CD4+ T cells. The frequency of IL-2 producing CD4+ T cells was slightly higher than the frequency of CD4+ T cells producing IFN- $\gamma$ . There was a high frequency of IFN- $\gamma$  expressing CD4+ T cells and very low levels of IL-4 expressing CD4+ T cells suggesting a Th1-biased T cell response, consistent with prior preclinical data for BNT162b2. Notably, the magnitude of the T cell response to each lineage or sublineage was similar across all the vaccine groups following the 2 dose primary series, although the levels were lower compared to that of BNT162b2-experienced mice. These results suggest that polyclonal T cell responses in mice are not affected by mutations in emerging lineages or sublineages of SARS-COV-2.

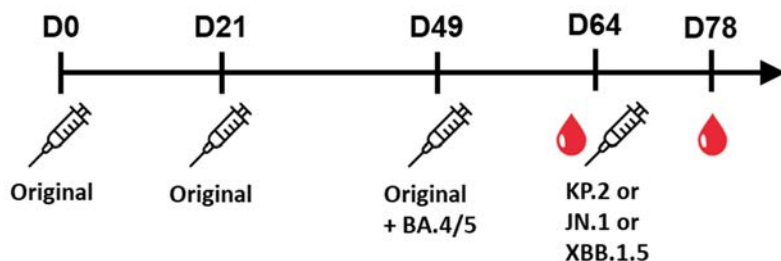
#### 2.6.2.8. Immunogenicity of BNT162b2 Monovalent Omicron KP.2 Vaccine Compared to BNT162b2 Monovalent Omicron JN.1 and BNT162b2 Monovalent Omicron XBB.1.5 Vaccines in Mice

##### 2.6.2.8.1. Vaccine-Experienced Study

We assessed the preclinical immunogenicity of a KP.2 variant-adapted vaccine as a fourth dose in female BALB/c mice (10/group) that were previously vaccinated with BNT162b2 (original wild type (WT) vaccine) on Days 0 and 21 and bivalent BNT162b2 (Original + Omicron BA.4/5) as a third dose on Day 49 ([Figure 2.6.2-25](#)). Against this background, given to approximate the vaccine antigenic exposures of the general human population, mice were given a fourth dose, on Day 64, of either the KP.2, JN.1 or XBB.1.5 vaccine. Sera were collected on Day 64 (prior to dose 4) and Day 78 (2 weeks post dose 4 for the assessment of neutralizing antibody responses in a pseudovirus neutralization test (pVNT) ([VR-VTR-11342](#)).



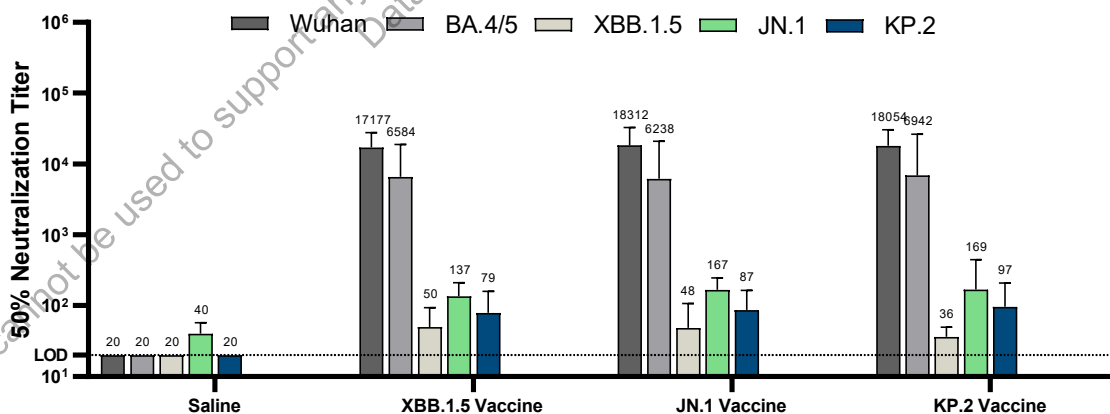
**Figure 2.6.2-25. Study Design for Immunogenicity of a Fourth Dose With BNT162b2 KP.2 Vaccine Compared to BNT162b2 XBB.1.5 and JN.1 Vaccines**



Groups of 10 female BALB/c mice were immunized intramuscularly (IM) on Days 0 and 21 with 0.5 µg of BNT162b2 Original and on Day 49 with 0.5 µg of bivalent BNT162b2 (Original + BA.4/5) to establish a vaccine experienced model. Mice were then immunized again on Day 64 with either XBB.1.5, JN.1, or KP.2 vaccine. Sera were collected on Day 64 and Day 78. Neutralizing antibody responses against a panel of pseudoviruses were measured by pVNT at 2 weeks post dose 3 and 2 weeks post dose 4.

Baseline serum neutralizing responses 2 weeks after a third dose with the bivalent Original + BA.4/5 vaccine (just prior to the fourth dose with either KP.2, JN.1 or XBB.1.5 vaccine) were highest against the Wuhan reference strain and the Omicron BA.4/5 lineage, and much lower against the XBB.1.5, JN.1 and KP.2 lineages (Figure 2.6.2-26). Baseline titers for each lineage were similar across the vaccine groups, allowing for direct comparisons of post-fourth dose titers.

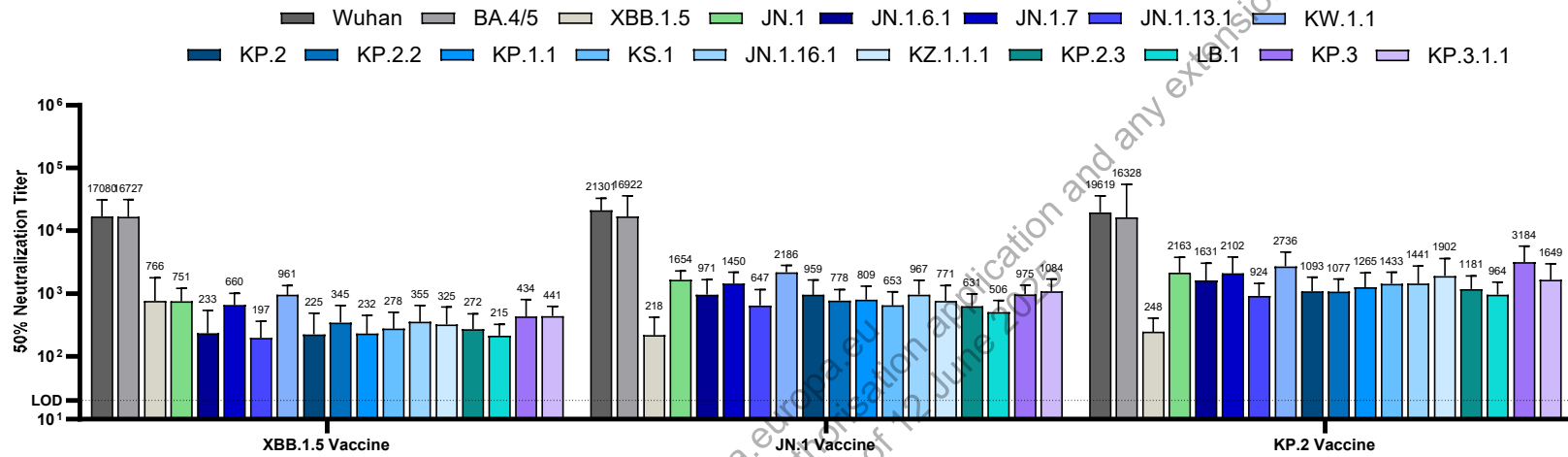
**Figure 2.6.2-26. Weeks Post Dose 3 Neutralizing Geometric Mean Titers (GMT) Following Immunization With 2 Doses of BNT162b2 Original, and 1 Dose of Bivalent BNT162b2 (Original +BA.4/5)**



Groups of 10 female BALB/c mice were immunized intramuscularly (IM) on Days 0 and 21 with 0.5 µg of BNT162b2 Original and on Day 49 with 0.5 µg of bivalent BNT162b2 (Original + BA.4/5) to establish a vaccine experienced mouse model. Neutralizing antibody responses against the pseudovirus of Wuhan reference strain, Omicron BA.4/5, XBB.1.5, JN.1, and KP.2 lineages, as shown in figure legend were measured by pVNT at 2 weeks post third dose. The numbers above each bar indicate the 50% neutralizing geometric mean titers (GMT).



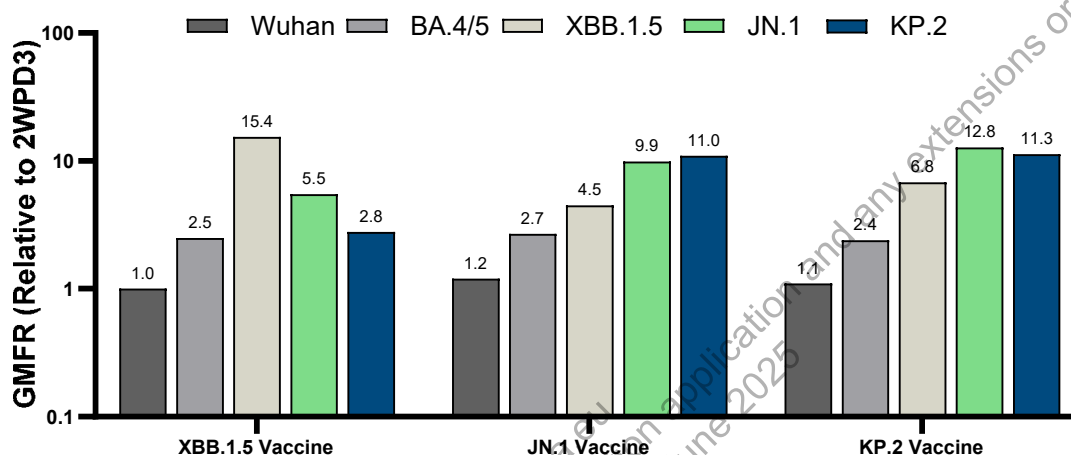
The KP.2 vaccine given as a fourth dose elicited neutralizing antibody geometric mean titers (GMT) against the JN.1 lineage and JN.1 sublineages, including KP.2 and KP.3, at 2 weeks post dose, that were approximately three-to-seven-fold higher than that elicited by the monovalent BNT162b2 XBB.1.5 vaccine and two-to-three-fold higher than that elicited by the JN.1 vaccine (Figure 2.6.2-27). The JN.1 vaccine elicited responses that were two-to-four-fold higher than those elicited by the XBB.1.5 vaccine. Both KP.2 and JN.1 vaccine responses effectively cross-neutralized all tested JN.1 sublineages with similar potency, including KP.2 and KP.3, which have been recently epidemiologically dominant (CDC, 2024).

**Figure 2.6.2-27. 2 Weeks Post Dose 4 Vaccination Neutralizing Geometric Mean Titers (GMT) Elicited by XBB.1.5, JN.1, and KP.2 Vaccines**

Groups of 10 female BALB/c mice were immunized intramuscularly (IM) on Days 0 and 21 with 0.5 µg of BNT162b2 Original, on Day 49 with 0.5 µg of bivalent BNT162b2 (WT + BA.4/5). 2 weeks following dose 3, mice were boosted with an additional dose of BNT162b2 XBB.1.5, JN.1, or KP.2 vaccine. Neutralizing antibody responses against pseudovirus of Wuhan reference strain (dark grey), Omicron BA.4/5 (light grey), XBB.1.5 (tan), JN.1 (green) and a broad panel of JN.1 sublineages listed and color-coded at the top of the plot were measured by pVNT at 2 weeks post fourth dose. The numbers above each bar signify the 50% neutralizing GMT.

The geometric mean fold rise (GMFR) in neutralizing titers from pre-to-post fourth dose vaccination, for the KP.2 vaccine group was 11.3-fold against Omicron KP.2 and nearly 13-fold against Omicron JN.1 (Figure 2.6.2-28). Similarly, GMFRs for the JN.1 vaccine were 9.9-fold and 11-fold against Omicron JN.1 and KP.2 lineages, respectively. In contrast, the XBB.1.5 vaccine elicited much lower GMFRs against KP.2 (2.8) and JN.1 (5.5).

**Figure 2.6.2-28. Neutralizing Antibody Titer Geometric Mean Fold Rise (GMFR) 2 Weeks Post Dose 4 Compared to Prior Vaccination**

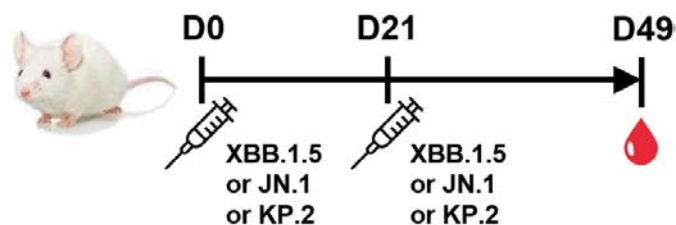


Groups of 10 female BALB/c mice were immunized intramuscularly (IM) on Days 0 and 21 with 0.5 µg of BNT162b2 Original, on Day 49 with 0.5 µg of bivalent BNT162b2 (WT + BA.4/5). 2 weeks following dose 3, mice were boosted with an additional dose of BNT162b2 XBB.1.5, JN.1, or KP.2 vaccine. Neutralizing antibody responses against pseudovirus of Wuhan reference strain (dark grey), Omicron BA.4/5 (light grey), XBB.1.5 (tan), JN.1 (green) and KP.2 (blue) listed and color-coded at the top of the plot were measured by pVNT at 2 weeks post third dose (pre-fourth dose) and 2 weeks post fourth dose. The numbers above each bar signify the fold-rise of the 50% neutralizing GMT from the pre-to-post-fourth dose timepoints.

#### 2.6.2.8.2. Primary Series Study

Groups of naïve female BALB/c mice (10/group) were immunized with monovalent BNT162b2 XBB.1.5, JN.1, or KP.2 vaccine on Days 0 and 21. Sera were collected on Day 49 (1 month post second dose) for assessment of neutralizing antibody responses in a pseudovirus neutralization test (pVNT). Spleens were collected on Day 49 to evaluate cell-mediated immune responses (VR-VTR-11341).

**Figure 2.6.2-29. Study Design for Immunogenicity of a Primary Series With BNT162b2 KP.2 Vaccine Compared to BNT162b2 XBB.1.5 and JN.1 Vaccines**

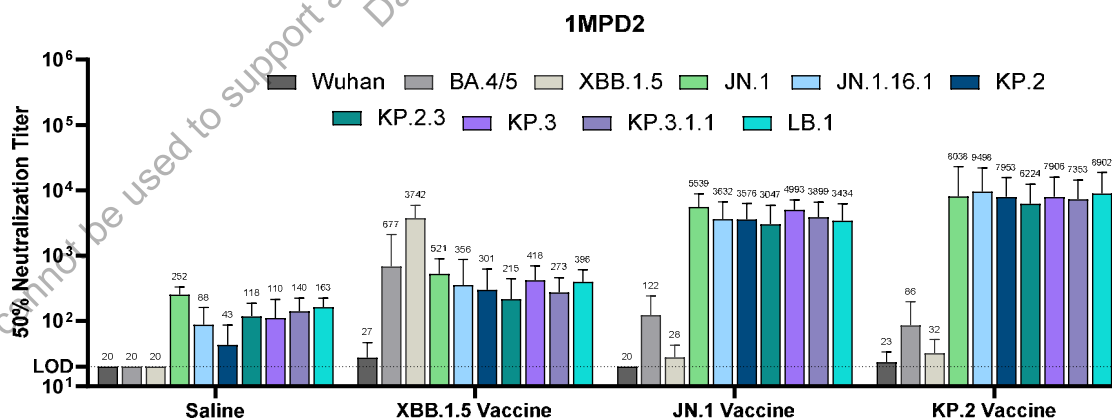


Groups of 10 female BALB/c mice were immunized intramuscularly (IM) on Days 0 and 21 with 0.5 µg of either BNT162b2 XBB.1.5, JN.1, or KP.2 vaccine. Sera and spleens were collected on Day 49. Neutralizing antibody responses against a panel of pseudoviruses were assessed by pVNT and T cell responses were evaluated by ICS on day 49.

#### 2.6.2.8.2.1. Functional Antibody Response

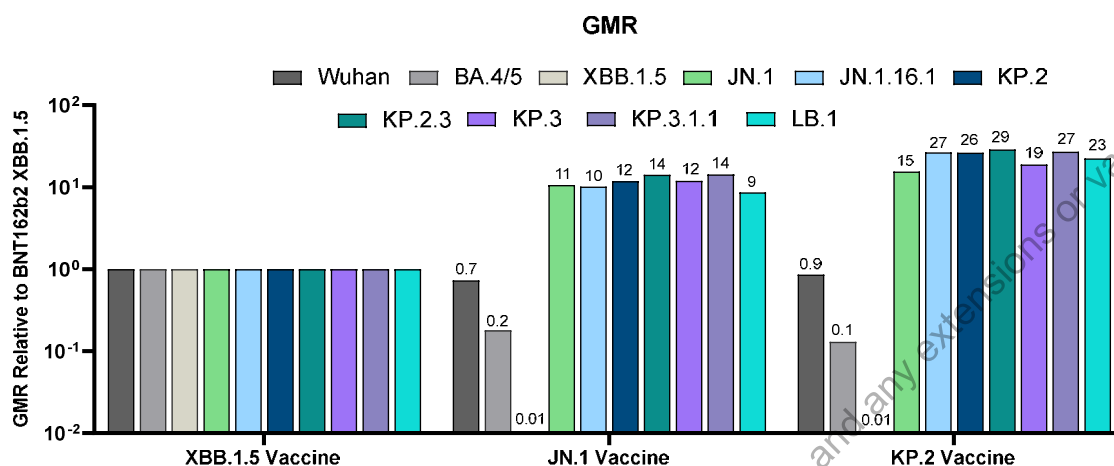
Intramuscular immunization of naïve BALB/c mice with two doses of monovalent BNT162b2 XBB.1.5, JN.1 or KP.2 vaccine induced strong neutralizing antibody responses against matched or closely matched sublineages (Figure 2.6.2-30 and Figure 2.6.2-31). BNT162b2 XBB.1.5 induced a robust neutralizing response against XBB.1.5, but much lower responses against JN.1, KP.2 and other JN.1 sublineages. The KP.2 vaccine elicited 15-to-29-fold higher neutralizing responses against epidemiologically relevant JN.1 sublineages, as compared to the XBB.1.5 vaccine; the JN.1 vaccine elicited 9-to-14-fold higher responses relative to the XBB.1.5 vaccine.

**Figure 2.6.2-30. 1 Month Post Dose 2 Neutralizing Geometric Mean Titers (GMT) With BNT162b2 XBB.1.5, BNT162b2 JN.1, or BNT162b2 KP.2 Monovalent Vaccines as a Primary Series**



Groups of 10 female BALB/c mice were immunized IM on Days 0 and 21 with a 0.5 µg of XBB.1.5, JN.1, or KP.2 vaccine. Sera were collected on Day 49 (1 month post 2nd dose). Neutralizing antibody responses against a broad panel of SARS-CoV-2 lineage pseudoviruses listed and color coded in the legend at the top of the plot were measured by pseudovirus neutralization assay. The numbers above each bar signify the 50% neutralizing GMT.

**Figure 2.6.2-31. Geometric Mean Ratios (GMR) of the 1 Month Post Dose 2 Neutralizing Geometric Mean Titers (GMT) Elicited by KP.2 and JN.1 Vaccines, Relative to XBB.1.5 Vaccine, as a Primary Series**

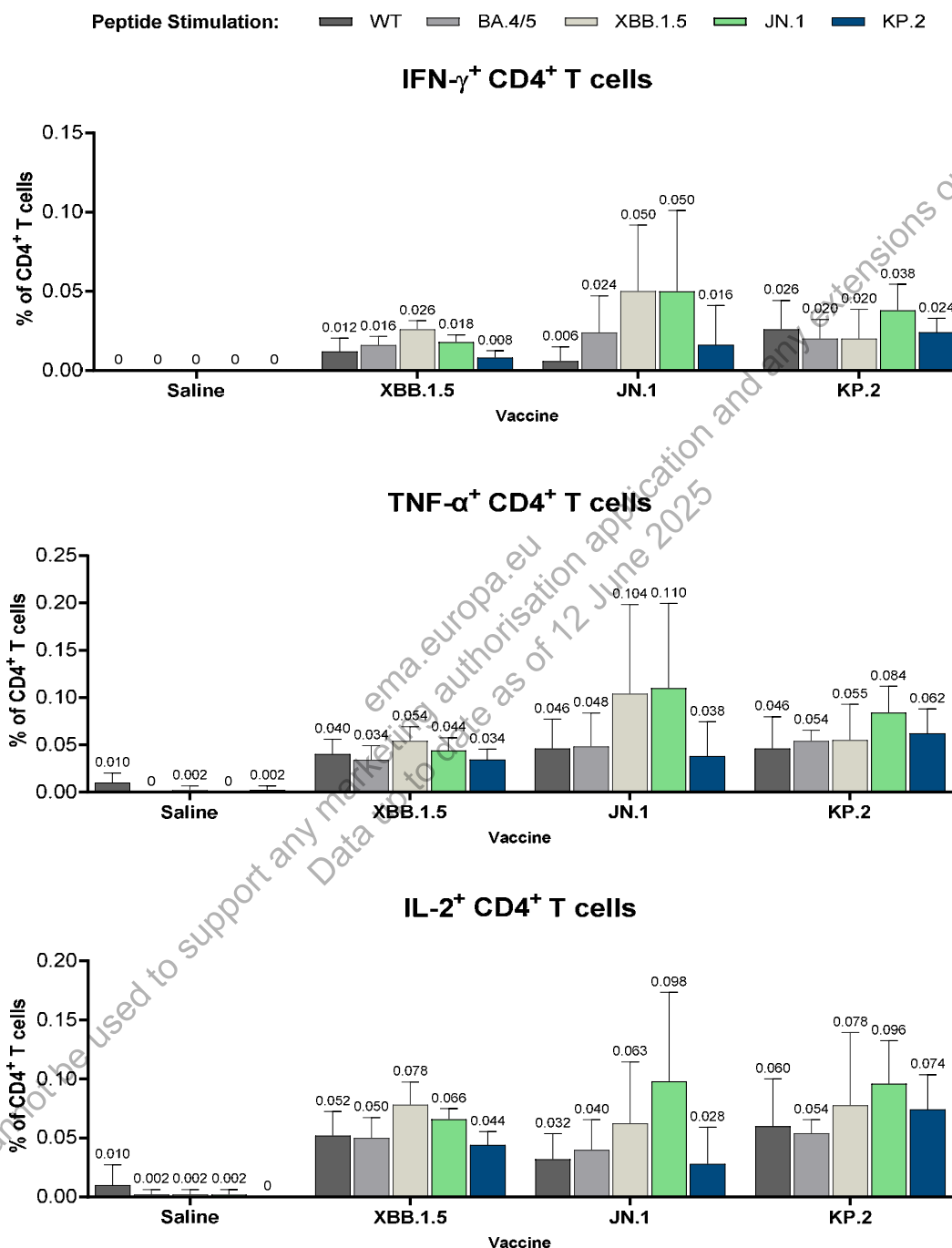


Groups of 10 female BALB/c mice were immunized IM on Days 0 and 21 with a 0.5 µg of monovalent BNT162b2 XBB.1.5, JN.1, or KP.2. Sera were collected on Day 49 (1 month post 2nd dose). Geometric mean ratios (GMR) of the geometric mean neutralizing antibody titers of the JN.1 vaccine and KP.2 vaccine relative to the XBB.1.5 against a broad panel of SARS-CoV-2 lineage pseudoviruses listed and color coded in the legend at the top of the plot are presented.

#### 2.6.2.8.2.2. T Cell Response

SARS-CoV-2 spike-specific T cell responses were assessed in splenocytes by intracellular cytokine staining (ICS) assay at 1 month following administration of the second dose in a primary series where mice received either monovalent BNT162b2 XBB.1.5, monovalent BNT162b2 JN.1 or monovalent BNT162b2 KP.2 vaccine. Peptide pools representing the full-length spike protein from the Wuhan wild type (WT) virus and Omicron BA.4/5, XBB.1.5, JN.1 and KP.2 were used to assess antigen-specific T cell responses. Vaccination with BNT162b2 KP.2 vaccine elicited similar frequencies of cytokine expressing (IFN-γ, TNF-α, IL-2) CD4+ T cells (Figure 2.6.2-32) and CD8+ T cells (Figure 2.6.2-33) compared to both the BNT162b2 JN.1 and BNT162b2 XBB.1.5 vaccines. The KP.2 vaccine induced comparable CD4+ and CD8+ T cell responses against all the variants that were tested, indicating that the T cell responses are stable and highly cross-reactive. Overall, both the KP.2 and JN.1 vaccines elicited broadly reactive and more robust T cell responses against the JN.1 lineage/sublineage peptide pools than was elicited by the XBB.1.5 vaccine.

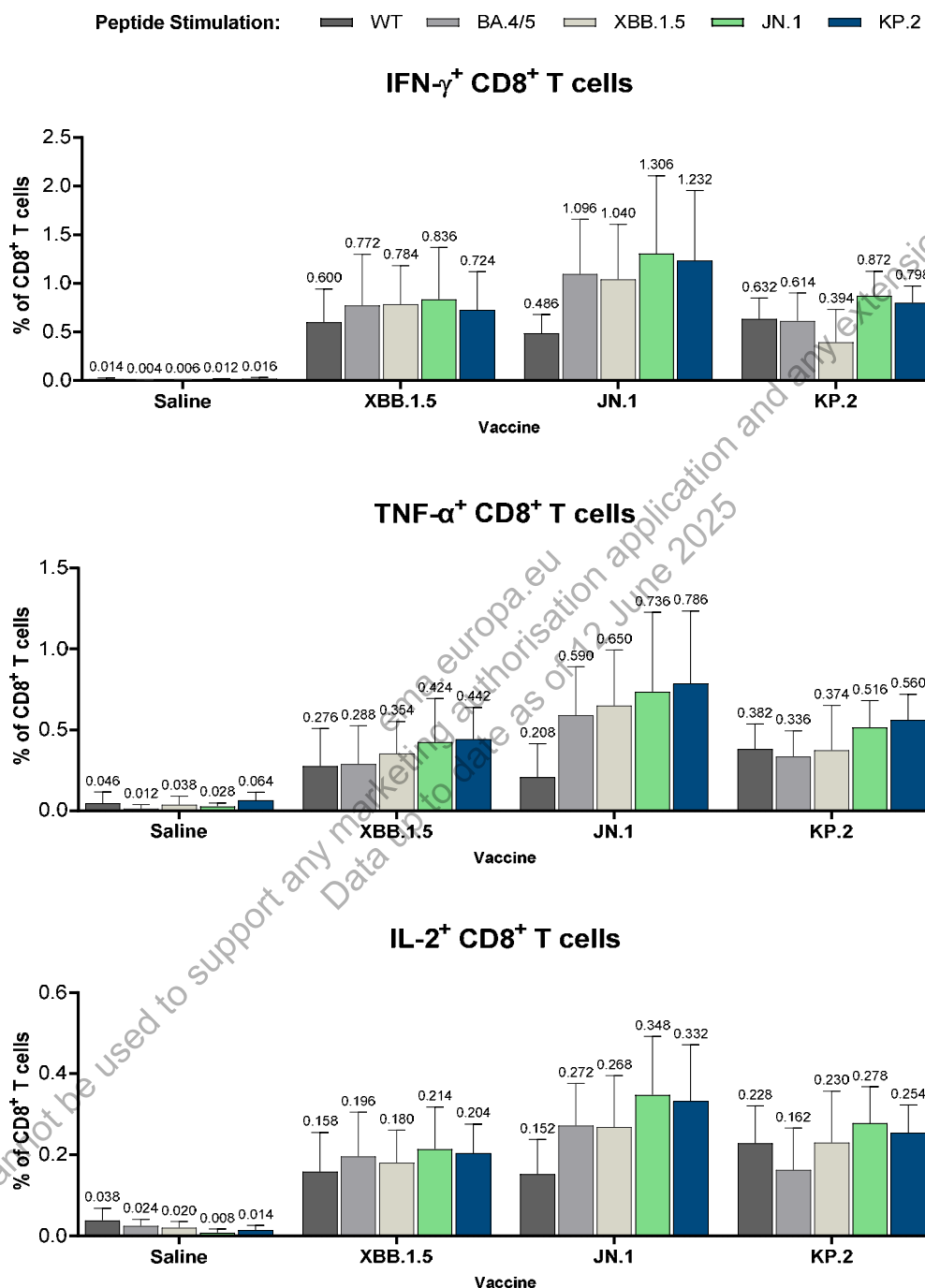
**Figure 2.6.2-32. Spike-Specific CD4<sup>+</sup> T Cell Response in Spleens Following Immunization With XBB.1.5, JN.1, or KP.2 Vaccine as a Primary Series**



Groups of 10 female BALB/c mice were immunized intramuscularly (IM) on Days 0 and 21 with 0.5  $\mu$ g of BNT162b2 XBB.1.5, JN.1, or KP.2 vaccine. 5 spleens/group were harvested on Day 49 (1 month post dose 2). CD4<sup>+</sup> T cell responses were measured by intracellular cytokine staining (ICS) following ex vivo stimulation of splenocytes with WT, BA.4/5, XBB.1.5, JN.1 and KP.2 peptide pools noted in the color-coded legend. Bars depict mean frequency with standard deviation (SD).



**Figure 2.6.2-33. Spike-Specific CD8<sup>+</sup> T Cell Response in Spleens Following Immunization With XBB.1.5, JN.1 or KP.2 Vaccine as a Primary Series**



Groups of 10 female BALB/c mice were immunized intramuscularly (IM) on Days 0 and 21 with 0.5  $\mu$ g of BNT162b2 XBB.1.5, JN.1, or KP.2 vaccine. 5 spleens/group were harvested on Day 49 (1 month post dose 2). CD8<sup>+</sup> T cell responses were measured by intracellular cytokine staining (ICS) following ex vivo stimulation of splenocytes with WT, BA.4/5, XBB.1.5, JN.1, and KP.2 peptide pools noted in the color-coded legend. Bars depict mean frequency with standard deviation (SD).

### **2.6.2.9. Immunogenicity of BNT162b2 Monovalent Omicron JN.1 and Monovalent Omicron XBB.1.5 in Mice**

#### **2.6.2.9.1. Vaccine-Experienced Study**

To assess the preclinical immunogenicity of a monovalent Omicron JN.1 variant-adapted vaccine administered as a fifth dose, female BALB/c mice (10/group) were immunized with BNT162b2 (original wild type (WT) vaccine) on Days 0 and 21, bivalent BNT162b2 (Original + Omicron BA.4/5) as a third dose, and monovalent BNT162b2 XBB.1.5 as a fourth dose on Days 49 and 93, respectively. Mice received this vaccine regimen to approximate the immune background of the general human population. A fifth dose with either the monovalent BNT162b2 JN.1 or monovalent BNT162b2 XBB.1.5 vaccine was administered on Day 129 (5 weeks post dose 4). Pre-vaccination sera were collected on Day 129 (prior to dose 5) and Day 156 (1 month post dose 5) for the assessment of neutralizing antibody responses in a pseudovirus neutralization test (pVNT). Spleens were collected on Day 156 to evaluate cell-mediated immune responses ([VR-VTR-11313](#)).

**Table 2.6.2-5. Study Design**

Group #	N/ group	Vaccination #1 (Day 0)	Vaccination #2 (Day 21)	Vaccination #3 (Day 49)	Vaccination #4 (Day 93)	Vaccination #5 (Day 129 – 5WPD4)	Vaccination (Day)	Bleed (Day)
1	10	Saline	Saline	Saline	Saline	Saline	0, 21, 49, 93, 129	129, 156 <sup>a</sup>
2		BNT162b2 WT	BNT162b2 WT	BNT162b2 Bivalent WT + BA.4/5 (co-formulated)	BNT162b2 XBB.1.5	BNT162b2 JN.1	0, 21, 49, 93, 129	129, 156 <sup>a</sup>
3						BNT162b2 XBB.1.5	0, 21, 49, 93, 129	129, 156 <sup>a</sup>

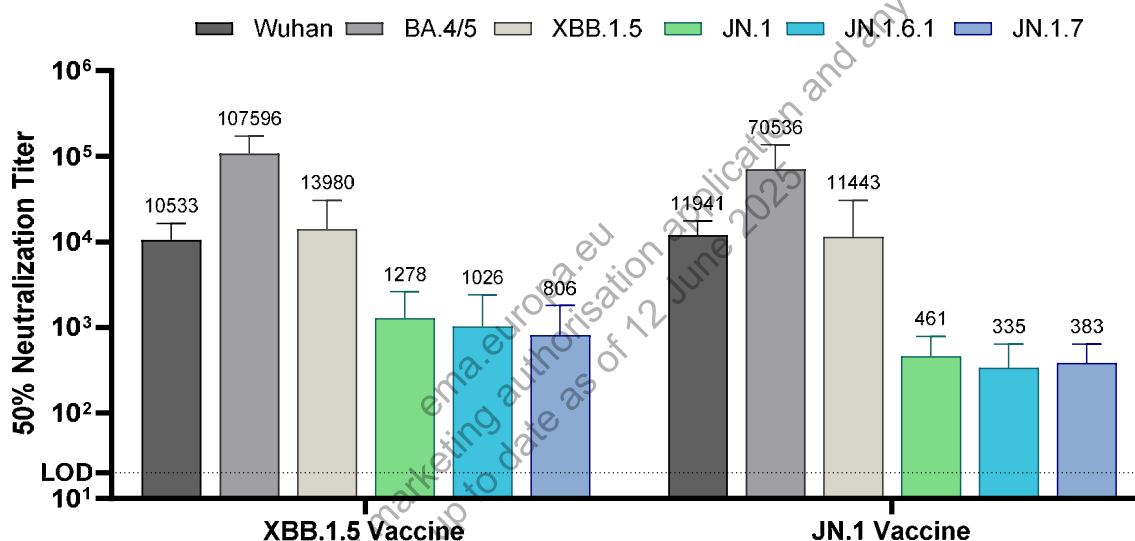
Vaccinations 1-4 were administered in previous studies. Vaccinations #1-3 were from PRL-COVID-Ms-2023-17 and Vaccination #4 was from PRL-COVID-Ms-2024-01. Experienced mice were transferred from PRL-COVID-Ms-2024-01 study.

a. 5 spleens per group were harvested on Day 156.

### 2.6.2.9.1.1. Functional Antibody Response

Baseline serum neutralizing responses 5 weeks after a fourth dose with the BNT162b2 XBB.1.5 vaccine (just prior to the fifth dose of either BNT162b2 XBB.1.5 or BNT162b2 JN.1) were highest against the Omicron BA.4/5 reference strain, lower against Wuhan reference strain and XBB.1.5, and further reduced against JN.1 and JN.1 sublineages (Figure 2.6.2-34). Slightly higher neutralizing responses were observed in the group that was assigned to receive BNT162b2 XBB.1.5 as a fifth dose (VR-VTR-11313).

**Figure 2.6.2-34. 5 Weeks Post Dose 4 Neutralizing Geometric Mean Titers (GMT) Following Immunization With 2 Doses of BNT162b2 Original, 1 Dose of Bivalent BNT162b2 (WT + BA.4/5) and 1 Dose of Monovalent BNT162b2 XBB.1.5**

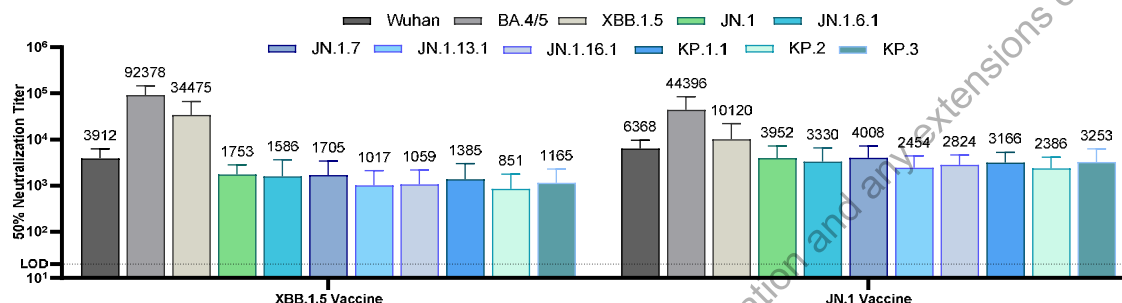


Groups of 10 female BALB/c mice were immunized intramuscularly (IM) on Days 0 and 21 with 0.5 µg of BNT162b2, on Day 49 with 0.5 µg of bivalent BNT162b2 (WT + BA.4/5) and on Day 93 with 0.5 µg of monovalent BNT162b2 XBB.1.5 to establish a BNT162b2 vaccine-experienced mouse model. Neutralizing antibody responses against pseudovirus of Wuhan reference strain (dark grey), Omicron BA.4/5 (light grey), XBB.1.5 (light yellow), JN.1 (green), JN.1.6.1 (blue), and JN.1.7 (blue-grey) variants of concern were measured by pVNT at 5 weeks post fourth dose. The numbers above each bar are the GMT.

IM immunization of BNT162b2-experienced BALB/c mice with monovalent BNT162b2 JN.1 vaccine as a fifth dose elicited neutralizing antibody geometric mean titers (GMT) against the JN.1 lineage and JN.1 sublineages, at one month post dose, that were two-to-threefold higher than that elicited by the monovalent BNT162b2 XBB.1.5 vaccine (Figure 2.6.2-35). In this study, monovalent JN.1 vaccine-elicited responses cross-neutralized all tested JN.1 sublineages with similar potency, including KP.2 that has gained some epidemiologic growth advantage.

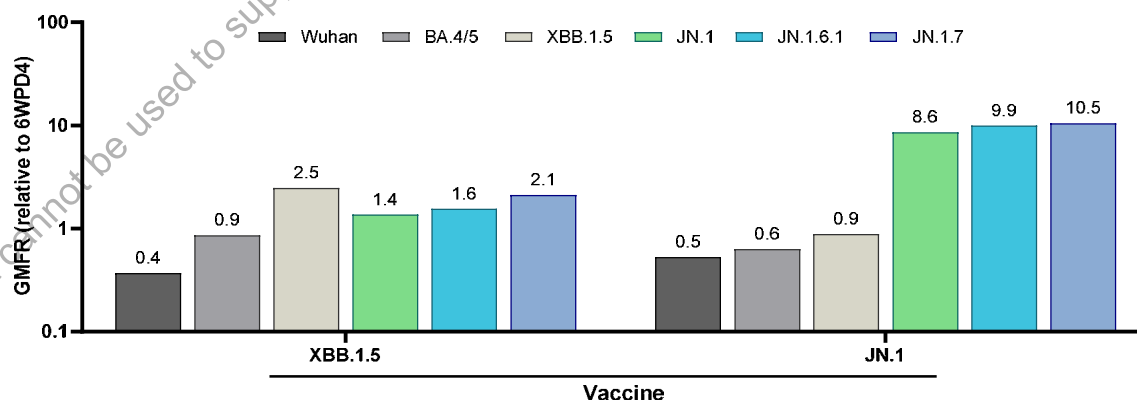
When neutralizing responses were evaluated as geometric mean fold rises (GMFR) from pre-to-post fifth dose vaccination, geometric mean titers rose by 8.6-fold against Omicron JN.1, and approximately 10-fold against JN.1.6.1, JN.1.7 (Figure 2.6.2-36). In contrast, XBB.1.5 vaccine elicited much lower fold rises in neutralizing activity against JN.1 and its sublineages.

**Figure 2.6.2-35. 1 Month Post Fifth Dose Vaccination Neutralizing Geometric Mean Titers (GMT) with BNT162b2 JN.1 and BNT162b2 XBB.1.5 Monovalent Vaccines**



Groups of 10 female BALB/c mice were immunized intramuscularly (IM) on Days 0 and 21 with 0.5 µg of BNT162b2, on Day 49 with 0.5 µg of bivalent BNT162b2 (WT + BA.4/5) and on Day 93 with 0.5 µg of monovalent BNT162B2 XBB.1.5; 5 weeks following dose 4, mice were boosted with an additional dose of monovalent BNT162 XBB.1.5 or BNT162b2 JN.1. Neutralizing antibody responses against pseudovirus of Wuhan reference strain (dark grey), Omicron BA.4/5 (light grey), XBB.1.5 (tan), JN.1 (green), JN.1.6.1 (dark turquoise), JN.1.7 (blue grey), JN.1.13.1 (sky blue), JN.1.16.1 (light blue-grey), KP.1.1 (blue), KP.2 (light turquoise) and KP.3 (teal) variants of concern were measured by pVNT at 1 month post fifth dose. The numbers above each bar signify the GMT.

**Figure 2.6.2-36. Neutralizing Antibody Geometric Mean Fold Rise (GMFR) 1 Month Post Dose 5 Compared to Prior Vaccination**

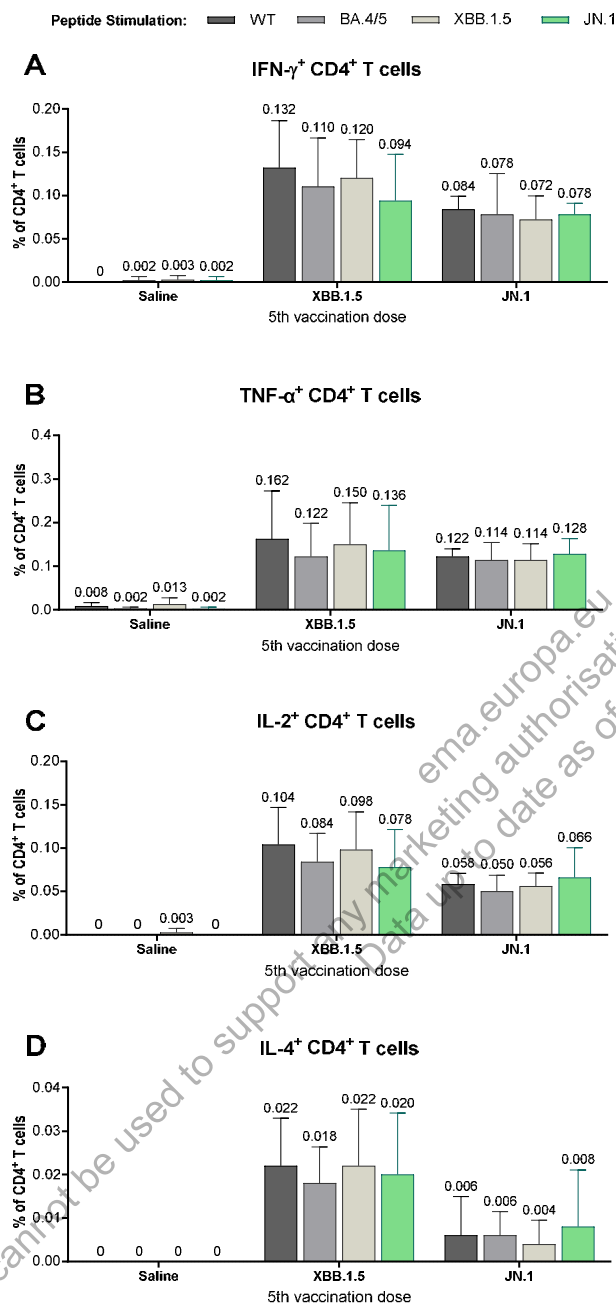


#### 2.6.2.9.1.2. T Cell Response

SARS-CoV-2 spike-specific T cell responses were assessed in splenocytes by intracellular cytokine staining (ICS) assay at 1 month following administration of the fifth dose in mice that received two prior doses of BNT162b2 (original WT vaccine), one dose of bivalent BNT162b2 (WT + BA.4/5), and one dose of BNT162b2 XBB.1.5. Peptide pools representing the full-length spike protein from either the Wuhan wild type (WT) virus, BA.4/5, XBB.1.5, or JN.1 were used to assess variant specific T cell responses. Fifth vaccination with monovalent BNT162b2 JN.1 vaccine elicited similar frequencies of cytokine-expressing (IFN- $\gamma$ , TNF- $\alpha$ , IL-2) CD4<sup>+</sup> T cells (Figure 2.6.2-37) and CD8<sup>+</sup> T cells (Figure 2.6.2-38) compared to monovalent BNT162b2 XBB.1.5 vaccine. The CD4<sup>+</sup> T cell response was Th1 dominant, with limited to no IL-4<sup>+</sup> CD4<sup>+</sup> T cells detected (Figure 2.6.2-37-D), consistent with prior studies of the BNT162b2 vaccine. Notably, the magnitude of T cell functional responses was similar against all variants that were tested within each vaccine group, indicating that the T cell responses are stable and highly cross-reactive (VR-VTR-11313).

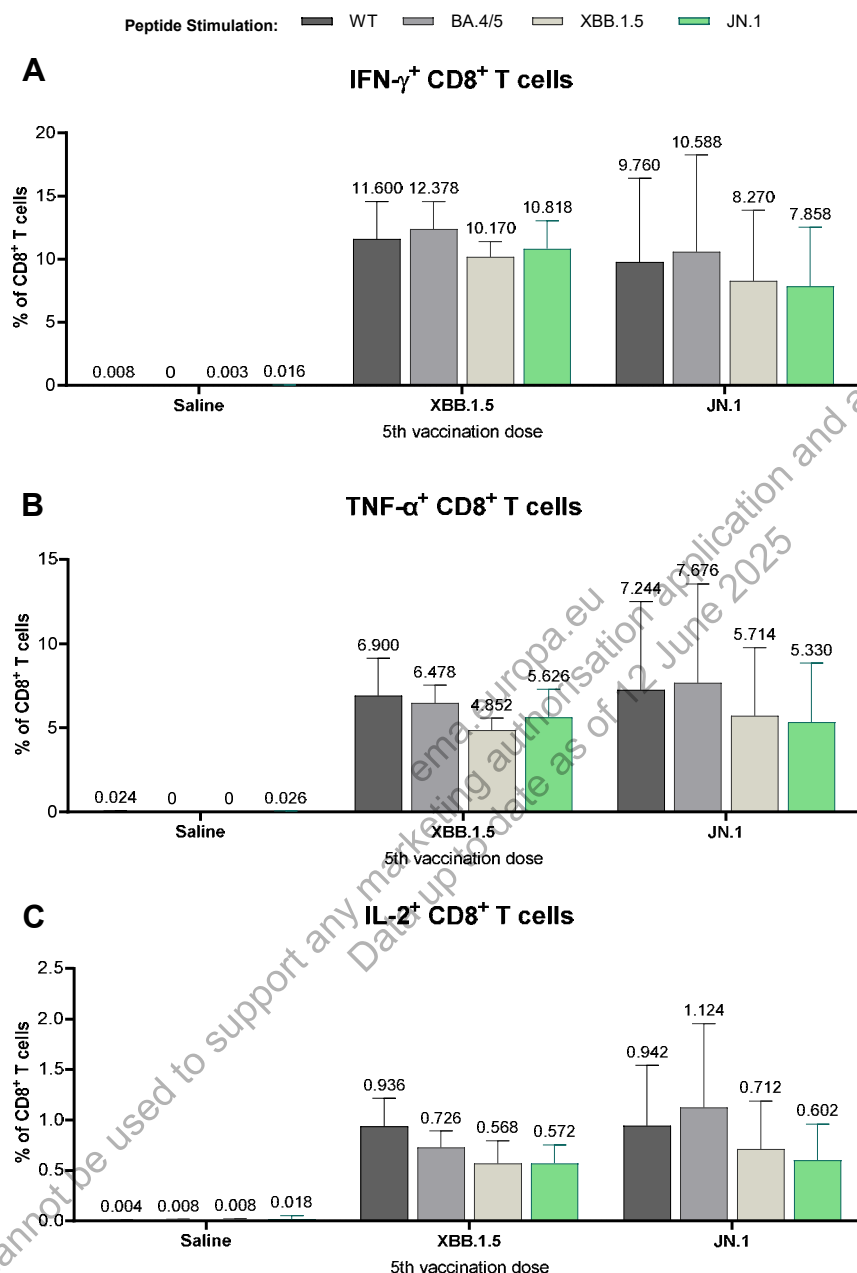


**Figure 2.6.2-37. Spike-Specific CD4<sup>+</sup> T Cell Response in Spleens Following Immunization of BNT162b2 Experienced Mice With JN.1 or XBB.1.5 as a Fifth Vaccination**



Groups of 10 female BALB/c mice were immunized intramuscularly (IM) on Days 0 and 21 with 0.5  $\mu$ g of BNT162b2, on Day 49 with 0.5  $\mu$ g of bivalent BNT162b2 (WT + BA.4/5) and on Day 93 with 0.5  $\mu$ g of monovalent BNT162b2 XBB.1.5; 5 weeks following dose 4, mice were vaccinated with an additional 0.5  $\mu$ g dose of monovalent BNT162b2 JN.1 or BNT162b2 XBB.1.5. 5 spleens/group were harvested on Day 156 (28 days post dose 5). CD4<sup>+</sup> T cell responses were measured by intracellular cytokine staining (ICS) following ex vivo stimulation of splenocytes with WT (dark grey), BA.4/5 (light grey), XBB.1.5 (light yellow) and JN.1 (green) peptide pools. Bars depict mean frequency with standard deviation (SD).

**Figure 2.6.2-38. Spike-Specific CD8<sup>+</sup> T Cell Response in Spleens Following Immunization of BNT162b2 Experienced Mice With JN.1 or XBB.1.5 as a Fifth Vaccination**



Groups of 10 female BALB/c mice were immunized intramuscularly (IM) on Days 0 and 21 with 0.5  $\mu$ g of BNT162b2, on Day 49 with 0.5  $\mu$ g of bivalent BNT162b2 (WT + BA.4/5) and on Day 93 with 0.5  $\mu$ g of monovalent BNT162b2 XBB.1.5; 5 weeks following dose 4, mice were vaccinated with an additional 0.5  $\mu$ g dose of monovalent BNT162b2 JN.1 or BNT162b2 XBB.1.5. 5 spleens/group were harvested on Day 156 (28 days post dose 5). CD8<sup>+</sup> T cell responses were measured by intracellular cytokine staining (ICS) following ex vivo stimulation of splenocytes with WT (dark grey), BA.4/5 (light grey), XBB.1.5 (light yellow) and JN.1 (green) peptide pools. Bars depict mean frequency with standard deviation (SD).

### 2.6.2.9.2. Primary Series Study

Groups of naïve female BALB/c mice (10/group) were immunized with monovalent BNT162b2 JN.1-adapted or BNT162b2 XBB.1.5-adapted vaccine on Days 0 and 21. Sera were collected on Day 35 (2 weeks post second dose) and Day 49 (1 month post second dose) for assessment of neutralizing antibody responses in a pseudovirus neutralization test (pVNT). Spleens were collected on Day 49 to evaluate cell-mediated immune responses (VR-VTR-11311).

**Table 2.6.2-6. JN.1 Primary Series Vaccine Mouse Immunogenicity Study Design**

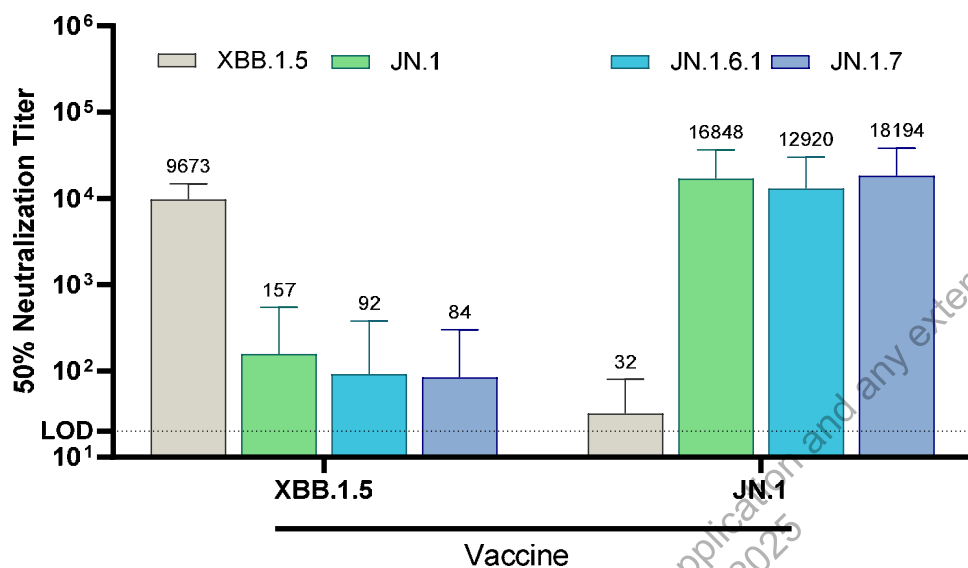
Group #	N/ group	Test Articles 0.5 µg	Vaccination (Day of Study)	Bleed (Day of Study)	Tissue Harvest (Day 49) (n=5)
1	10	Saline	0, 21	35, 49	Spleen
2		BNT162b2 JN.1	0, 21	35, 49	Spleen
3		BNT162b2 XBB.1.5	0, 21	35, 49	Spleen

#### 2.6.2.9.2.1. Functional Antibody Response

Intramuscular immunization of naïve BALB/c mice with two doses of monovalent BNT162b2 JN.1 or BNT162b2 XBB.1.5 vaccine induced strong neutralizing antibody responses against matched or closely matched sublineages (Figure 2.6.2-39) and Figure 2.6.2-40). BNT162b2 XBB.1.5 induced a robust neutralizing response against XBB.1.5, but much lower responses against JN.1 and JN.1 sublineages. The JN.1 adapted vaccine elicited potent neutralizing responses against JN.1 and all tested JN.1 sublineages (JN.1.6.1, JN.1.7, JN.1.13.1, JN.1.16.1, KP.1.1, KP.2 and KP.3).

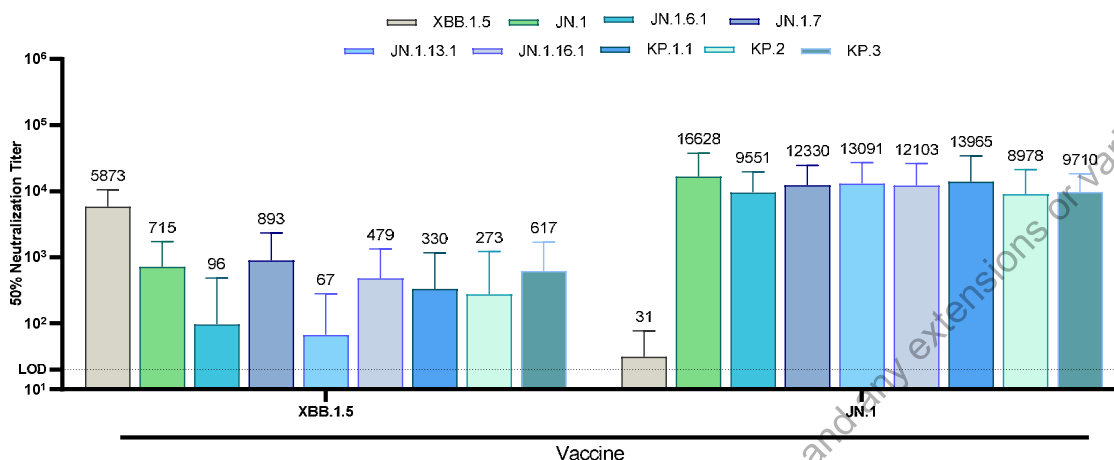
At 2 weeks post Dose 2, the JN.1 vaccine elicited neutralizing antibody responses against JN.1 lineages that were 100-to-200 fold higher than that elicited by the XBB.1.5 vaccine. (Figure 2.6.2-39). At 1 month post Dose 2, the JN.1 vaccine elicited neutralizing titers against JN.1 sublineages that were substantially higher, including a 33-fold higher response against the KP.2 sublineage, compared to neutralizing titers in the XBB.1.5 vaccine group, (Figure 2.6.2-40) (VR-VTR-11311).

**Figure 2.6.2-39. 2 Weeks Post Dose 2 Neutralizing Geometric Mean Titers (GMT) With BNT162b2 JN.1 and BNT162b2 XBB.1.5 Monovalent Vaccines as a Primary Series**



Ten BALB/c mice per group were immunized IM on Days 0 and 21 with a 0.5 µg of monovalent BNT162b2 JN.1 or BNT162b2 XBB.1.5. Sera were collected on Day 35 (2 weeks post 2nd dose). Neutralizing antibody responses against the XBB.1.5 (tan), JN.1 (green), JN.1.6.1 (dark turquoise), JN.1.7 (blue grey) variants of concern were measured by pseudovirus neutralization assay. The numbers above each bar signify the GMT.

**Figure 2.6.2-40. 1 Month Post Dose 2 Neutralizing Geometric Mean Titers (GMT) With BNT162b2 JN.1 and BNT162b2 XBB.1.5 Monovalent Vaccines as a Primary Series**

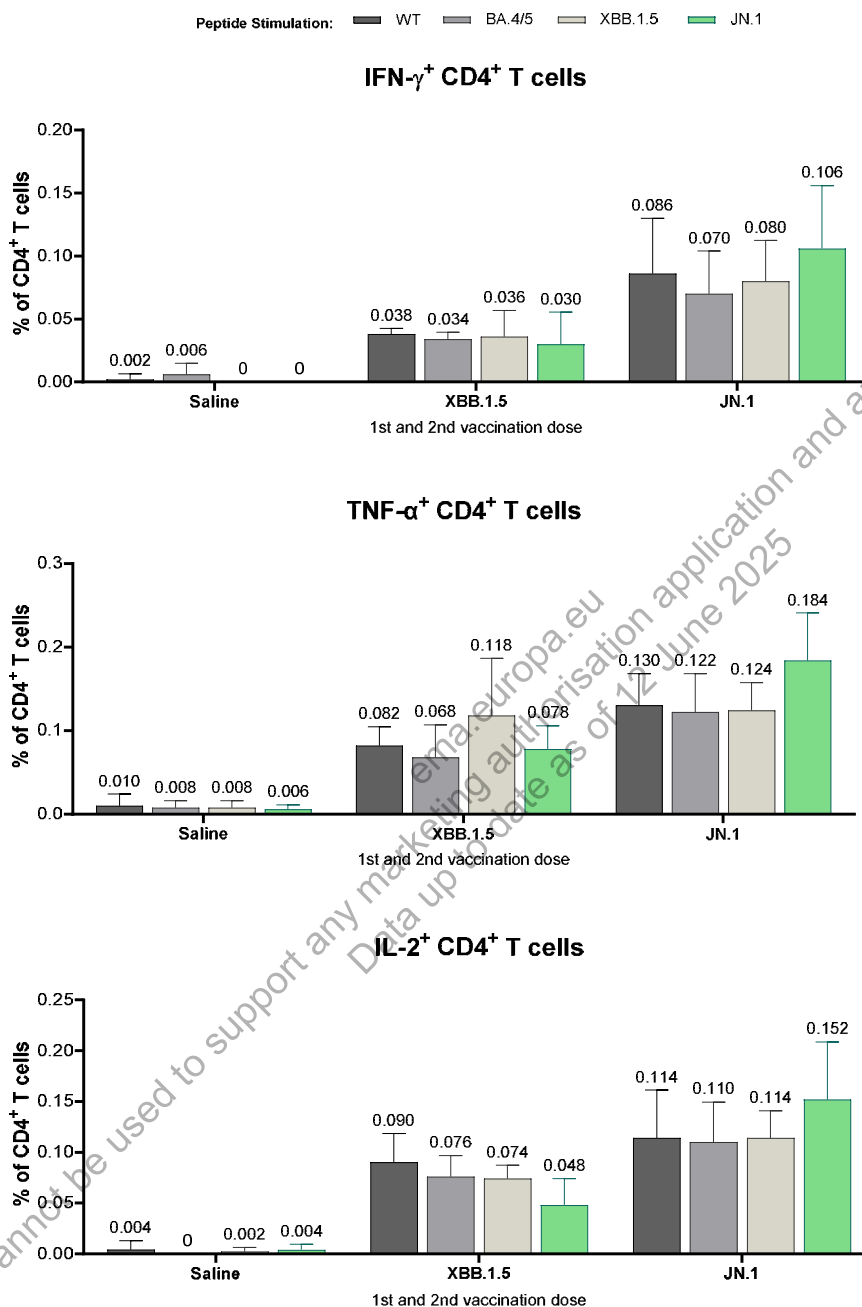


Ten BALB/c mice per group were immunized intramuscularly (IM) on Days 0 and 21 with 0.5 µg of either BNT162b2 JN.1 or BNT162b2 XBB.1.5. Sera were collected on Day 49 (1 month post second dose). Neutralizing antibody responses against pseudovirus of XBB.1.5 (tan), JN.1 (green), JN.1.6.1 (dark turquoise), JN.1.7 (blue grey), JN.1.13.1 (sky blue), JN.1.16.1 (dark blue grey), KP.1.1 (blue), KP.2 (light turquoise), and KP.3 (teal) variants of concern were measured by pVNT 1 month post second dose. The numbers above each bar signify the GMT.

#### 2.6.2.9.2.2. T Cell Response

SARS-CoV-2 spike-specific T cell responses were assessed in splenocytes by intracellular cytokine staining (ICS) assay at 1 month following administration of the second dose in a primary series where mice received either monovalent BNT162b2 JN.1 or monovalent BNT162b2 XBB.1.5. Peptide pools representing the full-length spike protein from the Wuhan wild type (WT) virus, BA.4/5, XBB.1.5 and JN.1 were used to assess variant specific T cell responses. Vaccination with BNT162b2 JN.1 elicited higher frequencies of cytokine-expressing (IFN-γ, TNF-α, IL-2) CD4+ T cells (Figure 2.6.2-41) and CD8+ T cells (Figure 2.6.2-42) compared to BNT162b2 XBB.1.5, particularly against the JN.1 variant peptide pool. Notably, JN.1 induced T cell responses against all the variants that were tested, indicating that the T cell responses are stable and highly cross-reactive (VR-VTR-11311).

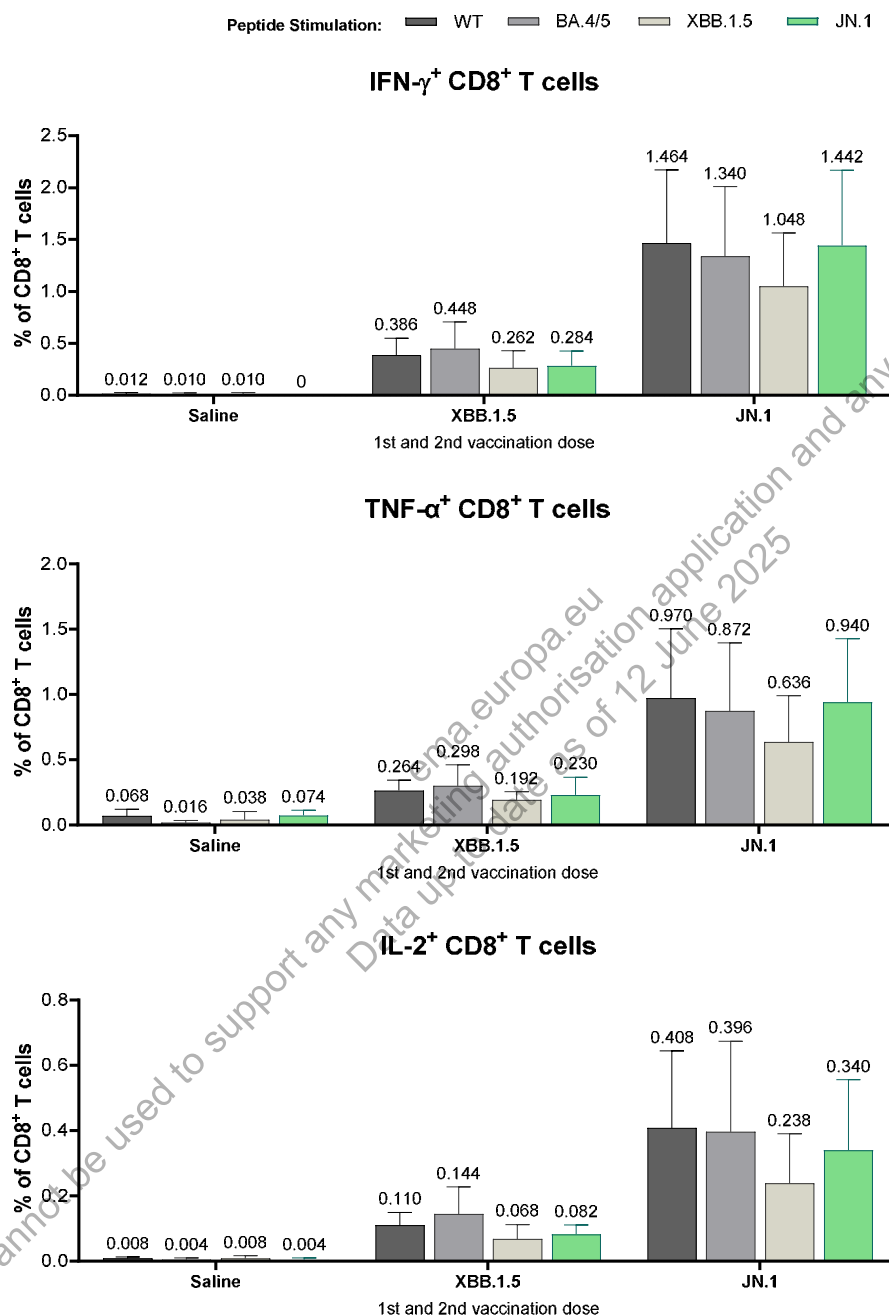
**Figure 2.6.2-41. Spike-Specific CD4<sup>+</sup> T Cell Response in Spleens Following Immunization With BNT162b2 JN.1 or BNT162b2 XBB.1.5 as a Primary Series**



Groups of 10 female BALB/c mice were immunized intramuscularly (IM) on Days 0 and 21 with 0.5  $\mu$ g of BNT162b2 JN.1 or BNT162b2 XBB.1.5. 5 spleens/group were harvested on Day 49 (1 month post dose 2). CD4<sup>+</sup> T cell responses were measured by intracellular cytokine staining (ICS) following ex vivo stimulation of splenocytes with WT (dark grey), BA.4/5 (light grey), XBB.1.5 (light yellow) and JN.1 (green) peptide pools. Bars depict mean frequency with standard deviation (SD).



**Figure 2.6.2-42. Spike-Specific CD8<sup>+</sup> T Cell Response in Spleens Following Immunization With BNT162b2 JN.1 or BNT162b2 XBB.1.5 as a Primary Series**



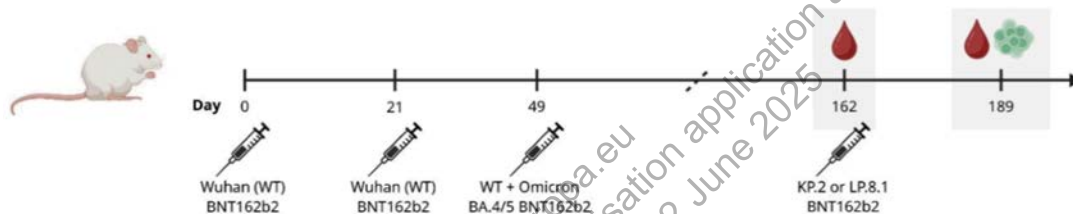
Groups of 10 female BALB/c mice were immunized intramuscularly (IM) on Days 0 and 21 with 0.5  $\mu$ g of BNT162b2 JN.1 or BNT162b2 XBB.1.5. 5 spleens/group were harvested on Day 49 (1 month post dose 2). CD8<sup>+</sup> T cell responses were measured by intracellular cytokine staining (ICS) following ex vivo stimulation of splenocytes with WT (dark grey), BA.4/5 (light grey), XBB.1.5 (light yellow) and JN.1 (green) peptide pools. Bars depict mean frequency with standard deviation (SD).

### 2.6.2.10. Immunogenicity of BNT162b2 Monovalent Omicron LP.8.1 and Monovalent Omicron KP.2 in Mice

#### 2.6.2.10.1. Vaccine-Experienced Study

To assess the preclinical immunogenicity of a monovalent Omicron LP.8.1 variant-adapted vaccine administered as a fourth dose, female BALB/c mice (10 per group) were immunized with BNT162b2 (Original) on Days 0 and 21, and bivalent BNT162b2 (Original + BA.4/5) as a third dose on Day 49. Mice received this vaccine regimen to approximate the immune background of the general human population. A fourth dose with either the monovalent BNT162b2 LP.8.1 or KP.2 vaccine was administered on Day 162. Sera were collected on Day 162 (prior to dose 4) and Day 189 (1 month post dose 4) for the assessment of neutralizing antibody responses in a pseudovirus neutralization test (pVNT). Spleens were collected on Day 189 to evaluate cell-mediated immune responses ([VR-VTR-11466](#)).

**Figure 2.6.2-43. Study Design for the Immunogenicity Evaluation of a Fourth Dose of the BNT162b2 LP.8.1 Vaccine Compared to KP.2**

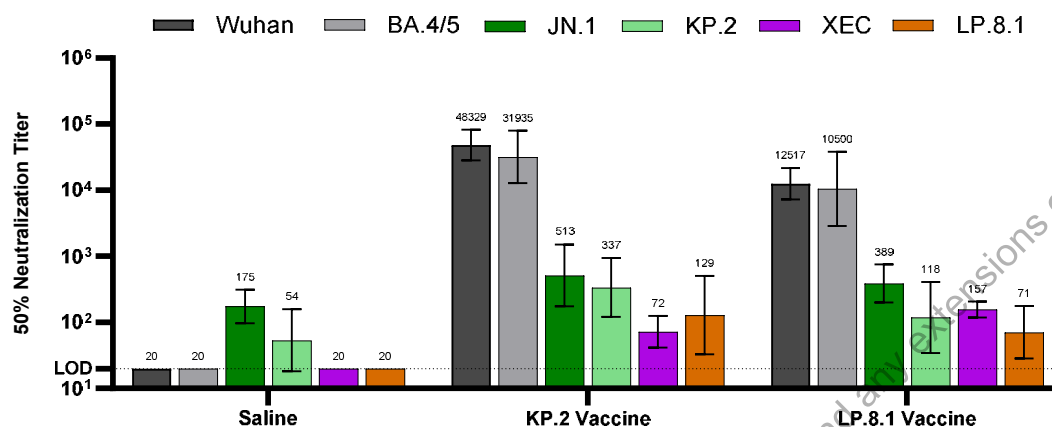


Groups of 10 female BALB/c mice were immunized intramuscularly (IM) on Days 0 and 21 with 0.5 µg of BNT162b2 (Original), on Day 49 with 0.5 µg of bivalent BNT162b2 (Original + BA.4/5), and on Day 162 (4 months post dose 3) with 0.5 µg of BNT162b2 KP.2 or LP.8.1 vaccine. Sera was collected and spleens were harvested at indicated time points to evaluate neutralizing antibody responses and cell-mediated immune responses.

#### 2.6.2.10.1.1. Functional Antibody Response

Baseline serum neutralizing responses with the BNT162b2 LP.8.1 or KP.2 vaccine (prior to the fourth dose) were highest against the Wuhan and Omicron BA.4/5 reference strains, and lower against JN.1 sublineages including JN.1, KP.2, XEC, and LP.8.1 ([Figure 2.6.2-44](#)).

**Figure 2.6.2-44. Neutralizing Antibody Geometric Mean Titers (GMT) Following Immunization with 2 Doses of BNT162b2 (Original) and 1 Dose of Bivalent BNT162b2 (Original + BA.4/5) (Pre-Boost)**

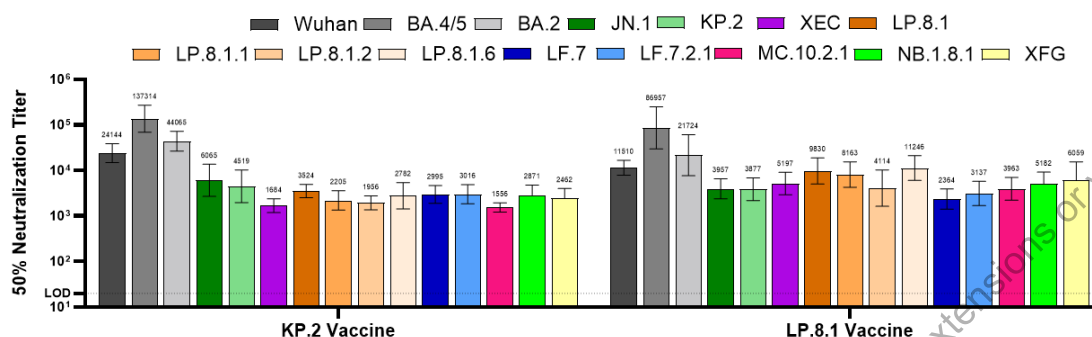


Groups of 10 female BALB/c mice were immunized intramuscularly (IM) on Days 0 and 21 with 0.5 µg of BNT162b2 (Original) and on Day 49 with 0.5 µg of bivalent BNT162b2 (Original + BA.4/5) to establish a vaccine-experienced mouse model. The X axis indicates the variant-adapted vaccine that will be given as the fourth dose. Neutralizing antibody responses against the pseudovirus of the Wuhan reference strain, Omicron BA.4/5, JN.1, KP.2, XEC, and LP.8.1 variants were measured by pVNT on Day 162 (4 months post dose 3). The numbers above each bar indicate the 50% neutralizing geometric mean titer (GMT).

The LP.8.1-adapted vaccine as a fourth dose elicited 1.8-to-4 -fold higher neutralizing responses against XEC, LP.8.1 sublineages (LP.8.1, LP.8.1.1, LP.8.1.2, and LP.8.1.6), MC.10.2.1, NB.1.8.1, and XFG compared to those elicited by the KP.2-adapted vaccines (Figure 2.6.2-45, and Figure 2.6.2-46). While the LP.8.1-adapted vaccine's immunogenicity against LF.7 and LF.7.2.1 variants was relatively lower, it remained similar to that of the KP.2-adapted vaccines.

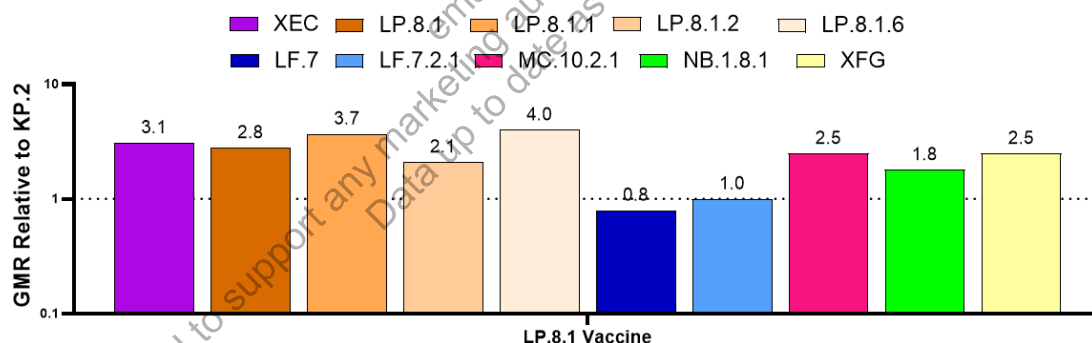
From pre- to post-fourth dose, the LP.8.1-adapted vaccine increased neutralizing antibody responses against LP.8.1 by 139-fold, against KP.2 and XEC by 33-fold, and against BA.4/5 and JN.1 by 8-to-10-fold, while antibody titers against Wuhan were unchanged (Figure 2.6.2-46).

**Figure 2.6.2-45. Neutralizing Antibody Geometric Mean Titers (GMT) Following Immunization of BNT162b2 Experienced Mice with BNT162b2 KP.2 or LP.8.1 as a Fourth Vaccination**



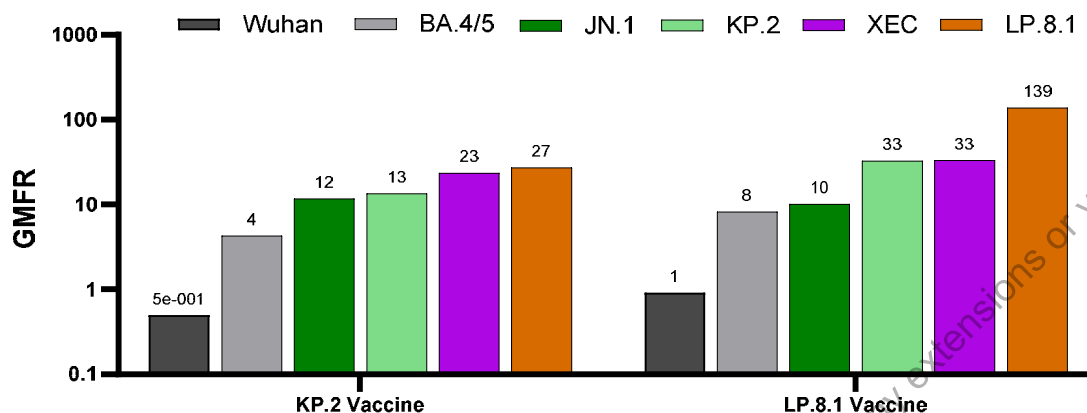
Groups of 10 female BALB/c mice were immunized intramuscularly (IM) on Days 0 and 21 with 0.5 µg of BNT162b2 (Original), on Day 49 with 0.5 µg of bivalent BNT162b2 (Original + BA.4/5), and on Day 162 (4 months post dose 3) with 0.5 µg of BNT162b2 KP.2 or LP.8.1 vaccine (X axis). Neutralizing antibody responses against a panel of JN.1 sublineage pseudoviruses were measured by pVNT on Day 189 (1 month post dose 4). The numbers above each bar indicate the 50% neutralization geometric mean titer (GMT).

**Figure 2.6.2-46. Geometric Mean Ratio (GMR) of Neutralizing Antibody GMTs Elicited by the LP.8.1 Vaccine Groups Relative to KP.2 Vaccine**



The study details are as described in Figure 2.6.2-45. The number above each bar indicates the geometric mean ratio (GMR). For each pseudovirus strain tested, the GMR is defined as the ratio of the BNT162b2 LP.8.1 vaccine (X axis) GMT to the BNT162b2 KP.2 vaccine GMT.

**Figure 2.6.2-47. Neutralizing Antibody Geometric Mean Fold Rise (GMFR) 1 Month Post Dose 4 Compared to Pre-Boost**

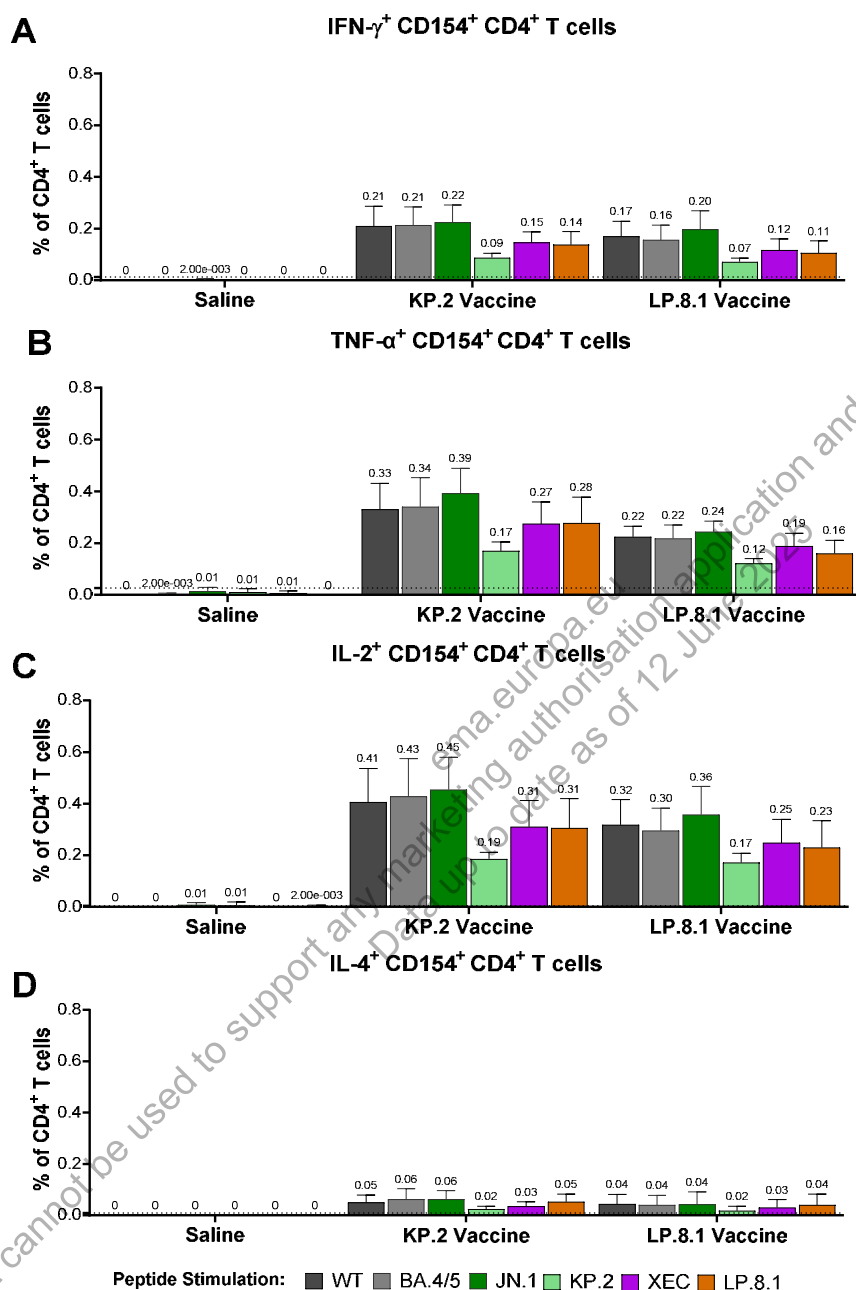


The study details are as described in Figure 2.6.2-45. The number above each bar indicates the geometric mean fold rise (GMFR). For each pseudovirus strain tested, the GMFR is defined as the fold increase of the post-fourth dose (X axis) GMT divided by the pre-fourth dose GMT.

#### 2.6.2.10.1.2. T Cell Response

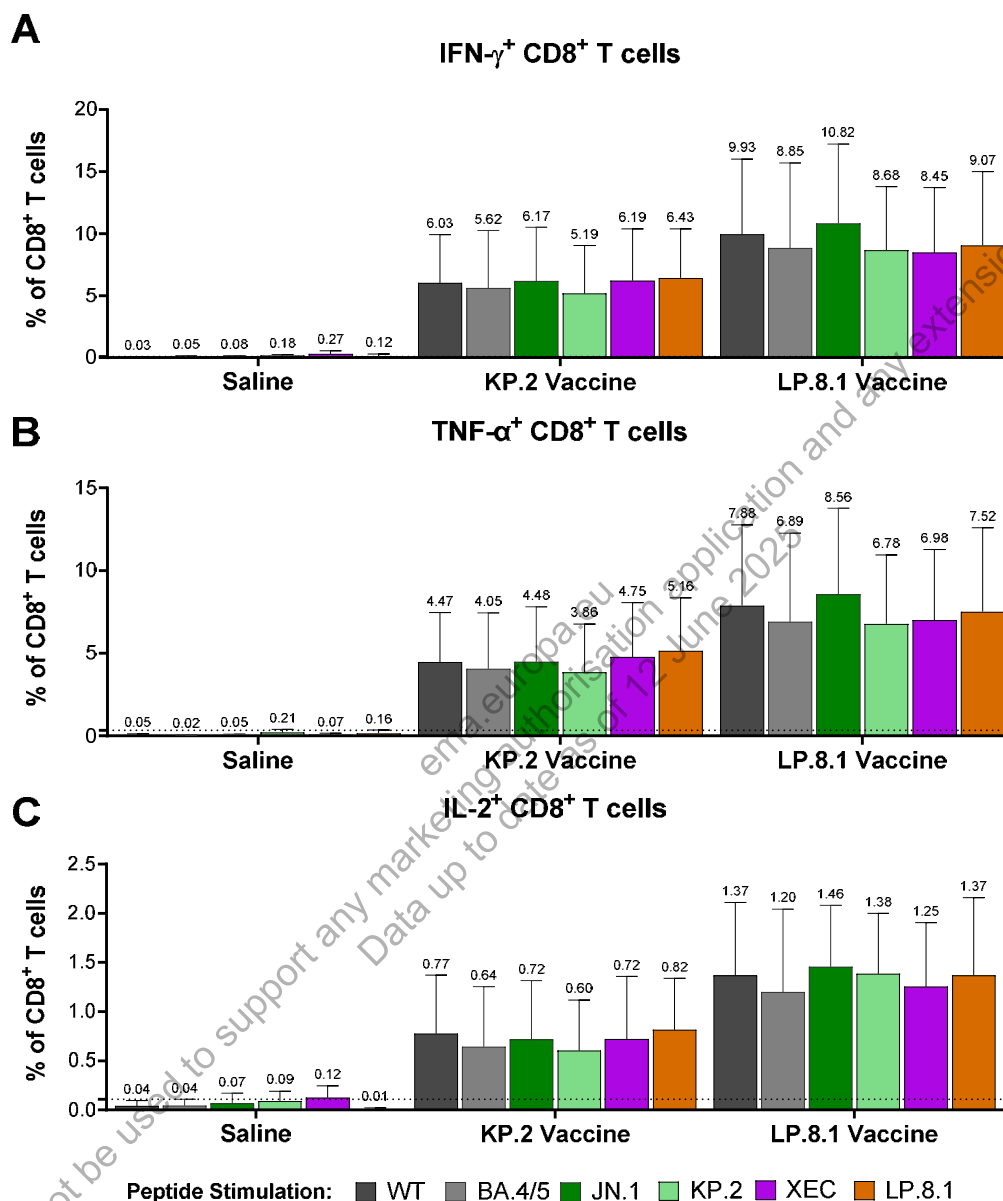
SARS-CoV-2 spike-specific T cell responses were assessed in splenocytes by intracellular cytokine staining (ICS) assay at 1 month following administration of the fourth dose in mice that received 2 doses of BNT162b2 (Original) and 1 dose of bivalent BNT162b2 (Original + BA.4/5). Peptide pools representing the full-length spike protein from the Wuhan wildtype (WT) virus, BA.4/5, JN.1, KP.2, XEC, or LP.8.1 strains were used to assess variant-specific T cell responses. A fourth vaccination, the monovalent BNT162b2 LP.8.1 vaccine elicited similar frequencies of cytokine-expressing (IFN- $\gamma$ , TNF- $\alpha$ , IL-2) CD4<sup>+</sup> T cells (Figure 2.6.2-48) and CD8<sup>+</sup> T cells (Figure 2.6.2-49) compared to the monovalent BNT162b2 KP.2 vaccine. The CD4<sup>+</sup> T cell response was Th1 dominant, with limited to no IL-4<sup>+</sup> CD4<sup>+</sup> T cells detected (Figure 2.6.2-48), consistent with prior studies of the BNT162b2 vaccine. Notably, the magnitude of T cell functional responses was similar against all variants that were tested within each vaccine group, indicating that the T cell responses are stable and highly cross-reactive (VR-VTR-11466).

**Figure 2.6.2-48. SARS-CoV-2 Spike-Specific CD4<sup>+</sup> T Cell Response in Spleens Following Immunization of BNT162b2 Experienced Mice with BNT162b2 KP.2 or LP.8.1 as a Fourth Vaccination**



Groups of 10 female BALB/c mice were immunized intramuscularly (IM) on Days 0 and 21 with 0.5  $\mu$ g of BNT162b2 (Original), on Day 49 with 0.5  $\mu$ g of bivalent BNT162b2 (Original + BA.4/5), and on Day 162 (4 months post dose 3) with 0.5  $\mu$ g of monovalent KP.2- or LP.8.1-adapted vaccines. Each group had 5 spleens harvested on Day 189 (1 month post dose 4). CD4<sup>+</sup> T cell responses were measured by intracellular cytokine staining (ICS) following ex vivo stimulation of splenocytes with Wild-type (dark grey), BA.4/5 (light grey), JN.1 (dark green), KP.2 (light green), XEC (purple), and LP.8.1 (orange) peptide pools. Bars depict the mean frequency with standard deviation (SD).

**Figure 2.6.2-49. SARS-CoV-2 Spike-Specific CD8<sup>+</sup> T Cell Response in Spleens Following Immunization of BNT162b2 Experienced Mice with BNT162b2 KP.2 or LP.8.1 as a Fourth Vaccination**



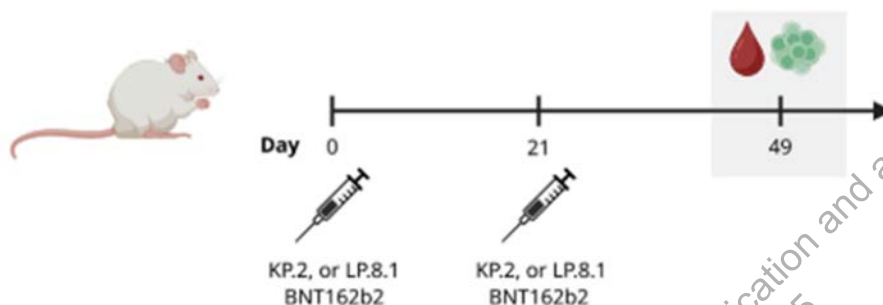
Groups of 10 female BALB/c mice were immunized intramuscularly (IM) on Days 0 and 21 with 0.5  $\mu$ g of BNT162b2 (Original), on Day 49 with 0.5  $\mu$ g of bivalent BNT162b2 (Original + BA.4/5), and on Day 162 (4 months post dose 3) with 0.5  $\mu$ g of monovalent KP.2- or LP.8.1-adapted vaccines. Each group had 5 spleens harvested on Day 189 (1 month post dose 4). CD8<sup>+</sup> T cell responses were measured by intracellular cytokine staining (ICS) following ex vivo stimulation of splenocytes with Wild-type (dark grey), BA.4/5 (light grey), JN.1 (dark green), KP.2 (light green), XEC (purple), and LP.8.1 (orange) peptide pools. Bars depict the mean frequency with standard deviation (SD).



#### 2.6.2.10.2. Primary Series Study

Groups of naïve female BALB/c mice (10 per group) were immunized with monovalent BNT162b2 LP.8.1 or KP.2 vaccine on Days 0 and 21. Sera were collected on Day 49 (1 month post dose 2) for assessment of neutralizing antibody responses in a pseudovirus neutralization test (pVNT). Spleens were collected on Day 49 to evaluate cell-mediated immune responses ([VR-VTR-11467](#)).

**Figure 2.6.2-50. Study Design for the Immunogenicity Evaluation of a Primary Series of the BNT162b2 LP.8.1 Vaccine Compared to KP.2**

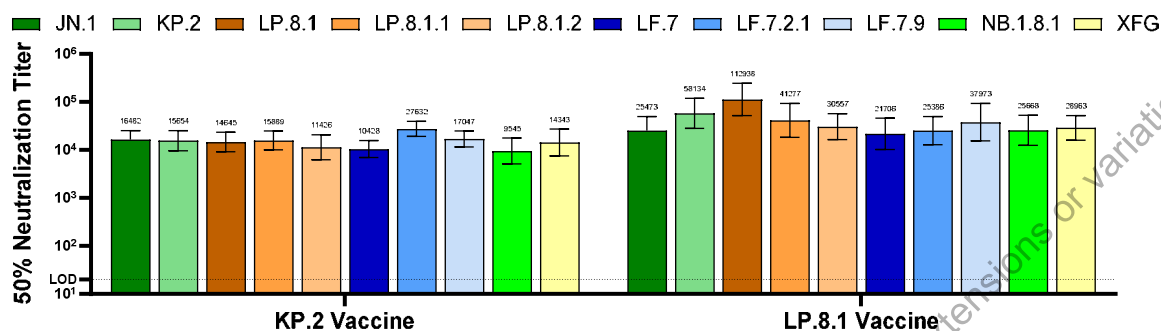


Groups of 10 female BALB/c mice were immunized intramuscularly (IM) on Days 0 and 21 with 0.5 µg of either BNT162b2 KP.2 or LP.8.1 vaccine. Sera was collected and spleens were harvested at indicated time points to evaluate neutralizing antibody responses and cell-mediated immune responses.

##### 2.6.2.10.2.1. Functional Antibody Response

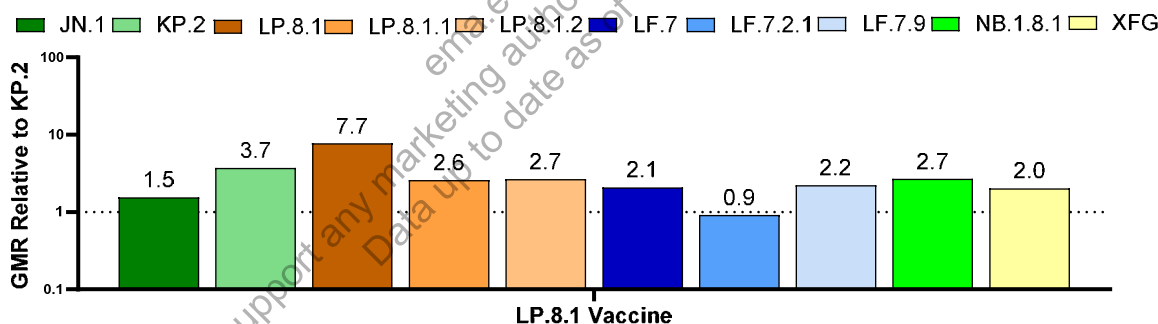
Intramuscular immunization of naïve BALB/c mice with 2 doses of monovalent BNT162b2 LP.8.1 or KP.2 vaccine induced strong neutralizing antibody responses against matched or closely matched sublineages ([Figure 2.6.2-51](#) and [Figure 2.6.2-52](#)). The LP.8.1-adapted vaccine as a 2-dose primary series elicited robust neutralizing antibody response that were 2-to-7.7-fold higher against LP.8.1 sublineages (LP.8.1, LP.8.1.1, and LP.8.1.2), XFG, and NB.1.8.1 compared to those elicited by the KP.2-adapted vaccine. LP.8.1-adapted vaccine immunogenicity against LF.7 sub-lineages (LF.7, LF.7.2.1, and LF.7.9) was similar to responses induced with the KP.2 adapted vaccine.

**Figure 2.6.2-51. Neutralizing Antibody Geometric Mean Titers (GMT) Following Immunization of Naïve Mice with BNT162b2 KP.2 or LP.8.1 as a Primary Series**



Groups of 10 female BALB/c mice were immunized intramuscularly (IM) on Days 0 and 21 with 0.5 µg of BNT162b2 KP.2 or LP.8.1 vaccine. Neutralizing antibody responses against a panel of JN.1 sublineage pseudoviruses were measured by pVNT on Day 49 (1 month post dose 2). The numbers above each bar indicate the 50% neutralization geometric mean titer (GMT).

**Figure 2.6.2-52. Geometric Mean Ratio (GMR) of Neutralizing Antibody GMTs Elicited by the LP.8.1 Vaccine Groups Relative to KP.2 Vaccine**



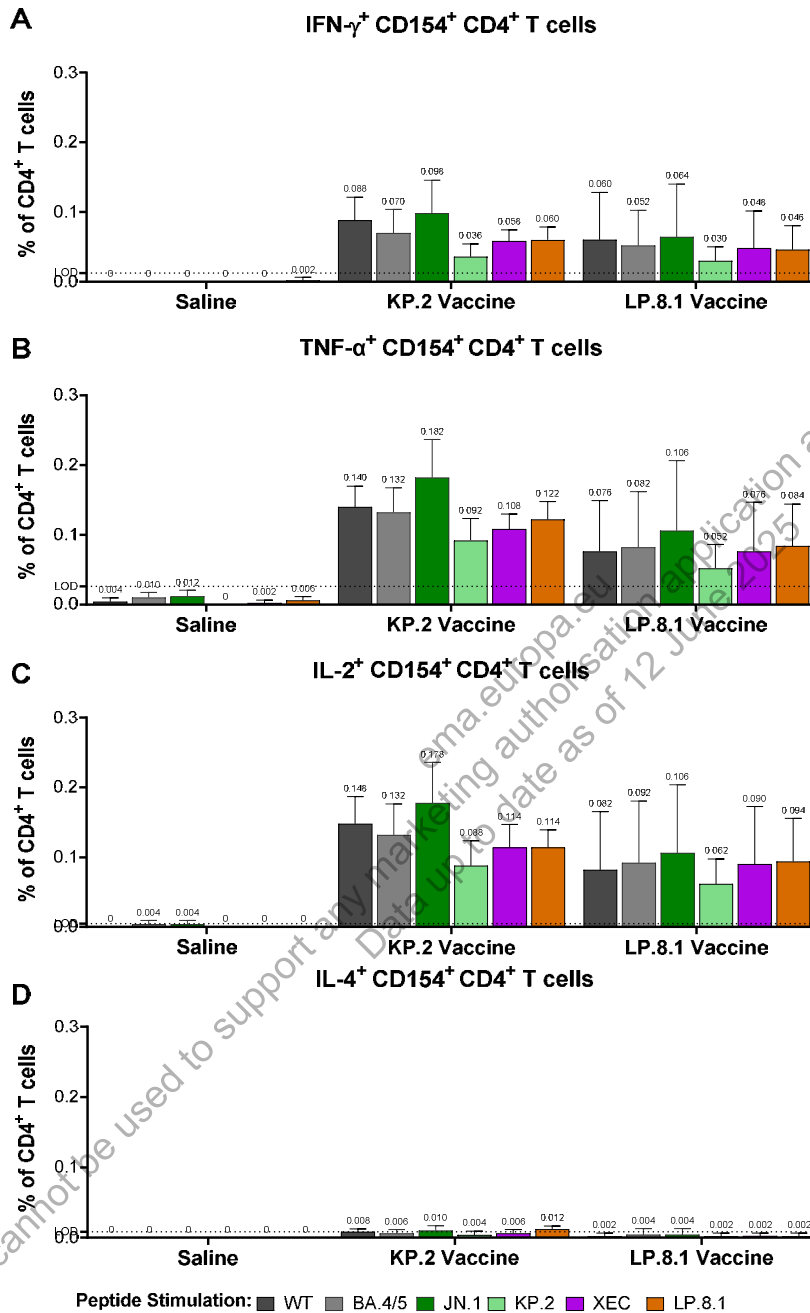
The study details are as described in Figure 2.6.2-51. The number above each bar indicates the geometric mean ratio (GMR). For each pseudovirus strain tested, the GMR is defined as the ratio of the BNT162b2 LP.8.1 vaccine (X axis) GMT to the BNT162b2 KP.2 vaccine GMT.

#### 2.6.2.10.2.2. T Cell Response

SARS-CoV-2 spike-specific T cell responses were assessed in splenocytes by intracellular cytokine staining (ICS) assay at 1 month following administration of the second dose in a primary series where mice received either KP.2- or LP.8.1-adapted vaccines. Peptide pools representing the full-length spike protein from the Wuhan wildtype (WT) virus, BA.4/5, JN.1, KP.2, XEC, or LP.8.1 strains were used to assess variant-specific T cell responses.

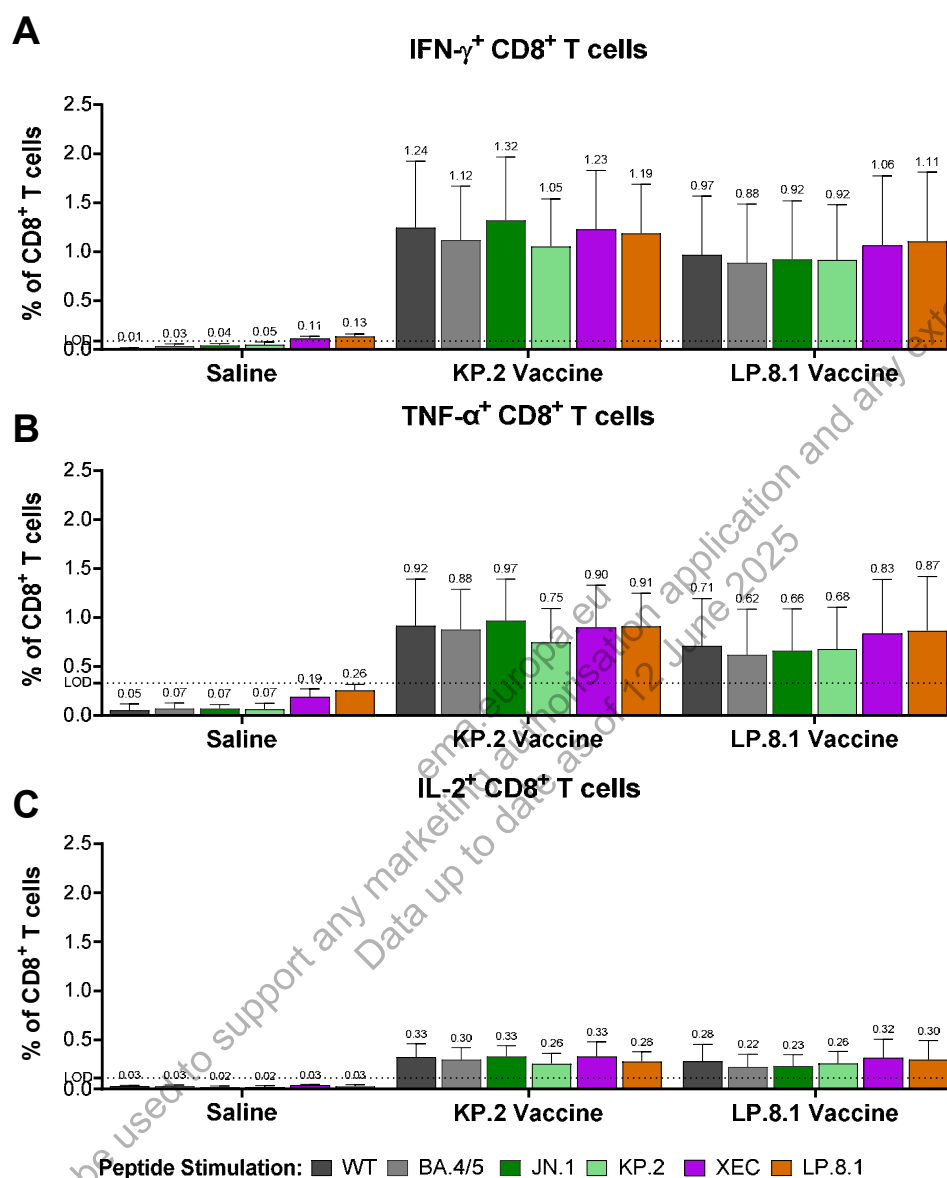
As a primary series, LP.8.1-adapted vaccines elicited similar frequencies of cytokine-expressing (IFN- $\gamma$ , TNF- $\alpha$ , IL-2) CD154<sup>+</sup> CD4<sup>+</sup> T cells (Figure 2.6.2-53) and CD8<sup>+</sup> T cells (Figure 2.6.2-54) compared to KP.2-adapted vaccines. All T cell responses within each vaccination group were similar in magnitude against all strains tested, demonstrating that T cell responses are highly cross-reactive. Finally, IL-4<sup>+</sup> CD4<sup>+</sup> T cell responses were very low across all vaccine groups (Figure 2.6.2-53), indicating that all variant-adapted BNT162b2 immunizations elicit a Th-1-biased response.

**Figure 2.6.2-53. SARS-CoV-2 Spike-Specific CD4<sup>+</sup> T Cell Responses in Spleens Following Immunization of Naïve Mice with BNT162b2 KP.2 or LP.8.1 as a Primary Series**



Groups of 10 female BALB/c mice were immunized intramuscularly (IM) on Days 0 and 21 with 0.5  $\mu$ g of monovalent KP.2- or LP.8.1-adapted vaccine. Each group had 5 spleens harvested on Day 49 (1 month post dose 2). CD4<sup>+</sup> T cell responses were measured by intracellular cytokine staining (ICS) following ex vivo stimulation of splenocytes with Wild-type (dark grey), BA.4/5 (light grey), JN.1 (dark green), KP.2 (light green), XEC (purple), and LP.8.1 (orange) peptide pools. Bars depict the mean frequency with standard deviation (SD).

**Figure 2.6.2-54. SARS-CoV-2 Spike-Specific CD8<sup>+</sup> T Cell Responses in Spleens Following Immunization of Naïve Mice with BNT162b2 KP.2 or LP.8.1 as a Primary Series**



Groups of 10 female BALB/c mice were immunized intramuscularly (IM) on Days 0 and 21 with 0.5  $\mu$ g of monovalent KP.2- or LP.8.1-adapted vaccine. Each group had 5 spleens harvested on Day 49 (1 month post dose 2). CD8<sup>+</sup> T cell responses were measured by intracellular cytokine staining (ICS) following ex vivo stimulation of splenocytes with Wild-type (dark grey), BA.4/5 (light grey), JN.1 (dark green), KP.2 (light green), XEC (purple), and LP.8.1 (orange) peptide pools. Bars depict the mean frequency with standard deviation (SD).

### 2.6.2.11. BNT162b2 Vaccine Immunogenicity and Evaluation of Protection Against SARS-CoV-2 Challenge in Rhesus Macaques

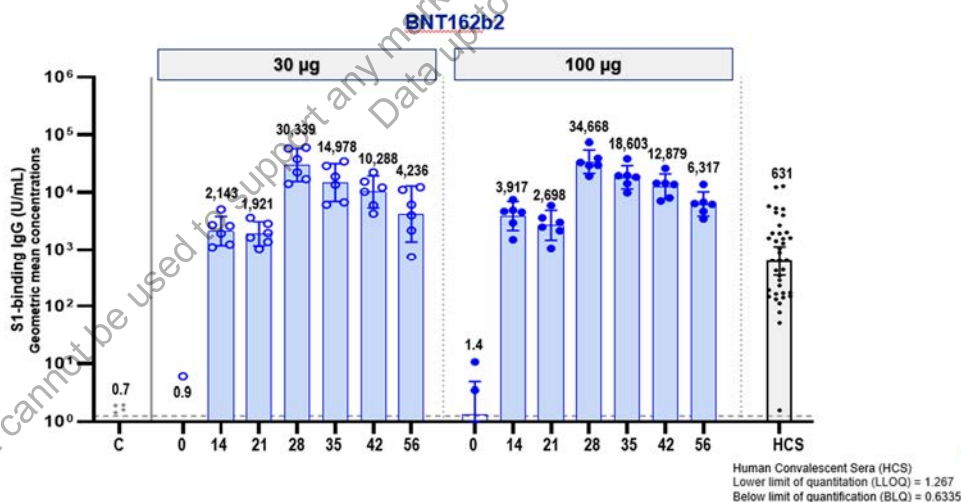
The ability of BNT162b2 immunization to protect rhesus macaques from live SARS-CoV-2 challenge was evaluated in 2–4 year old male rhesus macaques (VR-VTR-10671).

#### 2.6.2.11.1. Immunogenicity in Rhesus Macaques

Groups of 2-4 year old male rhesus macaques were immunized IM with 30 or 100 µg of BNT162b2 or saline control on Days 0 and 21. S1-binding IgG was readily detectable after a single immunization, and levels increased further seven days after the second immunization (Day 28) to geometric mean S1-binding IgG concentrations (GMCs) of 30,339 units (U)/mL (30 µg dose level) and 34,668 U/mL (100 µg dose level) (Figure 2.6.2-55). For comparison, the GMC of a panel of 38 SARS-CoV-2 convalescent human sera was 631 U/mL, substantially lower than the GMC of the immunized rhesus macaques after one or two doses.

Human convalescent sera (HCS) were drawn from SARS-CoV-2 infected individuals 18 to 83 years of age, at least 14 days after PCR-confirmed diagnosis, and at a time when individuals were asymptomatic. The serum donors predominantly had symptomatic infections (35/38), and one had been hospitalized. Based on the assumptions that the immune response to SARS-CoV-2 infection provides some measure of protection from disease upon subsequent exposure to the virus and that the neutralizing antibody response contributes to that protection, the neutralizing antibody titer of the convalescent serum panel provides a currently assessable benchmark to judge the quality of the immune response to the vaccine candidates.

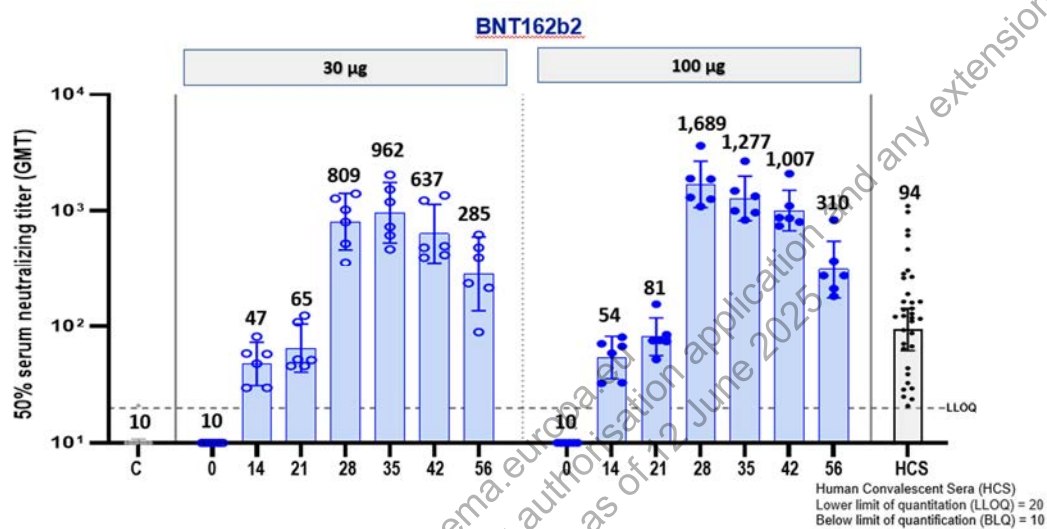
**Figure 2.6.2-55. S1-Binding IgG Levels Elicited by Immunization of Rhesus Macaques With BNT162b2**



S1-binding IgG concentrations elicited by immunization of rhesus macaques with BNT162b2. Numbers on the x-axis indicate the day post first immunization. Heights of bars indicate geometric mean concentrations (GMCs) in arbitrary units, which are written above the bars; whiskers indicate 95% CIs; dots represent individual monkey IgG concentrations. Dotted line indicates the lower limit of quantification (LLOQ 1.151 U/mL). Values at or below LLOQ were set to ½ LLOQ. C – saline-immunization control; HCS – human convalescent serum panel.

Fifty percent neutralization titers ( $VNT_{50}$ ), measured by an authentic SARS-CoV-2 neutralization assay (Muruato et al, 2020), were detectable in rhesus sera by Day 14 after a single immunization and peaked at geometric mean titers (GMTs) of 962 (on Day 35, 14 days after Dose 2 of 30  $\mu$ g) or 1,689 (on Day 28, 7 days after Dose 2 of 100  $\mu$ g; Figure 2.6.2-56). Robust neutralization GMTs of 285 for 30  $\mu$ g and 310 for 100  $\mu$ g dose levels persisted to at least Day 56 (most recent time point tested). For comparison, the 50% neutralization GMT of the human convalescent serum panel was 94.

**Figure 2.6.2-56. 50% Serum Neutralizing Titers Elicited by Immunization of Rhesus Macaques With BNT162b2**



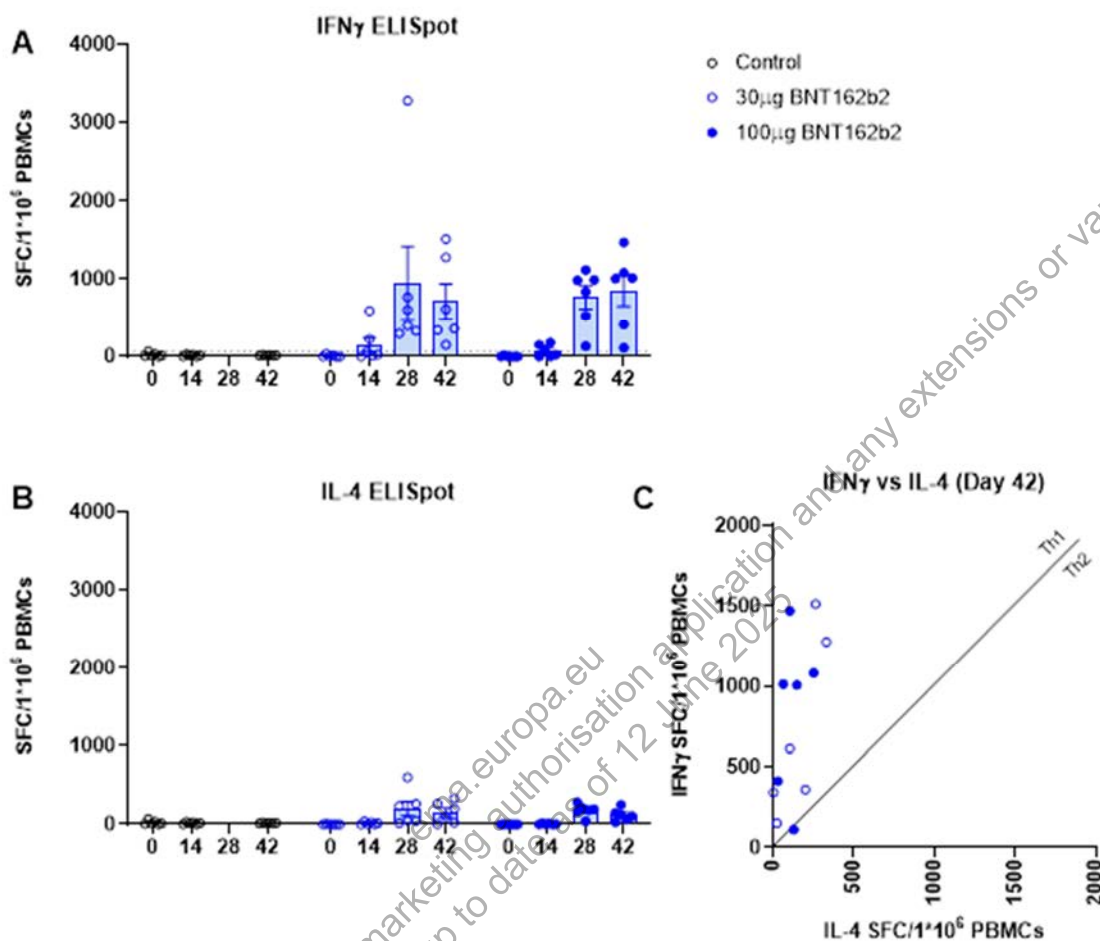
Numbers on the x-axis indicate the day post first immunization. Heights of bars indicate GMTs, which are written above the bars; whiskers indicate 95% confidence intervals; dots represent individual monkey titers. LLOQ = 20. Titers at or below LLOQ were set to  $\frac{1}{2}$  LLOQ. C – saline-immunization control; HCS – human convalescent serum panel.

Antigen-specific T cell responses play an important role in generation of antigen-specific antibody response as well as in elimination of infected cells to mediate protection against disease. S-specific T cell responses were analyzed in animals immunized with 30  $\mu$ g or 100  $\mu$ g of BNT162b2 and unimmunized controls (Control) by ELISpot and intracellular cytokine staining (ICS). PBMCs were collected before immunization (Day 0), 14 days post dose 1, 7 days post dose 2, and 21 days post dose 2.

S-specific T cells were low to undetectable in naïve animals. Strong  $IFN\gamma$  ELISpot responses but minimal IL-4 ELISpot responses were detected after the second 30 or 100  $\mu$ g dose of the vaccine candidate (Figure 2.6.2-57). ICS confirmed that BNT162b2 elicited strong S-specific  $IFN\gamma$  producing T cell responses, including a high frequency of CD4<sup>+</sup> T cells that produced  $IFN\gamma$ , IL-2, or TNF- $\alpha$  but a low frequency of CD4<sup>+</sup> T cells that produce IL-4, indicating a Th1-biased response (Figure 2.6.2-58A through D). BNT162b2 also elicited S-specific  $IFN\gamma$  producing CD8<sup>+</sup> T cell responses (Figure 2.6.2-58E).

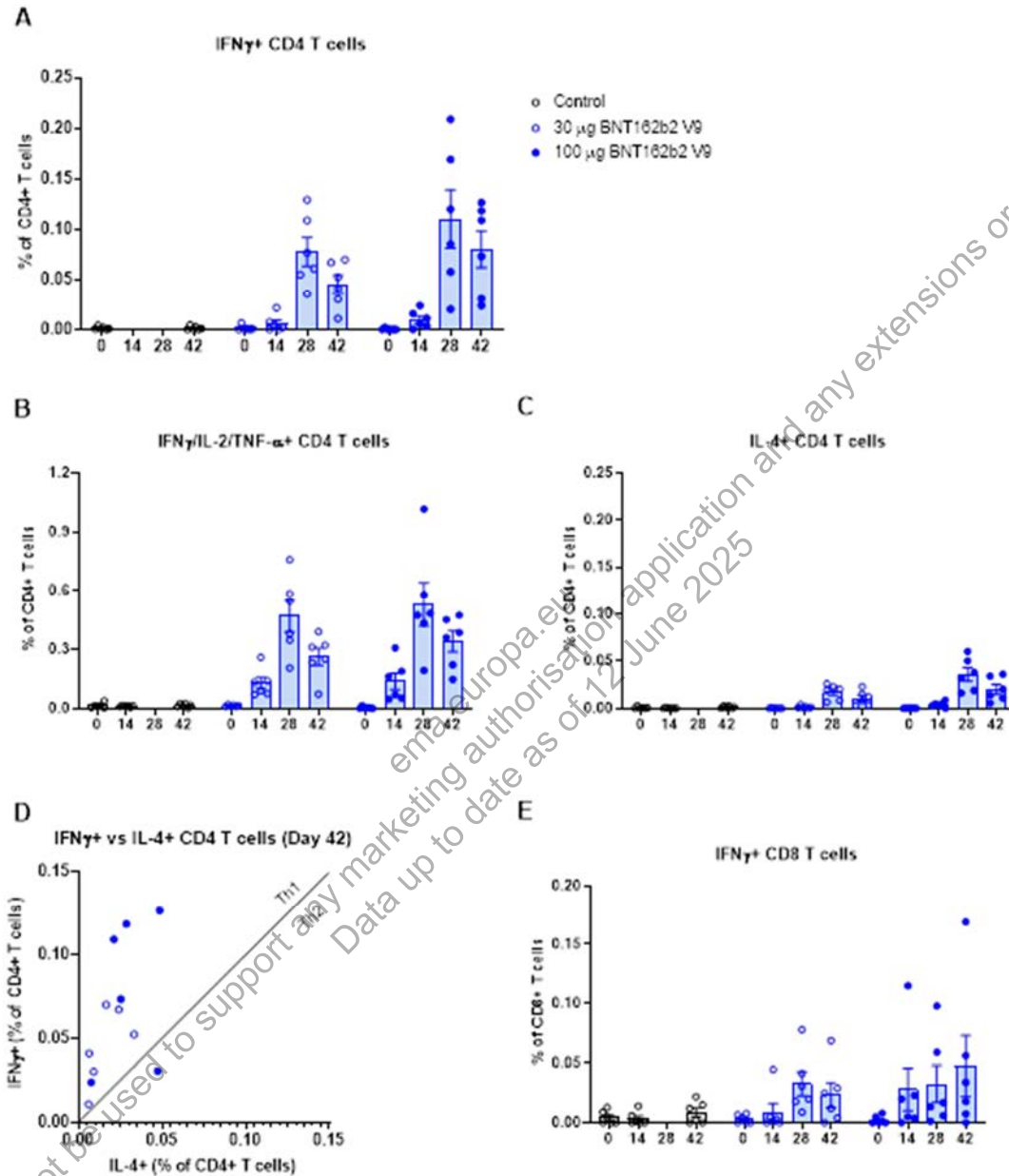


**Figure 2.6.2-57. IFN $\gamma$  and IL-4 ELISpot Results in BNT162b2 Immunized Animals**



Groups of six 2-4 year old rhesus macaques were immunized on Days 0 and 21 with 30 or 100  $\mu$ g BNT162b2 or buffer (Placebo). Height of bars indicates the mean; whiskers indicate the standard error of mean (SEM); and each symbol represents one animal. Dotted lines mark the lower limit of detection. (A) IFN $\gamma$  (B) IL-4 ELISpot analysis. (C) Correlation of frequency of IFN $\gamma$  or IL-4 producing cells 21 Days post dose 2.

**Figure 2.6.2-58. S-Specific CD4+ and CD8+ T Cell Response in BNT162b2 Immunized Animals as Measured by ICS Assay**



Height of bars indicates the mean; whiskers indicate the standard error of mean (SEM); and each symbol represents one animal. (A) Frequency of IFN $\gamma$ + CD4+ T cells. (B) Frequency of IFN $\gamma$ /IL-2/TNF- $\alpha$ + CD4+ T cells (C) Frequency of IL-4+ CD4+ T cells. (D) Correlation of frequency of IFN $\gamma$  or IL-4+ CD4+ T cells at 21 Days post dose 2. (E) Frequency of IFN $\gamma$ + CD8+ T cells.

#### 2.6.2.11.2. SARS-CoV-2 Challenge of BNT162b2-Immunized Nonhuman Primates

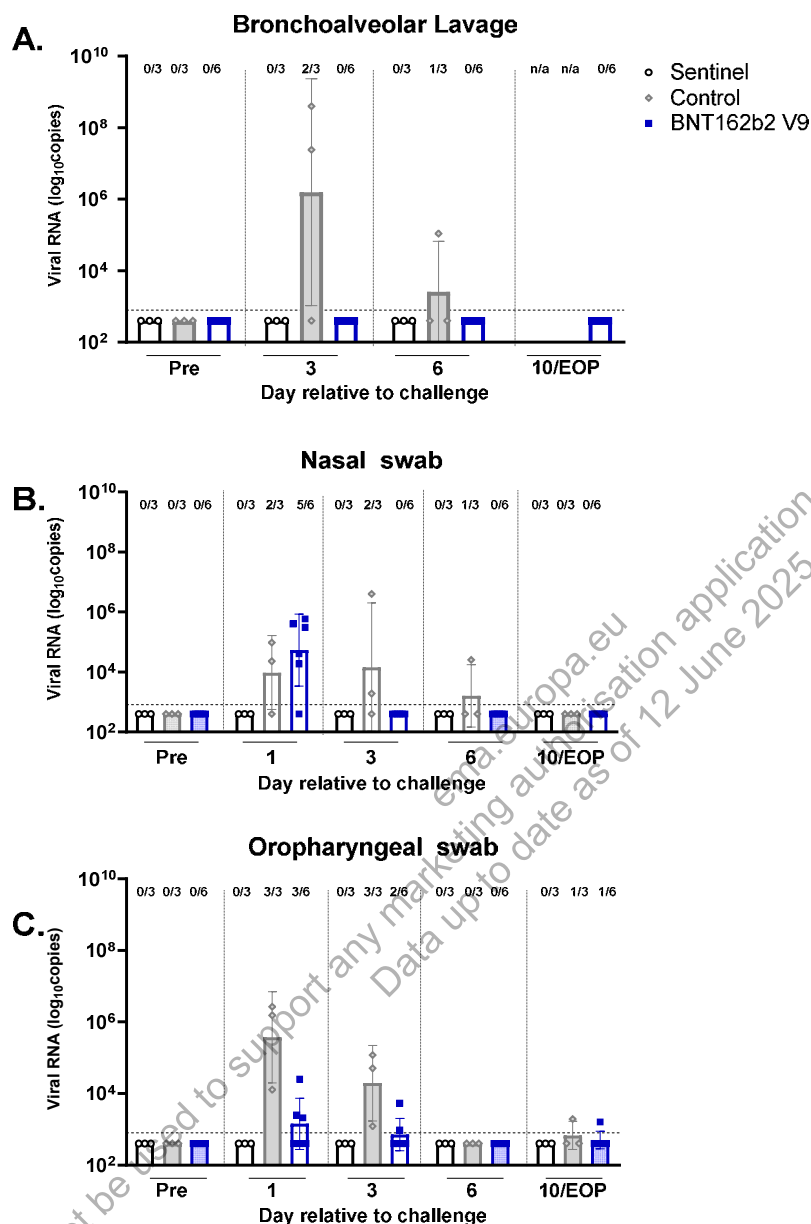
SARS-CoV-2 infection and COVID-19 in humans present diverse manifestation of signs, symptoms, and severity. Based on published reports, SARS-CoV-2 challenged rhesus macaques develop an acute, transient infection in the upper and lower respiratory tract and have evidence of viral replication in the gastrointestinal tract, similar to humans (Zou et al, 2020; Kim et al, 2020). Varying degrees of pulmonary inflammation, primarily at the peak of infection at approximately Day 2 to 4 post-challenge, have been reported in the literature (Munster et al, 2020). The human and rhesus ACE-2 receptor have 100% amino acid identity at the critical binding residues, which may account for the fidelity of this SARS-CoV-2 animal model (Zhou et al, 2020).

The groups of 2-4 year old male rhesus macaques that had received two intramuscular immunizations with 100 µg BNT162b2 (n=6) or buffer (Control; n=3) 21 days apart (described in Section 2.6.2.11.1) were challenged 55 days after the second immunization with  $1.05 \times 10^6$  plaque forming units of SARS-CoV-2 (strain USA-WA1/2020), split equally between the intranasal and intratracheal routes, as previously described (Singh et al, 2021). Three additional non-immunized, age-matched, rhesus macaques (sentinel) were mock-challenged with cell culture medium. Nasal and oropharyngeal (OP) swabs were collected and bronchoalveolar lavage (BAL) was performed at the times indicated, and the samples were tested for the presence of SARS-CoV-2 RNA (genomic RNA and subgenomic transcripts) by reverse-transcription quantitative polymerase chain reaction (RT-qPCR; Figure 2.6.2-59). All personnel performing the clinical, radiographic, histopathologic, and RT-qPCR evaluations were blinded to the group assignments of the macaques (VR-VTR-10671).

All samples obtained before the infectious challenge and all those obtained from sentinel animals lacked detectable SARS-CoV-2 RNA (Figure 2.6.2-59). Viral RNA was detected in BAL fluid from 2 of the 3 control-immunized macaques on Day 3 after challenge and from 1 of 3 on Day 6. At no time point sampled was viral RNA detected in BAL fluid from the BNT162b2-immunized and SARS-CoV-2 challenged macaques (Figure 2.6.2-59A). The difference in viral RNA detection in BAL fluid between BNT162b2-immunized and control-immunized rhesus macaques after challenge is statistically significant ( $p=0.0014$ ).

From control-immunized macaques, viral RNA was detected in nasal swabs obtained on Days 1, 3, and 6 after SARS-CoV-2 challenge; from BNT162b2-immunized macaques, viral RNA was detected only in nasal swabs obtained on Day 1 after challenge and not in swabs obtained on Day 3 or subsequently (Figure 2.6.2-59B). The pattern of viral RNA detection from OP swabs was similar to that for nasal swabs (Figure 2.6.2-59C).

**Figure 2.6.2-59. Viral RNA in BAL Fluid and Nasal and Oropharyngeal Swabs of Rhesus Macaques After Infectious SARS-CoV-2 Challenge**

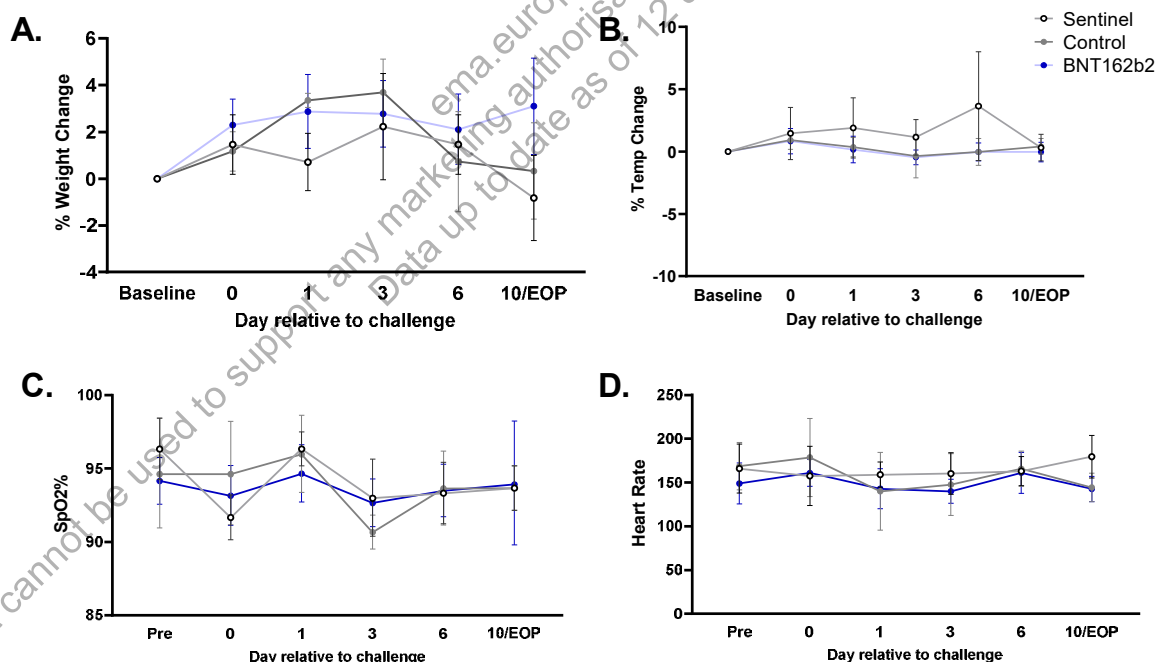


Groups of 2-4 year old rhesus macaques were immunized on Days 0 and 21 with 100 µg BNT162b2 (n=6), or buffer (Control; n=3). Fifty-five days after the second immunization, the animals were challenged with  $1.05 \times 10^6$  PFU of SARS-CoV-2 split equally between the IN and IT routes. Three age-matched male rhesus macaques were unimmunized and challenged with cell culture medium only (Sentinel). Viral RNA levels were detected by RT-qPCR in A) bronchoalveolar lavage, B) nasal swabs, and C) oropharyngeal swabs. EOP, end of project. Values below the LLOD set to  $\frac{1}{2}$  the LLOD. The viral RNA levels between control-immunized and BNT162b2-immunized animals after challenge were compared by a non-parametric analysis (Friedman's test), and the p-values are 0.0014 for BAL fluid, 0.2622 for nasal swabs, and 0.0007 for OP swabs. The Friedman's test is a non-parametric analysis based on the ranking of viral RNA shedding data within each day. PROC RANK and PROC GLM from SAS® 9.4 were used to calculate the p-values.

Despite the presence of viral RNA in BAL fluid from challenged control animals, none of the challenged animals, immunized or control, showed clinical signs of illness (Figure 2.6.2-60), indicating that the 2-4 year old male rhesus monkey challenge model appears to be an infection model, but not a clinical disease model. Lung radiograph (Figure 2.6.2-61A) and computerized tomography (CT) (Figure 2.6.2-61B) scores were determined by two board-certified veterinary radiologist who were blinded to treatment group. Data in Figure 2.6.2-61 represent the average of the two scores. Radiographic evidence of pulmonary abnormality was observed in challenged controls but not in challenged BNT162b2-immunized animals nor in unchallenged sentinels. No radiographic evidence of vaccine-elicited enhanced disease was observed. At necropsy on Day 7 or 8 after virus challenge, there were no significant gross pathology findings in any organs. Microscopically, the main finding in the lung was inflammation. The lung inflammation area score was similar between saline-immunized and BNT162b2-immunized animals, and there was no evidence of enhanced respiratory disease (Figure 2.6.2-62).

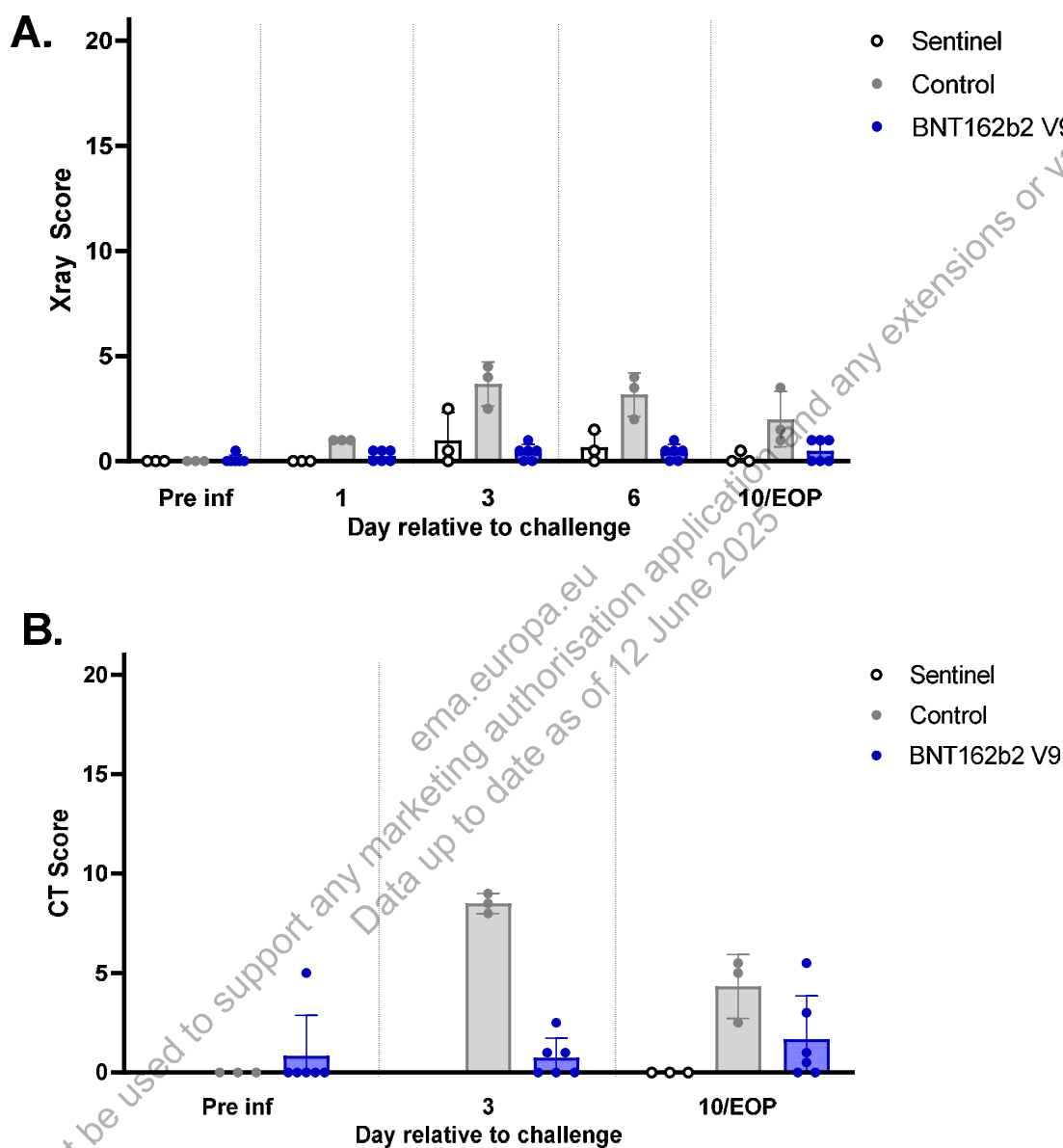
Overall, these data demonstrate that, compared to control, BNT162b2 immunization provided complete protection in the lungs from infectious SARS-CoV-2 challenge in rhesus macaques with no evidence of vaccine-elicited disease enhancement.

**Figure 2.6.2-60. Clinical Signs in Rhesus Macaques After Immunization With BNT162b2 and Challenge With Infectious SARS-CoV-2**



Rhesus macaques were immunized with BNT162b2, or saline, and challenged with SARS-CoV-2 or cell culture medium as described in the Figure 2.6.2-59 legend. Clinical signs were recorded on the days indicated. EOP, end of project. BNT162b2-immunized (n=6), control (n=3), and sentinel (n=3) macaques. (A) Body weight. (B) Temperature. (C) Oxygen saturation. (D) Heart rate.

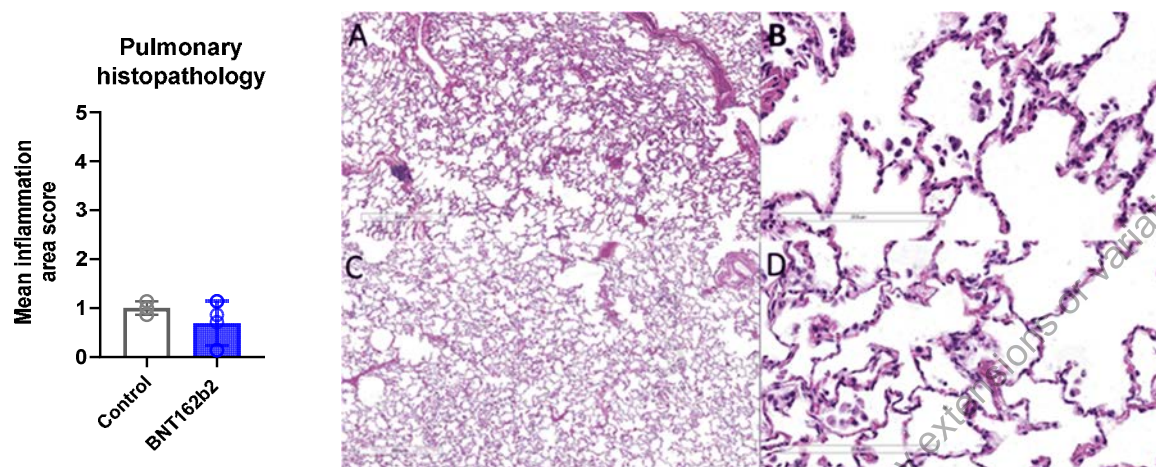
**Figure 2.6.2-61. Radiograph and CT Scores of Rhesus Macaque Lungs After Infectious SARS-CoV-2 Challenge**



Fifty-five days after the second immunization, BNT162b2 or Control (saline)-immunized animals were challenged with  $1.05 \times 10^6$  PFU of SARS-CoV-2 split equally between the IN and IT routes. Three age-matched unimmunized rhesus macaques were challenged with cell culture medium only (Sentinel). Chest X-rays and CT scans were performed prior to challenge and at the times indicated on the x-axis. EOP, end of project. Radiograph (A) and CT (B) scores were assigned to a total of 7 regions on a scale of 1-20. Images were evaluated by two board-certified veterinary radiologists blinded to treatment group. Individual data points represent the average of the two scores. The height of the bars indicates the mean score. Error bars indicate the standard deviation.



**Figure 2.6.2-62. Lung Inflammation Area Score After IN/IT SARS-CoV-2 Challenge**



Graph (left panel): Lung inflammation area score on Day 7 or 8 after IN/IT SARS-CoV-2 challenge. Each data point represents the mean lung inflammation area score of a single animal (mean score of the 7 lung lobes). Saline-immunized and challenged animals (Control; n=3) are shown in grey and BNT162b2-vaccinated and challenged animals (BNT162b2; n=6) are shown in blue. Each dot represents the inflammation mean area score for an individual animal. Bars indicate the geometric mean area scores within each group. Photomicrographs (right panel; 2.5x objective, A and C; 20x objective, B and D) of hematoxylin and eosin-stained lung sections from Control animals (A and B) and lungs from BNT162b2-immunized and challenged animals (C and D).

#### 2.6.2.12. Immunogenicity Testing of Rats in the GLP Compliant Repeat Dose Toxicity Studies and Developmental and Reproductive Toxicity Study

Immunogenicity results from two GLP-compliant repeat-dose toxicity studies as well as a DART study ([Study 20256434](#)) with BNT162b2 are presented below.

##### 2.6.2.12.1. Repeat-Dose Toxicity Study of Three LNP-Formulated RNA Platforms Encoding for Viral Proteins by Repeated Intramuscular Administration to Wistar Han Rats

The immunogenicity of BNT162b2 in the GLP-compliant repeat-dose rat toxicity study ([Study 38166](#)) was analyzed.

Male and female Wistar Han rats received three weekly doses of 100 µg of BNT162b2. Serum samples were collected and analyzed (5 animals/sex) from main study animals on Day 17, two days after the third administration, at the end of the dosing phase as well as from recovery cohorts at the end of the study on Day 38. Treatment with the BNT162b2 vaccine elicited binding IgG against the S1 fragment and the RBD of SARS-CoV2 S. There was a strong antibody response at both analyzed time points. The group mean IgG concentration against S1 and RBD are given in [Table 2.6.2-7](#). Antibody concentrations against S1 and RBD increased over time.



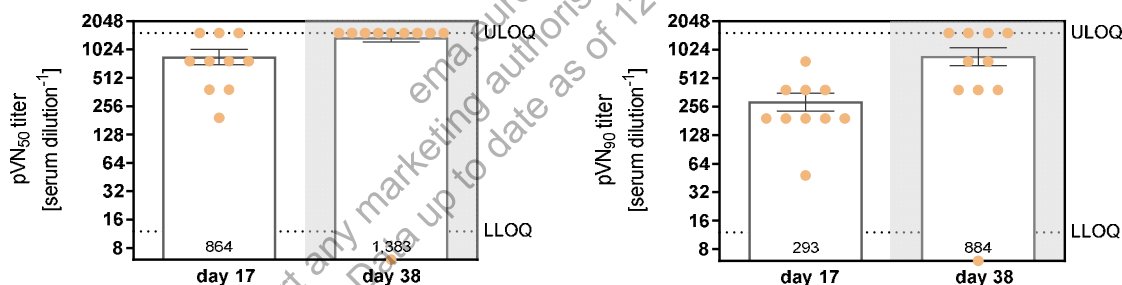
**Table 2.6.2-7. IgG Antibody Concentration [mg/mL] Against the Viral Antigen in Wistar Han Rats After BNT162b2 Immunization**

		BNT162b2 (100 µg)
17 days after first immunization	Against S1	1.76 ± 0.16
	Against RBD	2.33 ± 0.19
38 days after first immunization	Against S1	3.46 ± 0.52
	Against RBD	4.90 ± 0.87

Pseudovirus neutralization results mirrored the antigen binding results.

Treatment of rats with BNT162b2 resulted in the elicitation of neutralizing antibodies against pseudovirus infection. Neutralizing antibody titers in vaccinated animals increased over time with the recorded neutralizing activity being consistent with the ELISA data shown above. Serum titers resulting in 50% pseudovirus neutralization exceeded the upper limit of quantification (ULOQ) of a reciprocal titer of 1536 in more than 8 out of 10 animals on Day 38, and therefore a neutralization titer of 90% was evaluated as well (Figure 2.6.2-63).

**Figure 2.6.2-63. Pseudovirus Neutralization Activity in Rats After BNT162b2 Immunization**



Wistar Han rats were immunized IM with three weekly injections of 100 µg BNT162b2. On Day 17 and Day 38, animals were bled, and the sera were tested for titers of pseudovirus neutralizing antibodies. Individual titers resulting in 50% pseudovirus neutralization (pVNT<sub>50</sub>, left graph) or 90% pseudovirus neutralization (pVNT<sub>90</sub>, right graph) are shown by dots; group mean values are indicated by horizontal bars and are included in the figure (±SEM, standard error of the mean). Group size for analysis was n=5 male and n=5 female rats. Mean titers are given in the bars. All control serum samples were below the lower limit of quantification (LLOQ); ULOQ = upper limit of quantification.

#### 2.6.2.12.2. 17-Day Intramuscular Toxicity Study of BNT162b2 in Wistar Han Rats With a 3-Week Recovery

The immunogenicity of the COVID-19 vaccine BNT162b2 in the GLP compliant repeat-dose rat toxicity study ([Study 20GR142](#)) was analyzed. The summary of the results described below will focus on only BNT162b2.

Wistar Han rats (15/sex/group) were administered IM doses of 0 (saline) or 30 BNT162b2 µg RNA/dose per animal. Doses were administered once a week for 3 weeks (Days 1, 8, and 15). Following the dosing phase, 10 animals/sex from each group were euthanized 2 days post last immunization for post-mortem assessments. The remaining 5 animals/sex/group were euthanized following a 3-week recovery phase.

Administration of 3 once-weekly doses of BNT162b2 elicited SARS-CoV-2 neutralizing antibody responses in males and females at the end of the dosing (Day 17) and recovery (Day 21) phases of the study. SARS-CoV-2 neutralizing antibody responses were not observed in animals prior to vaccine administration or in saline-administered control animals (Table 2.6.2-8).

**Table 2.6.2-8. Group Mean Titers of SARS-CoV-2 Neutralizing Antibodies**

Study Day	Sex	Saline (0 µg RNA)	BNT162b2 (30 µg RNA)
Prior to Dosing Initiation (Day -5)	Male	5	5
	Female	5	5
End of Dosing Phase (Day 17)	Male	5	1114
	Female	5	2501
End of Recovery Phase (RP Day 21)	Male	5	5120
	Female	5	5120

RP = Recovery phase.

#### 2.6.2.12.3. A Combined Fertility and Developmental Study (Including Teratogenicity and Postnatal Investigations) of BNT162b1, BNT162b2 and BNT162b3 by Intramuscular Administration in the Wistar Han Rat

The immunogenicity of the COVID-19 vaccine candidate BNT162b2 in the GLP compliant DART ([Study 20256434](#)) was analyzed. The summary of the results described below will focus on only BNT162b2.

Female Wistar Han rats (44 animals/group) were administered saline or 30 µg RNA/dosing day of BNT162b2 by IM injection for a total of 4 doses (21 and 14 days prior to mating and on GDs 9 and 20). On GD 21, half of the females in each group underwent Cesarean section. The remaining females in each group were allowed to naturally deliver their pups and both maternal animals and their offspring were monitored out through the end of weaning (LD 21/PND 21). SARS-CoV-2 neutralizing antibodies were assessed in maternal animals prior to mating, on GD 21, and LD 21 as well as in fetuses on GD 21 and in pups on PND 21.

BNT162b2 elicited SARS-CoV-2 neutralizing antibody responses in all of the females just prior to mating (M 0), at the end of gestation (GD 21), and at the end of lactation (LD 21). SARS-CoV-2 neutralizing titers were detected in all offspring (fetuses on GD 21 and pups on PND 21). SARS-CoV-2 neutralizing antibody titers were not observed in animals prior to vaccine administration or in saline-administered control animals (Table 2.6.2-9).

**Table 2.6.2-9. Group Mean Titers of SARS-CoV-2 Neutralizing Antibodies**

Interval/Occasion	Saline (0 µg RNA)	BNT162b2 (30 µg RNA)
Prior to Dosing Initiation	5.0	5.3
Just Prior to Mating	5.0	3886.4
Gestation Day 21 (Dams)	5.0	3445.5
Lactation Day 21	5.0	3620.4
Fetuses (Gestation Day 21)	5.0	640.0
Pups (Postnatal Day 21)	5.0	4561.4

#### 2.6.2.13. Secondary Pharmacodynamics

No secondary pharmacodynamics studies were conducted with BNT162b2.

#### 2.6.2.14. Safety Pharmacology

No safety pharmacology studies were conducted with BNT162b2 as they are not considered necessary according to the WHO guideline (WHO, 2005).

#### 2.6.2.15. Pharmacodynamic Drug Interactions

Pharmacodynamic drug interaction studies with BNT162b2 have not been conducted.

#### 2.6.2.16. Discussion and Conclusions

The BNT162b2 vaccine candidate encoding the full-length P2 S induces an overall potent immune response in mice, rats and nonhuman primates. SARS-CoV-2 S is a primary target of neutralizing antibodies, and the modRNA that encodes the vaccine antigen induces a strong neutralizing antibody response. This is explained partly by data that show the recombinant form of the P2 S antigen encoded by the vaccine and transiently expressed on the surface of mammalian cells exhibits high affinity binding to a soluble ACE-2 receptor and to SARS-CoV-2 neutralizing monoclonal antibodies. Analysis of the P2 S trimer structure by cryogenic electron microscopy revealed high similarity to previously reported P2 S structures. The well-resolved trimeric prefusion structure and the high affinity binding to ACE-2 and human neutralizing antibodies demonstrate that the recombinant full-length P2 S authentically presents the ACE-2 binding site and other epitopes targeted by many SARS-CoV-2 neutralizing antibodies.

Nonclinical studies of the Original BNT162b2 vaccine in mice and nonhuman primates showed that both antigen-binding IgG and neutralizing antibody responses were detectable as early as 14 days post-immunization, with substantial increases after the second dose. Similar

results indicating robust immunogenicity were obtained in an accessory study to the GLP-compliant repeat-dose toxicology studies in rats ([Study 38166](#) and [Study 20GR142](#)) and DART study ([Study 20256434](#)). In a SARS-CoV-2 rhesus challenge model, BNT162b2 Original provided partial protection from infection in the upper airway, and no viral RNA was detected in the lower airways, sampled serially by BAL starting 3 days after challenge. No evidence of disease enhancement was observed in BNT162b2-immunized and SARS-CoV-2 challenged macaques ([VR-VTR-10671](#)).

Nonclinical mouse studies of variant-adapted formulas of BNT162b2, showed elicitation of potent neutralizing antibody responses against strains matched and closely-matched to the respective vaccine, when the vaccine was administered either as a two dose primary series or as an additional dose in BNT162b2-experienced mice. Similar to data with the original BNT162b2, variant-adapted vaccines also elicited a strong Th1-type CD4<sup>+</sup> T cell response and a CD8<sup>+</sup> IFN $\gamma$  response. Th1-type CD4<sup>+</sup> T cell response, and a CD8<sup>+</sup> IFN $\gamma$  response.

Overall, nonclinical studies of the variant-adapted BNT162b2 formulas in mice demonstrate that the more closely matched the vaccine composition is to the strains tested in humoral and cellular immune assays, the more robust the responses that are elicited. This diversity of elicited immune mechanisms could block virus infection as a first line of defense and clear virus-infected cells as a second line of defense.

This pattern has been consistently observed throughout multiple variant-adapted vaccine updates, including for Omicron BA.4/5, XBB.1.5, JN.1 and KP.2 adapted vaccines, as per the data presented here. Additionally, variant-adapted vaccines, such as the LP8.1-adapted vaccine, not only elicit potent neutralization of the vaccine-encoded matched variants but also elicit similar neutralizing responses against broad panels of pseudoviruses that derive from the parental variant, thus indicating a cross-neutralizing response that is likely to confer clinical protection against antigenically drifted subvariants, as has been observed for prior variant-adapted vaccines.

#### **2.6.2.17. Immunogenicity and Efficacy Methods**

##### **2.6.2.17.1. SARS-CoV-2 S1 and RBD Direct ELISA**

For preclinical studies in mice, antigen-based direct ELISAs measured S1-binding (S1 recombinant protein, Sino Biological) and RBD-binding (recombinant RBD, Sino Biological) IgG levels in serum samples. MaxiSorp plates (Thermo Fisher Scientific) were coated with recombinant protein (100 ng/100  $\mu$ L) in sodium carbonate buffer, and bound IgG was detected using an HRP-conjugated secondary antibody and TMB substrate (Biotrend). Data collection was performed using a BioTek Epoch reader and Gen5 software version 3.0.9. For concentration analysis, the signal of the specific samples was correlated to a standard curve of an isotype control.

##### **2.6.2.17.2. VSV/SARS-CoV-2 S Pseudovirus Neutralization Assay**

For preclinical immunogenicity studies in rodents, a pseudotype neutralization assay (pVNT) was used as a surrogate of virus neutralization (which, for SARS-CoV-2, requires BSL3 containment). The pVNT is based on a recombinant replication-deficient vesicular stomatitis virus (VSV) vector that encodes GFP instead of VSV-G (VSV $\Delta$ G-GFP). VSV $\Delta$ G-GFP was

pseudotyped with SARS-CoV-2 S protein according to published pseudotyping protocols. Serial dilutions of mouse sera were incubated with 300 PFU per well pseudotyped virus for 60 minutes at 37°C incubator before inoculating Vero cell monolayers in 96 well plates, after which additional media was supplemented onto the plates. The plates were then incubated for an additional 20 hours. At end of incubation, the plates were fixed with methanol for 10 minutes and stained with a rabbit anti-VSV-M [23H12] (Absolute Antibody, catalog# Ab01404-23.0) primary antibody followed by Alexa 488 conjugated Goat anti-Rb IgG (ThermoFisher, catalog# A-11008) secondary antibody to detect viral foci. The 50% neutralization titer is calculated as the last reciprocal serum dilution at which 50% of the virus is neutralized compared to wells containing virus only.

#### **2.6.2.17.3. SARS-CoV-2 S1-Binding and RBD-Binding Kinetics Using Surface Plasmon Resonance Spectroscopy**

Binding kinetics of murine S1- and RBD-binding serum IgGs was determined using a Biacore T200 device (Cytiva). An anti-mouse-Fc antibody (Jackson ImmunoResearch) was covalently coupled to immobilization level of ~10,000 response units (RU) on the CM5 sensor chip matrix. Bulk mouse IgGs were captured from diluted serum and binding analyses to histidine-tagged S1 (S1-His) or histidine-tagged RBD (RBD-His) (Sino Biological) were performed using a multi-cycle kinetic method with concentrations ranging from 25 to 400 nM or 1.5625 to 50 nM, respectively. Binding kinetics were calculated using a global kinetic fit to a 1:1 Langmuir model with Biacore T200 Evaluation Software Version 3.1 (Cytiva).

#### **2.6.2.17.4. SARS-CoV-2 S1-Binding IgG Luminex Assay**

For nonhuman primate studies, a direct binding Luminex immunoassay (dLIA) was used to quantify S1-binding serum IgG levels ([VR-MQR-10211](#)). A recombinant SARS-CoV-2 S1 with a C-terminal Avitag™ (Acro Biosystems) was bound to streptavidin-coated Luminex microspheres. Bound nonhuman primate S1-binding IgG was detected with a R-Phycoerythrin-conjugated goat anti-human polyclonal secondary antibody (Jackson Labs). Data were captured as median fluorescent intensities (MFIs) using a Luminex reader and converted to U/mL antibody concentrations using a reference standard curve with arbitrary assigned concentrations of 100 U/mL and accounting for the serum dilution factor. Assay results were reported in U/mL of IgG.

#### **2.6.2.17.5. SARS-CoV-2 Neutralization Assay**

For nonhuman primate studies, the same authentic SARS-CoV-2 neutralization assay used for clinical testing was applied ([VR-MQR-10214](#)). The SARS-CoV-2 neutralization assay used a previously described strain of SARS-CoV-2 (USA\_WA1/2020) that had been rescued by reverse genetics and engineered by the insertion of an mNeonGreen (mNG) gene into open reading frame 7 of the viral genome ([Xie et al, 2020](#)). This reporter virus generates similar plaque morphologies and indistinguishable growth curves from wild type virus ([Murua et al, 2020](#)). Viral master stocks used for the neutralization assay were grown in Vero E6 cells as previously described ([Xie et al, 2020](#)). Serial dilutions of heat inactivated sera were incubated with the reporter virus for 1 hour at 37°C before inoculating Vero CCL81 cell monolayers in 96 well plates to allow accurate quantification of infected cells. Virus was added at  $2 \times 10^4$  PFU per well to yield a target of 10-30% of infected cells in the



monolayer. Total cell counts per well were enumerated by nuclear stain (Hoechst 33342) and fluorescent virally infected foci were detected 16-24 hours after inoculation with a Cytation 7 Cell Imaging Multi-Mode Reader (Biotek) with Gen5 Image Prime version 3.09. Titers were calculated in GraphPad Prism version 8.4.2 by generating a 4-parameter (4PL) logistical fit of the percent neutralization at each serial serum dilution. The 50% neutralization titer was reported as the interpolated reciprocal of the dilution yielding a 50% reduction in fluorescent viral foci.

#### 2.6.2.17.6. Cytokine Profiling Immunoassays in Mice

Antigen-specific T cell responses were analyzed in fresh or frozen splenocytes with a flow cytometry based intracellular cytokine staining (ICS) assay. For frozen samples, splenocytes were thawed, washed and rested in cRPMI for 1h at 37°C. After resting, splenocytes were washed and counted prior to plating. Splenocytes ( $2 \times 10^6$  cells/well) were cultured in cRPMI with media-DMSO (unstimulated) or specific peptide libraries (15mers with 11aa overlap at the final concentration of 2 µg/mL/peptide) representing the full-length spike sequences of SARS-CoV-2 WT (JPT, PM-WCPV-S-1), Omicron BA.4/5 (JPT, PM-SARS2-SMUT10-2), XBB.1.5 (JPT, PM-SARS2-SMUT15), JN.1 (JPT, PM-SARS2-SMUT21-1) and KP.2 (Mimotopes, Custom) lineages separately, for 5 hours at 37°C in the presence of anti-CD107a APC antibody and protein transport inhibitors, GolgiPlug and GolgiStop. Following stimulation, splenocytes were first incubated with Fixable Viability Dye eFluor 506 (10 minutes at RT) followed by staining with fluorescent-conjugated antibodies to the surface proteins CD19, CD3, CD4 and CD8 for  $25 \pm 5$  minutes at RT followed by fixation, permeabilization and staining for intracellular proteins CD154, IFN-γ, TNF-α and IL-2 for  $25 \pm 5$  minutes at RT. After staining, cells were washed and resuspended in flow cytometry staining buffer. Samples were acquired on a 5-Laser Aurora system (Cytek®) using the SpectroFlo® Software version 3.1.2. The instrument was subject to daily quality control procedures using SpectroFlo® QC Beads as per the manufacturer recommendations. Acquired data files were analyzed using OMIQ software. Results are background (media-DMSO) subtracted and shown as percentage of cytokine-expressing CD4+ and CD8+ T cells.

For prior studies, ELISpot was performed with mouse IFNγ ELISpot<sup>PLUS</sup> kits according to the manufacturer's instructions (Mabtech). Briefly, a total of  $5 \times 10^5$  splenocytes were ex vivo restimulated with the full-length S peptide mix (0.1 µg/mL final concentration per peptide, JPT) or controls (gp70-AH1 [SPSYVYHQF] (Slansky et al, 2000), JPT). Streptavidin-ALP and BCIP/NBT-plus substrate were added, and spots counted using an ELISpot plate reader (ImmunoSpot® S6 Core Analyzer, CTL). Spot numbers were evaluated using ImmunoCapture Image Acquisition Software V7.0 and ImmunoSpot 7.0.17.0 Professional. For T cell subtyping, CD8+ T cells were isolated from splenocyte suspensions using MACS MicroBeads (CD8a [Ly-2], Miltenyi Biotec) according to the manufacturer's instructions. The flow-through served as a source of CD4+ T cells. CD8+ or CD4+ T cells were subsequently restimulated with syngeneic bone marrow-derived dendritic cells loaded with full-length S peptide mix (0.1 µg/mL final concentration per peptide) or medium as control. For cytokine profiling in mice by bead-based immunoassays, mouse splenocytes were re-stimulated for 48 hours with full-length S peptide mix (0.1 µg/mL final concentration per peptide) or cell culture medium (no peptide) as control. Concentrations of

IFN $\gamma$ , IL-2, IL-4, IL-5 and (for splenocytes from BNT162b2-immunised mice) IL-13 in supernatants were determined using a bead-based, 11-plex Th1/Th2 mouse ProcartaPlex multiplex immunoassay (Thermo Fisher Scientific) according to the manufacturer's instructions. Fluorescence was measured with a Bioplex200 system (Bio-Rad) and analysed with ProcartaPlex Analyst 1.0 software (Thermo Fisher Scientific). Values below the lower limit of quantification (LLOQ) were set to zero.

#### 2.6.2.17.7. ELISpot and Intracellular Cytokine Staining Assays in NHPs

Cryopreserved NHP PBMCs were thawed in pre-warmed AIM-V media (Thermo Fisher Scientific, US) with Benzonase (EMD Millipore, US), washed once, and the concentration was adjusted to  $2.5 \times 10^6$  cells/mL in AIM-V.

For ELISpot assays, commercially available NHP IFN- $\gamma$  and IL-4 ELISpot assay kits were used (Mabtech, Sweden). Briefly, pre-coated PVDF 96-well microplates were washed with PBS and blocked with AIM-V. PBMCs were added at  $1.0 \times 10^5$  cells/well for IFN- $\gamma$  and  $2.5 \times 10^5$  cells/well for IL-4. Cells were stimulated with a peptide pool spanning the entire S protein (15 mers, 11aa overlap, JPT, Germany) at 1  $\mu$ g/mL for 24 hours for IFN- $\gamma$  and 48 hours for IL-4 at 37°C in 5% CO<sub>2</sub>. Tests were performed in triplicate wells; media-DMSO, a CMV peptide pool (JPT, Germany) and PHA (Sigma, USA) were included as controls. Cells were removed, plates washed, and spots detected using a biotinylated detection antibody followed by a Streptavidin-HRP secondary antibody and AEC chromogenic substrate (BD, US) for 10 minutes for IFN- $\gamma$  and 30 minutes for IL-4 at room temperature until red spots were developed. Dried plates were scanned and counted using a CTL ImmunoSpot S6 Universal Analyzer (CTL, US). Reported results are background (media-DMSO) subtracted and normalized to spot forming cells (SFC)/ $10^6$  PBMCs.

For intracellular cytokine staining (ICS) flow cytometry-based analysis, thawed PBMCs rested for 3 to 4 hours were stimulated in AIM-V medium in 96-well plates with the peptide pool spanning the entire S protein at 1  $\mu$ g/mL; Staphylococcus enterotoxin B (SEB; 2  $\mu$ g/mL) was used as a positive control; and 0.2% DMSO was used as a negative control. An APC-conjugated CD107a monoclonal antibody, GolgiStop, and GolgiPlug were added to each well, and cells were incubated at 37°C for 12 to 16 hours. Cells were then stained with Viability Dye eFluor 780 and Fc block prior to surface staining with mAbs specific for CD4, and CD8. Following staining for surface markers, cells were fixed and permeabilized with BD CytoFix/CytoPerm solution, and intracellular staining performed with mAbs specific for the following proteins, diluted in permeabilization buffer: CD154, IFN- $\gamma$ , IL-2, IL-4, TNF- $\alpha$ , CD3. Cells were washed, resuspended in 2% fetal bovine serum (FBS)/ phosphate buffered saline (PBS) buffer and acquired on a LSR Fortessa. Data were analyzed by FlowJo (10.4.1). Cytokine-expressing cells were gated within the CD154<sup>+</sup> CD4<sup>+</sup> T cells and CD69<sup>+</sup> CD8<sup>+</sup> T cells. Results shown are background (media-DMSO) subtracted.



#### 2.6.2.17.8. Quantitative RT-PCR for Detection of SARS-CoV-2 Viral RNA

For quantification of SARS-CoV-2 virus in nonhuman primate challenge model swabs and bronchoalveolar lavage (BAL) specimens, the US Centers for Disease Control-developed 2019-nCoV\_N1 assay, a sensitive reverse transcription-polymerase chain reaction (RT-PCR)-based assay that detects both viral genomic RNA and RNA transcripts, was used (Singh et al, 2021).

#### 2.6.2.17.9. Lung Radiographs and Computed Tomography Scans

Lung radiographs (X-rays) and computed tomography (CT) scans were performed under anesthesia as previously described (Singh et al, 2021; Kaushal et al, 2015). For radiographic imaging, 3-view thoracic radiographs (ventrodorsal, right and left lateral) were obtained one week prior to challenge, and post-challenge on Days 1, 3, 6 and end of project (Day 7/8) or Day 10. High-resolution CT was performed one week prior to challenge and post-challenge on Days 3 and 6, for BNT162b2-immunized and control NHP and end of project (Day 7/8) or Day 10 for all groups. The animals were anesthetized using Telazol (2-6 mg/kg) and maintained by inhaled isoflurane delivered through a Hallowell 2002 ventilator anesthesia system (Hallowell, Pittsfield, MA). Animals were intubated to perform end inspiratory breath-hold using a remote breath-hold switch. Lung field CT images were acquired using Multiscan LFER150 PET/CT (MEDISO Inc., Budapest, Hungary) scanner. Image analysis was performed using 3D ROI tools available in Vivoquant (Invicro, Boston, MA). Images were interpreted by two board-certified veterinary radiologists blinded to treatment groups. Scores were assigned to a total of 7 lung regions on a severity scale of 0-3 per region, with a maximum severity score of 21. Pulmonary lesions that could not be unequivocally attributed to the viral challenge (such as atelectasis secondary to recumbency and anesthesia) received a score of "0".

#### 2.6.2.17.10. Macroscopic and Microscopic Pathology

Histopathological assessments were performed at Days 7 or 8 following infectious SARS-CoV-2 challenge on the BNT162b2-immunized animals (100 µg dose level; n=6) and age- and sex-matched saline-immunized and SARS-CoV-2-challenged control animals that were included in the histopathology animal cohort (n=3). Tissues collected and microscopically evaluated included lung (7 sections- 1 sample of each lobe on L & R), kidney, liver, spleen, skin, large and small intestine, heart [with coronary arteries], bone marrow, nasal septum, tongue, trachea, mediastinal lymph node, and mucocutaneous junctions. Tissues were fixed in 10% neutral buffered formalin and routinely processed into paraffin blocks, sectioned to 5 µm and stained with hematoxylin and eosin.

Microscopic evaluation was performed independently by two pathologists, both blinded to treatment group. Lungs were evaluated using a semi-quantitative scoring system with inclusion of cell types and/or distribution as appropriate. An inflammation area score, based on the estimated area of the lung section with inflammation, was used to grade each lung lobe: 0=normal; 1≤10%; 2=11-30%; 3=30-60%; 4=60-80%; 5≥80%. Samples were unblinded after agreement on diagnoses and severity grades. For each animal, the inflammation area score for each lung lobe was averaged to generate a single inflammation area score for that animal. That score was used to evaluate the severity of respiratory disease after SARS-CoV-2 challenge.

### 2.6.2.18. References

Al-Amri SS, Abbas AT, Siddiq LA, et al. Immunogenicity of candidate MERS-CoV DNA vaccines based on the spike protein. *Sci Rep.* 2017;7:44875.

Brouwer PJM, Caniels T G, van der Straten KJ. Potent neutralizing antibodies from COVID-19 patients define multiple targets of vulnerability. *Science.* 2020;369(6504):643-50.

Cai Y, Zhang J, Xiao T, et al. Distinct conformational states of SARS-CoV-2 spike protein. *Science.* 2020;10.1126/science.abd4251.

Centers for Disease Control and Prevention. COVID Data Tracker. Atlanta, GA: U.S. Department of Health and Human Services, CDC; 2024, July 31. Available from: <https://covid.cdc.gov/covid-data-tracker/#variant-proportions>. Accessed: 31 Jul 2024

de Wit E, van Doremalen N, Falzarano D, et al. SARS and MERS: recent insights into emerging coronaviruses. *Nat Rev Microbiol.* 2016;14(8)(08):523-34.

Henderson R, Edwards RJ, Mansouri K, et al. Controlling the SARS-CoV-2 spike glycoprotein conformation. *Nat Struct Mol Biol.* 2020;(Jul):Online.

Hoffmann M, Kleine-Weber H, Schroeder S, et al. SARS-CoV-2 cell entry depends on ACE2 and TMPRSS2 and is blocked by a clinically proven protease inhibitor. *Cell.* 2020;181(2):271-80.e8.

Hulswit RJ, de Haan CA, Bosch BJ. Coronavirus spike protein and tropism changes. *Adv Virus Res* 2016;96:29-57.

Hutloff A. Regulation of T follicular helper cells by ICOS. *Oncotarget* 2015;6(26)(Sep):21785-6.

Kariko K, Buckstein M, Ni H, et al. Suppression of RNA recognition by Toll-like receptors: the impact of nucleoside modification and the evolutionary origin of RNA. *Immunity* 2005;2(Aug):165-75.

Kaushal D, Foreman TW, Gautam US, et al. Mucosal vaccination with attenuated *Mycobacterium tuberculosis* induces strong central memory responses and protects against tuberculosis. *Nat Commun.* 2015;6:8533.

Ke Z, Oton J, Qu K. et al. Structures and distributions of SARS-CoV-2 spike protein trimers on intact virions. *Nature.* 2020; 588:498-502

Kim JY, Ko JH, Kim Y, et al. Viral load kinetics of SARS-CoV-2 infection in first two patients in Korea. *J Korean Med Sci.* 2020;35(7)(Feb):e86.

Liu L, Wang P, Nair MS, et al. Potent neutralizing antibodies against multiple epitopes on SARS-CoV-2 spike. *Nature*. 2020;584(7821):450-6.

Munster VJ, Feldmann F, Williamson BN, et al. Respiratory disease in rhesus macaques inoculated with SARS-CoV-2. *Nature*. 2020;585:268-72

Muruato AE, Fontes-Garfias CR, Ren P, et al. A high-throughput neutralizing antibody assay for COVID-19 diagnosis and vaccine evaluation. *Nat Commun*. 2020;11(1):4059.

Pallesen J, Wang N, Corbett KS, et al. Immunogenicity and structures of a rationally designed prefusion MERS-CoV spike antigen. *Proc Natl Acad Sci USA*. 2017;114(35):E7348-57.

Pardi N, Parkhouse K, Kirkpatrick E, et al. Nucleoside-modified mRNA immunization elicits influenza virus hemagglutinin stalk-specific antibodies. *Nat Commun*. 2018;9(1)(08):3361.

Report R-20-0085: Immunogenicity Study of the LNP-Formulated ModRNA Encoding the Viral S Protein-V9.

Robbiani DF, Gaebler C, Muecksch F, et al. Convergent antibody responses to SARS-CoV-2 infection in convalescent individuals. *Nature*. 2020;584:437-42

Sahin U, Karikó K, Türeci Ö. mRNA-based therapeutics - developing a new class of drugs. *Nat Rev Drug Discov*. 2014;13(10):759-80.

Singh DK, Singh B, Ganatra SR et al. Responses to acute infection with SARS-CoV-2 in the lungs of rhesus macaques, baboons and marmosets. *Nat Microbiol*. 2021;6:73-86

Slansky JE, Rattis FM, Boyd LF, et al. Enhanced antigen-specific antitumor immunity with altered peptide ligands that stabilize the MHC-peptide-TCR complex. *Immunity*. 2000;13(4):529-38.

Study 38166. Repeat-Dose Toxicity Study of Three LNP-Formulated RNA Platforms Encoding for Viral Proteins By Repeated Intramuscular Administration to Wistar Han Rats.

Study 20GR142. Giovanelli M. 17-Day Intramuscular Toxicity Study of BNT162B2 (V9) and BNT162B3C in Wistar Han Rats with a 3-Week Recovery. Study ongoing.

Study 20256434 (RN9391R58). Bouressam M. A Combined Fertility and Developmental Study (Including Teratogenicity and Postnatal Investigations) of BNT162b1, BNT162b2 and BNT162b3 by Intramuscular Administration in the Wistar Rat. 22 Dec 2020.

Vogel AB, Kanevsky I, Che Y, et al. BNT162b vaccines protect rhesus macaques from SARS-CoV-2. *Nature*. 2021;592:283-9.

VR-MQR-10211 Method Qualification Report for a Single-Plex Direct Luminex Assay for Quantitation of IgG Antibodies to SARS-CoV-2 S1 Protein in Human Sera.

VR-MQR-10214 Qualification of the SARS-CoV-2 mNeonGreen Virus Microneutralization Assay.

VR-VTR-10671 BNT162b2 (V9) Immunogenicity and Evaluation of Protection against SARS-CoV-2 Challenge in Rhesus Macaques.

VR-VTR-10741 Structural and Biophysical Characterization of SARS-CoV-2 Spike Glycoprotein (P2 S) as a Vaccine Antigen.

VR-VTR-10944 Evaluation of COVID-19 Variant-Modified Vaccines in Mice.

VR-VTR-10976 Immunogenicity of Monovalent and Bivalent BA.4/BA.5 Variant-Modified Vaccines in Mice.

VR-VTR-11122 Immunogenicity of COVID-19 Monovalent and Bivalent XBB.1.5 Sublineage-Modified Vaccines in Naïve Mice as a Primary Series

VR-VTR-11123 Immunogenicity of COVID-19 Monovalent and Bivalent XBB.1.5 Sublineage-Modified Vaccines in BNT162b2 Experienced Mice as a Fourth Dose Booster

VR-VTR-11311 Immunogenicity Evaluation of BNT162b2 JN.1 as a Primary Series in Mice

VR-VTR-11313 Immunogenicity Evaluation of BNT162b2 JN.1 as a Fifth Vaccination in Mice

VR-VTR-11341 Immunogenicity Evaluation of KP.2 and JN.1-Adapted BNT162b2 as a Primary Series in Mice

VR-VTR-11342 Immunogenicity Evaluation of KP.2 and JN.1-Adapted BNT162b2 as a Fourth Vaccination in Vaccine-Experienced Mice

VR-VTR-11466 Immunogenicity Evaluation of XEC- and LP.8.1-Adapted BNT162b2 in Vaccine-Experienced Mice

VR-VTR-11467 Immunogenicity Evaluation of XEC- and LP.8.1-Adapted BNT162b2 in Naïve Mice

World Health Organization. WHO guidelines on nonclinical evaluation of vaccines. Annex 1. In: World Health Organization. WHO technical report series, no. 927. Geneva, Switzerland; World Health Organization; 2005:31-63.

Wrapp D, Wang N, Corbett KS, et al. Cryo-EM structure of the 2019-nCoV spike in the prefusion conformation. Science. 2020;367(6483):1260-3.

Wu Y, Wang F, Shen C, et al. A noncompeting pair of human neutralizing antibodies block COVID-19 virus binding to its receptor ACE2. Science. 2020; 368(6496):1274-8.

Xie X, Muruato A, Lokugamage KG, et al. An infectious cDNA clone of SARS-CoV-2. Cell Host Microbe. 2020; 27(5):841-848.e3.

Yong CY, Ong HK, Yeap SK, et al. Recent advances in the vaccine development against middle east respiratory syndrome-coronavirus. Front Microbiol. 2019;10:1781.

Yuan M, Wu NC, Zhu X, et al. A highly conserved cryptic epitope in the receptor binding domains of SARS-CoV-2 and SARS-CoV. Science. 2020; 368(6491):630-3.

Zakhartchouk AN, Sharon C, Satkunarajah M, et al. Immunogenicity of a receptor-binding domain of SARS coronavirus spike protein in mice: implications for a subunit vaccine. Vaccine. 2007;25(1):136-43.

Zhou M, Zhang X, Qu J. Coronavirus disease 2019 (COVID-19): a clinical update. Front Med. 2020(Apr):1-10.

Zou L, Ruan F, Huang M, et al. SARS-CoV-2 viral load in upper respiratory specimens of infected patients. N Engl J Med. 2020;382(12)(03):1177-9.